A THEORETICAL STUDY OF THE PROPERTIES OF PHOTOEXCITED HOT CARRIERS IN GERMANIUM

by

ALEJANDRO NOGUERA BECERRA

A dissertation submitted to the University of Warwick for admission to the degree of Doctor of Philosophy, School of Physics, March 1978.

CAPTION TABLES:

LIST OF TABLES:

LIST OF FIGURES (continued)

LIST OF FIGURES (continued)

MEMORANDUM

This dissertation is submitted to the University of Warwick in support of my application for admission to the degree of Doctor of Philosophy. It contains account of my own work performed at the School of Physics of the University of Warwick in the period October 1974 to October 1977, under the general supervision of Doctor C. J. Hearn. No part of this dissertation has been used previously in a degree thesis submitted to this or any other university. The work described in this thesis is the result of my own independent research, except where specifically acknowledged in the text.

March 1978

A. Noguera Becerra

ACKNOWLEDGEMENTS

The author wishes to express his deep gratitude to Doctor C. J. Hearn, for his continued interest and encouragement throughout the course of this work. I wish also to thank the University of Warwick for providing the facilities for research within the School of Physics. Furthermore, I would like to thank Doctor J. McInnes for many useful and fruitful discussions.

I gratefully acknowledge the financial support provided by the Universidad de los Andes, Venezuela.

Finally, I wish to thank Ms. Terri Moss for her skill and patience in typing this thesis, and also thank my wife Conchita for her continued support and encouragement.

ABSTRACT

This thesis is about a theoretical study of the properties of photoexcited holes in p-type Ge samples at low temperatures. The emphasis is on those carriers which are in non-equilibrium with the lattice. The energy distribution function for these carriers are obtained by a numerical solution of a rate equation which involves excitation, recombination and lattice scattering. Two models of a semiconductor are considered. The complicated band structure of p-type Ge is first approximated by a parabolic heavy hole band; later developments make necessary the inclusion of a parabolic light hole band.

Two types of photoexcitation are analysed. In the first, carriers are generated by a narrow spectrum of photoexcitation and the distribution function is studied as function of the initial excitation energy, the spectrum bandwidth and the density of the compensating impurities. For a very narrow excitation spectrum, the distribution of carriers exhibits a series of equally spaced peaks at carrier wavevectors equal to and below the photoexcitation wavevector. At compensation densities greater than or about equal to 10^{13} cm^{-3} and photoexcitation energies about 30 meV the distribution function resembles a Maxwellian function with carriers temperature much greater than that of the lattice.

The second excitation spectrum involves room temperature blackbody radiation. In the one band model, the distribution function is, for Cu-doped Ge with compensation densities less than or equal to 10^{13} cm^{-3}, nearly a Maxwellian function with the carrier temperature obtained from an energy balance equation. Good agreement with experimental mobility data is found for the same compensation densities. For higher compensation densities a parabolic light hole band is then included in the model of semiconductor and the experimental photohall mobility data for Cu-and Ga-doped Ge samples are used to deduce a value for the deformation potential a. This parameter is found to depend on both the compensation density and lattice temperature.

It is also reported additional calculations which suggest ways to improve the theoretical model.

PUBLICATION

Various aspects of the work described in this thesis have been published in the Scientific Literature. The paper involved is published jointly with Dr. C. J. Hearn.

"Properties of hot photoexcited holes in Cu-doped Germanium at low temperature". Solid-State Electronics 21, 171 (1978).

CHAPTER 1

INTRODUCTION

It is only recently that a comprehensive information about low-temperature-transport properties of photoexcited holes in p-type Ge has become available. These properties are in general very sensitive to the form of the carrier energy distribution. This thesis presents a theoretical study of the non-equilibrium photohole distribution functions and their consequences as regards hole properties. The objectives is to relate measurements of phototransport and trapping parameters to the knowledge of the interaction of holes with phonons and the recombination processes at low temperatures. Particular emphasis is placed on hot carrier phenomena, that is, carriers with average energy much greater than that of equilibrium.

A complete knowledge of the distribution of carriers is essential in order to understand many of the transport and trapping properties of semi-conductors. It is well known that for carriers in thermal equilibrium with the lattice, the Fermi-Dirac distribution is applicable to the case of degenerate systems. This function reduces to the Maxwell-Boltzmann function for non-degenerate systems. However the initially excited carriers may be unable to dissipate the energy excess received from the external source during their lifetime and departure from thermal equilibrium may occur.

At low temperatures, the mobility of free carriers is strongly influenced by the presence of ionised impurities. The degree of this influence decreases as the carrier energy increases. Consequently carrier mobilities will reflect changes in the energy

distribution function. Furthermore, the carrier lifetime is governed by capture of free carriers at impurity centres. Their capture probability is a function of the average carrier energy. The energy of a hot distribution has no direct dependence on the lattice temperature. Therefore the carrier lifetime will not show a strong temperature dependence as in thermal cases. The carrier lifetime can be systematically varied by changing the recombination density enabling one to pass from a thermal to a hot distribution function.

Experiments by Norton and Levinstein [1] suggest that hot holes occur in Cu-doped Germanium at low temperatures and for compensating donor concentrations (N_D) greater than 10^{13} cm^{-3}. Samples with compensating densities around 10^{13} cm^{-3} involve a carrier lifetime of the same order as the energy relaxation time τ_{ac} and warm carriers are observed [1]. Holes were photoexcited by room temperature blackbody radiation and so have initial energies much greater than the thermal energy ($k_B T$). Using the same radiation and similar type of experiments, Bannaya et.al. [2] arrived also at the conclusion that in Ga-doped Ge hot holes occur for $N_D \geq 10^{14}$ cm^{-3}.

Further experimental evidence in support of hot photoexcited holes in Cu-doped Ge has been obtained by studying the Oscillatory Photoconductivity. This is produced by monochromatic light of wavelength λ and photon energy greater than the ionization energy of copper centres i.e. $\varepsilon_{ph} \geq 42.86$ meV. The ionised hole will be ejected with an initial energy (ε_{ph}-42.86) eV. If this energy is

greater than the optical phonon threshold energy (ε_{op} = 0.037 eV), an optical phonon will be emitted in about 10^{-12} second. This process will continue until the hole energy becomes less than ε_{op}. This phenomena has been illustrated by Stoker et.al. [3] for n-type materials. The carrier energy exhibits a repetition ramp form as a function of the photon energy [1]. In the case of high compensation densities ($N_D \geq 10^{14}$ cm^{-3}) hole lifetimes are very short, typically about 10^{-10} sec at $10^{o}K$. Therefore carriers have no time to come into equilibrium with the lattice. The photoconductivity, under this condition, will show a behaviour characteristic of the product of mobility, lifetime and photo-conization cross section. Assuming that the photoconization is constant for photons with $\varepsilon_p > 42.86$ e.V one may write the photoconductivity as

$$\sigma(\varepsilon) = e\ \mu(\varepsilon)\ \tau(\varepsilon) = e\ \tau_o\ \mu(\varepsilon)\ \varepsilon^n$$

where $\mu(\varepsilon)\ \tau(\varepsilon)$ is the product of mobility and carrier lifetime as a function of the carrier energy and n is approximately ½ for Cu-doped Ge. Since ε is a repetitive ramp, the photoconductivity will exhibit the same dependence with increasing photon energy. Besfamil'naya et.al [4] measured this effect in Cu,Au,Zu and Cd doped Ge. They demonstrated that the oscillations become more pronounced as the compensation is increased, and this response was not due to oscillations in the absorption coefficient. No attemps were made to separate the contribution to oscillations from carrier lifetime and mobility. This latter effect was separated by Godik [5] in Cu-doped Ge samples. Oscillatory mobilities were found for compensation $N_D \geq 10^{13}$cm.

This work has direct relevance to experimental measurements by Norton and Levinstein [1], Bannaya et.al [2] and Godik [5]. Calculations are aimed at obtaining the energy distribution function which consequently will be used in a discussion of some of the carriers properties which are of interest in explaining transport data.

The first theoretical investigation of hot photoexcited carriers was made by Mattis [6]. He discussed the problem of calculating the photoexcited carrier distribution function within the framework of a variational principle. The theory was based on a simple model involving accoustic deformation scattering of non-degenerate carriers in the band in the presence of cascade capture into shallow impurities. Although the distribution was not derived, Mattis showed that significant departures from the Maxwell-Boltzmann distribution are possible at very low temperatures. These effects were associated with a rapid decreasing of carrier lifetime with lattice temperature. Hearn [7,8] considered the criteria for the applicability of an effective temperature to describe the steady-state distribution function. Carriers were photoexcited into one of the bands of a simple semi-conductor by a monochromatic source. Inter-carrier collisions were important but non-degeneracy was assumed. Departures from a Maxwellian form depends essentially on the carrier lifetime. On the other hand, Ladyzhinskii [9] studied the form of a "hot" distribution function in connection with the theory of photoconductivity. This study assumes monochromatic radiation, momentum and energy relaxation by acoustic deformation scattering within one band of a semi-conductor. The calculated distribution function gives different

results for average lifetime and photoconductivity as compared with the case of the Boltzmann function. Finally, another work of interest is that of Barker and Hearn [10]. This work investigates the properties of photoexcited electrons into one of the bands of a semi-conductor. Detailed numerical calculations are made of the carrier distribution function in Ge and Si at low temperatures. Excitation by room temperature blackbody radiation and cascade capture into shallow impurities have been assumed. Calculations used acoustic deformation and non-polar optical scattering. The theory shows that carrier heating occur below $30^{o}K$ and impurity densities of the order of 10^{15} cm^{-3}. Good agreement with early photo Hall mobility data for one Cu-doped Ge sample [11] is obtained.

This report deals with the transport properties of photo-excited holes for two models of a semiconductor. The complicated band structure of p-type Ge is first approximated by a parabolic heavy hole band; later developments make necessary the inclusion of a parabolic light hole band. The distribution function is derived from a rate equation involving photoexcitation, re-combination into either deep or shallow impurities and lattice scattering. Holes are photoexcited either by room temperature radiation or by a narrow band of photoexcitation. Acoustic deformation scattering and instantaneous optical phonon emission account for the lattice scattering. The isotropic distribution function occurring in the absence of an electric field is determined numerically and the low field mobility and carrier lifetime are then obtained as suitable averages over the zero-field distribution function.

In Chapter II the physics of photoexcited carriers in p-type Germanium samples at low temperatures is investigated. Holes are excited by a narrow spectrum of photoexcitation. Special interest is paid to the variation of the form of the energy distribution function when the excitation linewidth, photoexcitation energy and the energy dependence of the recombination lifetime are changed. The mobility is then calculated for a Cu-doped Ge sample at two lattice temperatures and various excitation energies. Results are compared with photohall mobility data of Godik [5].

In Chapter III the properties of photoexcited carriers in the heavy hole band of Cu-doped Germanium samples at low temperatures are studied. Holes are now photoexcited by room temperature blackbody radiation. The energy distribution function is compared with a Maxwellian function, with the carrier temperature evaluated from an energy balance equation. The mobility and carrier lifetime are then averaged over both kinds of distribution functions. Results are finally compared with the photohall data of Norton and Levinstein [1].

Chapter IV begins with a brief review of the experimental status of the three deformation potentials for the lattice scattering in the valence band of Ge. It is noted that, the deformation potential conventionally denoted by a is very uncertain in value. Photoexcitation gives a wide class of carrier distribution functions and this opens up the possibility of obtaining a value for the deformation parameter a by fitting the calculated hot hole mobilities to those measured by Norton and Levinstein [1] and

Bannaya et.al [2]. This course of investigation is pursued throughout the rest of the chapter, and leads to results which cannot be derived from equilibrium transport measurements.

Chapter V discusses some of the problems raised by this work, and presents additional results which partially explain those difficulties. These new results suggest areas for future research at both theoretical and experimental levels.

The Appendices contain mathematical information about the scattering processes used in the calculations.

CHAPTER II

THE ENERGY DISTRIBUTION OF PHOTOEXCITED HOLES IN P-TYPE GERMANIUM LASER ILLUMINATION

2.1. INTRODUCTION

In this chapter we investigate the physics of photoexcited holes in the valence band of a simple model of semi-conductor. Details of the theoretical model are given in Section 2.2. The distribution of holes generated by a narrow spectrum of photo-excitation is derived from a rate equation involving photoexcitation, recombination and lattice scattering. The isotropic distribution function occurring in the absence of an electric field is determined numerically. Thus the carriers properties are obtained as suitable averages over the zero-field distribution function. The method of calculation is presented in Section 2.3.

In thermodynamic equilibrium the distribution function is mainly determined by acoustic and optical phonon scattering. To produce changes in the distribution function one requires an external stimulus strong enough to transfer energy and momentum to the carriers at rates which compare significantly with rates of any other scattering process present. This effect is significant when the capture rate by an impurity matches or exceeds the scattering rates. The distribution function may then deviate sharply from a thermal Maxwell-Boltzmann function. This situation can occur in Germanium at low temperatures. Ridley and Harris [12] have suggested that the form of the distribution function may depend crucially on the excitation bandwidth ($\hbar\,\Delta\omega$). Section 2.4 presents the salient features of the distribution function for various values of the bandwidth. The distribution function exhibits

a series of equally spaced peaks at carrier wave-vectors equal and below the photoexcitation wave-vector (K_{ph}) at very narrow excitation spectrum. The wave-vector ΔK between peaks corresponds to the minimum momentum that a carrier should have in order to emit an acoustic phonon. On increasing the bandwidth the peaks disappear.

The form of the distribution function depends strongly on carrier lifetime, although no important changes are seen when the energy dependence of the carrier lifetime is varied. The carrier lifetime can become comparable with the energy relaxation time ($\tau_{ac}(k_BT)$) in Ge at low temperatures. Under these conditions one can expect that the photocarrier behaviour will depend on the radiation energy ε_{ph}. Godik [5] has reported one experiment of this type in Cu-doped Ge at low temperatures. Calculations of the low field Hall mobilities involve the average of the total momentum relaxation time over the zero-field distribution function (Section 2.5). The form of the distribution function is given in Section 2.6 for various excitation energies ε_{ph} and carrier lifetimes. The form of the distribution function resembles a Maxwellian function as the excitation energy comes close to the optical phonon threshold energy (ε_{op} = 0.037 m.e.V).

It is noted that the deformation potential, of the one-deformation parameter theory, changes in value when one attempts to fit the calculated mobilities to the experimental data [5], at two lattice temperatures.

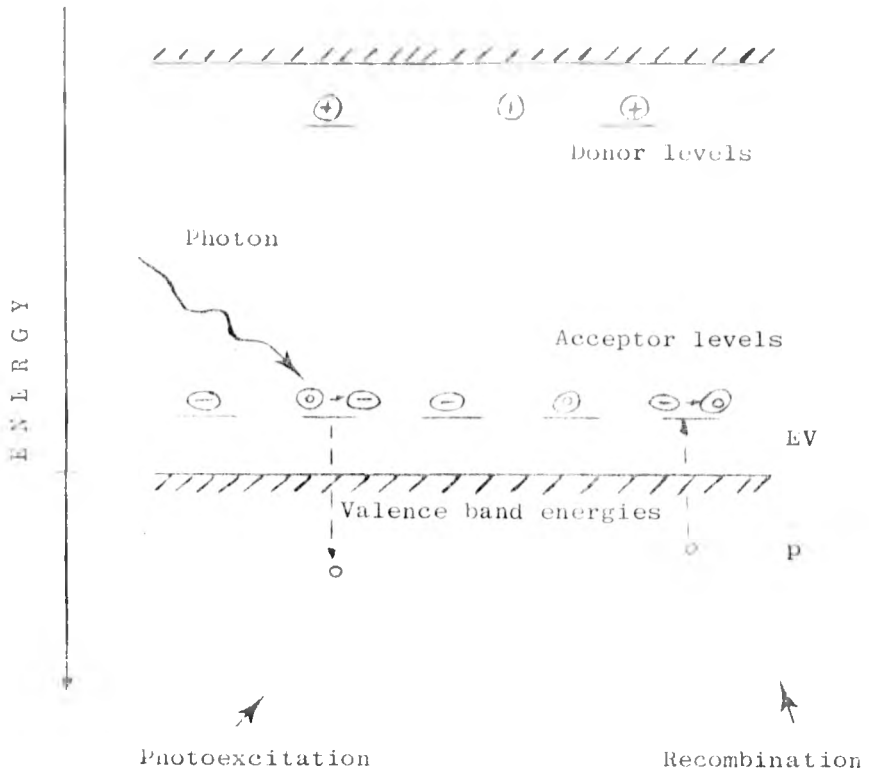

CODE	
○	hole
⊙	neutral impurity
⊖	negatively charge impurity
⊕	positively charge impurity
E_c	energy of minimum conduction band
EV	energy of maximum valence band
p	density of holes

Illustration of the dynamics of extrinsic photoexcitation. Holes are excited from the neutral acceptors into the band and subsequently recombine with the ionised impurities.

2.2. THE THEORETICAL MODEL

The complicated valence band structure of Ge is approximated by a parabolic heavy hole band so that the carrier energy dispersion relation is

$$\varepsilon(\underset{\sim}{k}) = \frac{\hbar^2 k^2}{2 m_2}$$

where m_2 is identified with the heavy-hole effective mass (.33 m_e, m_e is the mass of a free electron), $\underset{\sim}{k}$ is the hole wave-vector. A steady state rate equation is set up to investigate the energy distribution of holes in that band. This equation expresses the balance at which carriers enter and leave a state $\underset{\sim}{k}$. Carriers are photogenerated from acceptor levels by a narrow spectrum of photoexcitation. We assume that this radiation gives rise to a spatially uniform rate of excitation of carriers into the band. Transport effects can then be ignored. The only effect of the radiation is considered to be that of generation of carriers. In particular free-carrier absorption within the band is neglected. Also transition processes within the solid is supposed not to be affected by the radiation. Under these conditions the effective bandwidth of carriers arriving at the band is essentially determined by the radiation linewidth. At low temperatures broadening of the optical transition lifetime will broaden the bandwidth. We will leave the bandwidth as parameter.

Since the optical excitation is isotropic in $\underset{\sim}{k}$-space, we assume that the distribution function $f_o(\underset{\sim}{k})$ in the absence of external electric field depends only on energy. Only inelastic scattering processes are effective in determining $f_o(\underset{\sim}{k})$. The linear response region is considered only. This corresponds to

a low carrier concentration so that effects of degeneracy, inter-carrier scattering and non-equilibrium of phonons can be ignored. The steady rate equation describing photoexcitation of carriers into a single band obeys a linear integral equation:

$$\left.\frac{\partial f_o(\underset{\sim}{k})}{\partial t}\right|_{ph} + \left.\frac{\partial f_o(\underset{\sim}{k})}{\partial t}\right|_{rec} + \left.\frac{\partial f_o(\underset{\sim}{k})}{\partial t}\right|_{lattice} = 0 \qquad 2.2.1.$$

this equation (2.2.1) includes photoexcitation (ph), recombination into impurity centres (rec) and lattice scattering. Conservation of the total number of carriers given by

$$\sum_{k} \left.\frac{\partial f_o(\underset{\sim}{k})}{\partial t}\right|_{lattice} = 0$$

leads to a useful sum rule

$$\sum_{k} \left.\frac{\partial f_o(\underset{\sim}{k})}{\partial t}\right|_{ph} = - \sum_{k} \left.\frac{\partial f_o(\underset{\sim}{k})}{\partial t}\right|_{rec} \qquad 2.2.2.$$

which may be used as a boundary condition.

In a steady state situation the total rate of photoexcitation W_{ph} equals the total rate of recombination W_{rec}, that is, $W_{ph} = W_{rec} \equiv W$. The shape distribution function becomes independent of the total excitation rate W; and can be conveniently rewritten in terms of a reduced distribution function $\phi(K)$, normalised to unit rate of photoexcitation W [10].

$$\phi(K) \equiv 4\pi\rho \quad \alpha^{-3} \; f_o(K) \; W^{-1} \qquad 2.2.3.$$

where $K^2 = \alpha^2 \; k^2 \equiv \frac{\varepsilon(\underset{\sim}{k})}{k_B T} \equiv \frac{\hbar^2 \; k^2}{2m_2 k_B T}$ with ρ and T being the density of states in $\underset{\sim}{k}$-space and lattice temperature respectively.

a low carrier concentration so that effects of degeneracy, inter-carrier scattering and non-equilibrium of phonons can be ignored. The steady rate equation describing photoexcitation of carriers into a single band obeys a linear integral equation:

$$\left.\frac{\partial f_o(\underset{\sim}{k})}{\partial t}\right|_{ph} + \left.\frac{\partial f_o(\underset{\sim}{k})}{\partial t}\right|_{rec} + \left.\frac{\partial f_o(\underset{\sim}{k})}{\partial t}\right|_{lattice} = 0 \qquad 2.2.1.$$

this equation (2.2.1) includes photoexcitation (ph), recombination into impurity centres (rec) and lattice scattering. Conservation of the total number of carriers given by

$$\sum_{k} \left.\frac{\partial f_o(\underset{\sim}{k})}{\partial t}\right|_{lattice} = 0$$

leads to a useful sum rule

$$\sum_{k} \left.\frac{\partial f_o(\underset{\sim}{k})}{\partial t}\right|_{ph} = - \sum_{k} \left.\frac{\partial f_o(\underset{\sim}{k})}{\partial t}\right|_{rec} \qquad 2.2.2.$$

which may be used as a boundary condition.

In a steady state situation the total rate of photoexcitation W_{ph} equals the total rate of recombination W_{rec}, that is, $W_{ph} = W_{rec} \equiv W$. The shape distribution function becomes independent of the total excitation rate W; and can be conveniently rewritten in terms of a reduced distribution function $\phi(K)$, normalised to unit rate of photoexcitation W [10].

$$\phi(K) \equiv 4\pi\rho \quad \alpha^{-3} \; f_o(K) \; W^{-1} \qquad 2.2.3.$$

where $K^2 = \alpha^2 \; k^2 \equiv \dfrac{\varepsilon(\underset{\sim}{k})}{k_B T} \equiv \dfrac{\hbar^2 \; k^2}{2m_2 k_B T}$ with ρ and T being the density of states in $\underset{\sim}{k}$-space and lattice temperature respectively.

The rate equation becomes

$$\bar{\omega}_{ph}(K) - \frac{\phi(K)\ K}{\tau_{rec}(K)} = K\ J_{lattice}\ (\phi) \qquad 2.2.4.$$

where the reduced rate of photoexcitation is given by

$$\bar{\omega}_{ph}(K) = 4\pi\rho\ \alpha^{-3}\ W^{-1}\ K \left.\frac{\partial f_o(K)}{\partial t}\right|_{ph}$$

Equation 2.2.2 leads the distribution function to satisfy the normalization condition

$$2\int_o^\infty dK \frac{K^2\ \phi(K)}{\tau_{rec}\ (K)} = 1 \qquad 2.2.5.$$

(The factor 2 arises from a summation over spin states) and $\bar{\omega}_{ph}(K)$ becomes also normalised

$$\int_o^\infty \bar{\omega}_{ph}(K)\ dK^2 = 1 \qquad 2.2.6.$$

$J(\phi)$ is the total intraband scattering rate out of state K. This scattering rate is based on acoustic deformation scattering and instantaneous optical phonon emission. The acoustic deformation scattering uses, in the one band model, the one-parameter deformation theory. The detailed form of J for acoustic scattering is discussed in detail in the literature (in particular by Conwell [13] and Barker [14]). For completeness the form of J is given in Appendix 1. As far as acoustic scattering is concerned the numerical calculations involve no approximation in J.

The instantaneous-optical-phonon-emission assumption can be expressed in the following way: carriers with energy in excess of

the optical phonon emission threshold (0.037 e.V) will lose this excess energy by instantaneous emission of one or more optical phonons. This hypothesis seems to be valid because the optical phonon emission process occurs in a time which is much faster than the carrier lifetime and the acoustic relaxation time. Optical phonon emission takes place in about 10^{-12} sec [1], so that after a very short time carriers will all have energies below 37 m.e.V. This automatically reduces the range of integration in J to a maximum energy 37 m.e.V. and the distribution of carriers with energies greater than 0.037 e.V is ignored.

Holes are excited from neutral acceptors in a partially compensated p-type semiconductor. At low temperatures the neutral acceptor concentration N_A^o is given by

$$N_A^o = N_A - N_D$$

where N_A is the density of acceptors and N_D is the total donor density (considered fully ionised). The rate of generation of carriers by a flux of photons incident on neutral acceptors depends on N_A, the photoionization cross-section and the intensity of radiation. The photoionization cross-section is supposed to be constant for all photons with energy greater than the activation energy. Thus the form of the excitation rate is mainly determined by the external source. Fortunately calculations have shown that the distribution function $\phi(K)$ is not critically dependent on the exact form of the radiation spectrum. We then choose for convenience an excitation rate of the form

$$\bar{\omega}_{ph}(K) = C_o K e^{-\nu(K^2-\bar{K}_o^2)^2} \qquad 2.2.7.$$

where the parameter ν defines the bandwidth of the excitation and K_o^2 corresponds to the value of K^2 at which the excitation is maximum. C_o is the normalization constant.

The normalized rate of recombination is characterised by a recombination lifetime $\tau_{rec}(K)$ which varies with carrier energy as follows:

$$\tau_{rec}(K) = \tau_o K^n = [\langle v \rangle \sigma N_D]^{-1} K^n \qquad 2.2.8.$$

recombination to shallow acceptors is assumed to take place via a cascade mechanism of the Lax-type [15] and n=3 is consequently adopted. Measurements of carrier concentration with applied electric field in p-type Germanium doped with deep impurities [16] are consistent with n=1 which will be used when dealing with Cu impurities. $\langle v \rangle$ is the average thermal velocity and σ is the capture cross-section. This latter quantity has been measured for low compensated samples at low temperature. Norton and Levinstein [17] have reported such measurements in Cu-doped Ge and Stannard [17] for shallow acceptors. We assume that their data are also valid for higher compensation densities. Finally, recombination into neutral acceptors is neglected because the cross section associated with this process is very much smaller than σ into ionised impurities and N_A is nearly of the same order of N_D.

2.3. Method of Calculation

The rate equation 2.2.4 is an integral equation for the distribution function ϕ and is solved following an iterative technique due to Hearn [8]. To apply this technique it is better

to rewrite first the rate equation in a more convenient form. Note that KJ(ϕ) represents the balance between scattering in and out of the state K, and can be written as follows:

$$K\,J(\phi) = Z(K)\;\phi(K) - Y(\phi(K)) \qquad 2.3.1.$$

the distribution function is then formally given by

$$\phi(K) = \frac{\bar{\omega}_{ph}(K) + Y(\phi(K))}{\frac{K}{\tau_{rec}(K)} + Z(K)} \qquad 2.3.2.$$

An assumption implicit in the iterative technique is that if $\phi_n(K)$ is an approximated solution for the distribution function after n iterations, then a better approximation $\phi_{n+1}(K)$ is now given by

$$\phi_{n+1}(K) = \frac{\bar{\omega}_{ph}(K) + Y(\phi_n(K))}{K/\tau_{rec}(K) + Z(K)} * N_{n+1} \qquad 2.3.3.$$

where the normalization constant N_{n+1} represents a measure of the convergency of the iterative process. The solution obtained by the iterative technique converges to a physical acceptable solution of the rate equation only when N_{n+1} reaches a steady value equal to 1. The results of numerical calculations indicate that N_{n+1} is an oscillatory function around 1, and in general this parameter converges to 1 at $n \sim 35$ iterations. It is noted however that in the evaluation of a given transport parameter we must go to slightly higher number of iterations, say 50 iterations, to obtain better convergence of that transport parameter. This

criterion is adopted to stop the iterative process. In order to check the validity of this convergency criterion the distribution function ϕ_n (n=N) is input into the rate equation in order to calculate an effective rate of photoexcitation ω^*_{ph}. If ϕ_n is the exact solution of the rate equation then ω^*_{ph} and $\bar{\omega}_{ph}$ (equation 2.2.7) must be equals. The proposed criterion to stop the iterative procedure ensures that the two rates of photoexcitation are very close to each other, that is, the root mean square error is about or less than 1%. A thermal Maxwell-Boltzmann function is used for the starting distribution function ϕ_1. However for a broader spectrum of photoexcitation the Maxwellian distribution function with carrier temperature obtained from the energy balance equation (Chapter III) is used.

In numerical calculations the continuous variable K is replaced by a discrete one which goes from zero to $K_{max} = 220\Delta$, where Δ is the mesh gauge given by

$$\Delta = \frac{1}{6} \left| mS^2 / 2k_B T \right|^{\frac{1}{2}} ,$$

where S is the sound velocity. Δ may be thought of as a small portion of a typical energy transferred in an electron-phonon collision. The integrations are carried out by the use of the Simpson's rule. Computation was carried out on the Burroughs B 6700 computer, University of Warwick.

2.4. Dependence of the Distribution function on the Radiation Bandwidth

It is well known that the phonon wavevector q involved in the emission or absorption of an acoustic phonon takes values going from zero to 2k, where k is the magnitude of the carrier wavevector.

Consequently the acoustic phonon energy is in the range from zero to about $2\hbar kS$ ($= \hbar\omega_{ac}$). This range of energies available for the interacting phonon allows a given carrier state to enter into contact with other states lying within this energy range above and below by emission or absorption of an acoustic phonon. Ridley and Harris [12] have suggested that the distribution function may depend critically on the bandwidth ($\hbar\Delta\omega$). Three cases may occur:

(1) $\Delta\omega << \omega_{ac}$, (2) $\Delta\omega = \omega_{ac}$ and (3) $\Delta\omega >> \omega_{ac}$

The third case corresponds to a very broad spectrum of photo-excitation and resembles a blackbody radiation; and this kind of radiation is used in the next two chapters.

A rough measure of the excitation bandwidth is given by

$$\frac{\hbar\Delta\omega}{k_B T} \sim \sqrt{2/\nu} \qquad 2.4.1.$$

exact for a gaussian spectrum but an approximation in our case. ν is a parameter which enters in the reduced radiation rate (equation 2.2.7). Equation 2.4.1 is then compared with $\frac{\hbar\omega_{ac}}{k_B T}$ and is given by

$$\frac{\hbar\omega_{ac}}{k_B T} = \frac{2\hbar kS}{k_B T} = 4\sqrt{\frac{m_2 S^2}{2k_B T}}\sqrt{\frac{\varepsilon_{ph}}{k_B T}} = 4\, K_A\, K_{ph} \qquad 2.4.2.$$

A very narrow spectrum of photoexcitation gives rise to a series of peaks in the distribution function. These peaks occur at energies equal to and lower than the excitation energy ε_{ph} (<0.037 e.V) The sharpest of these peaks occur at $\varepsilon = \varepsilon_{ph}$, while the others

become increasingly broader as the energy decreases. If the distribution function is drawn against K instead of K^2, it is noted that the peaks occur at equally spaced intervals ΔK. This interval ΔK corresponds to the minimum value in K for an electron to be able to emit an acoustic phonon (equal to KA, equation 2.4.2). The same interval appears in the expression for the total acoustic scattering rate out of state K. This is because the carrier state K is in contact with states lying in the range from K to K + KA (K-KA) by the absorption (emission) of acoustic phonons. The peaks in the distribution function gradually disappear as the spectrum bandwidth is increased to values of the same order of ω_{ac}. In other words, this occurs when the bandwidth of the excitation spectrum is greater than the interval ΔK. All these factors suggest that the appearance of the peaks in the distribution function is related to the ability of the newly excited carriers to emit one or more acoustic phonons, with wavevectors equal to ΔK, immediately after the excitation. This condition occurs when the radiation spectrum is very narrow and the probability of scattering out of state K_{ph} by emission of an acoustic phonon is much greater than the scattering in by absorption of acoustic phonons. The increase in the radiation spectrum bandwidth implies that both processes are comparable. Therefore the presence of the peaks disappear.

For acoustic relaxation times much smaller than the carrier lifetime, the distribution function is nearly a thermalised Maxwellian function. At lower values of the recombination lifetime the form of the distribution function is more complicated. This will be discussed further later in this chapter. It is noted that the form of the distribution function is not critically dependent on the

energy dependence of the recombination lifetime. Figures 2.1, 2.2 and 2.3 compare the form of the distribution function for two values of the parameter ν and three compensation densities at $4^{o}K$. A list of the data used in these calculations appears in Table 2.1.

2.5. LOW FIELD TRANSPORT

The trapping and low field transport parameters will be averaged over the isotropic zero-field distribution function $\phi(K)$, in a similar fashion to conventional transport perturbation in which $\phi(K)$ replaces the average thermal equilibrium function [18]. This approach is justified if the response to the external electric fields is ohmic. For Cu-doped Ge the critical field is around 5 V/cm [16]. In order to evaluate the mobility at a given temperature, the energy dependence of the scattering process must be averaged over the distribution function $\phi(K)$. To this end the total momentum relaxation time must be obtained as the harmonic sum of all scattering times and averaged over $\phi(K)$ to give the mobility. Three scattering mechanisms are considered. The acoustic deformation -, ionised and neutral-impurity-scattering. At very low temperatures the optical scattering is neglegible and therefore ignored. The acoustic deformation scattering is based on the theory of Bir, Normantas and Pikus [19] which includes inter- and intra-band transitions and uses two deformation parameters. Bir et.al [19] have given the expressions to relate these two parameters with those of the more general three-parameter theory [20] and Lawaetz [21] has found a relationship to connect these three deformation potentials

with the parameter of the one-deformation theory. This relationship arises from a study of the low-field mobility and galvanomagnetic data for holes in Ge at high temperatures. We assume that identical formula is valid at low temperatures. The relationship is given by

$$D^2 = a^2 + \frac{C_\ell}{C_t}\left(b^2 + \frac{1}{2}d^2\right) \qquad 2.5.1.$$

where D is the deformation potential in the one-parameter theory. a, b and d are the three deformation potentials in the more general theory. C_ℓ and C_t are the average longitudinal and transverse elastic constants for an isotropic phonon spectrum [22],

$$C_\ell = \frac{1}{5}\left(3\,C_{11} + 2\,C_{12} + 4\,C_{44}\right)$$
$$C_t = \frac{1}{5}\left(C_{11} - C_{12} + 3\,C_{44}\right) \qquad 2.5.2.$$

We adopted for the shear deformation potentials b and d the following values: b = -2.2 eV and d = -4.5 eV [23] which implies $\bar{b}$ = -2.4 eV (the shear deformation potential in the two-parameter theory [19]). The deformation potential a, which characterises the shift in the valence band under hydrostatic pressure, has a very uncertain value in spite of several attempts to deduce a value from conventional low-field transport measurements [21]. It is therefore retained as a fitting parameter. The present status of the three deformation potentials parameters will be discussed in Chapter IV

The ionised impurity scattering time uses the Brooks-Herring-Dingle formula [24]. We have assumed that the singly ionised Cu-impurity has the scattering potential as a singly ionised shallow acceptor or donor. This is reasonable because most of

the contribution to the scattering cross-section comes from large values of the impact parameter, that is, at considerable distance from the core potential. At large distances the potentials are nearly identical. This is seen by the fact that the spacing in excited-state-energy spectrum of Cu and shallow impurities are in agreement [25,26]

The neutral scattering time is calculated from a modified version of the Erginsoy formula [27] (which is only valid for hydrogenic impurities). The new formula is obtained by multiplying the Erginsoy expression by a constant factor A. Norton and Levinstein [28] have applied, with success, all these scattering mechanisms to describe the mobility in a series of non-illuminated Cu-doped Ge, and derived experimentally the non-hydrogenic multiplicity factor A for the neutral impurity scattering time. Details of the scattering mechanisms are given in Appendix 2, and a different expression for the neutral impurity scattering time is studied in Chapter V. This new expression gives values for the neutral impurity scattering time which are in agreement with those obtained by the use of the modified Erginsoy formula.

In order to calculate the mobility the heavy - and light-hole distribution functions are needed. However the rate equation 2.2.3, in the one band model, gives the heavy-hole distribution function $\phi_2(K)$ only, the light hole $\phi_1(K)$ one is then obtained by multiplying $\phi_2(K)$ by an appropriate density of states factor

$$\phi_1(K) = \left(\frac{m_1}{m_2}\right)^{3/2} \phi_2(K) \qquad 2.5.3.$$

where m_1 is the light hole effective mass. Mobility is then given by

$$\mu = -\frac{1}{3}(1+\gamma^3)^{-1}\left[\gamma^3 \langle C_{11}\rangle + \langle C_{22}\rangle\right] \qquad 2.5.4.$$

where

$$\gamma^2 = \frac{m_1}{m_2}$$

$$\langle C_{ii}\rangle = \int K^3 \frac{\partial \phi_i(K)}{\partial K} C_{ii}(K)\, dK$$

$$C_{11} = \frac{e\,\tau_{11}}{m_1\delta}\left(1+\gamma^2\frac{\tau_{22}}{\tau_{12}}\right)$$

$$C_{22} = \frac{e\,\tau_{22}}{m_1\delta}\left(1+\gamma^3\frac{\tau_{11}}{\tau_{12}}\right)$$

$$\delta = \left(1-\frac{\tau_{11}\,\tau_{22}}{\tau_{12}\,\tau_{21}}\right)$$

τ_{ii} is the total momentum relaxation time (i=j intraband transition, $i \neq j$ interband transitions, i = 1(2) corresponding to the light (heavy) hole band). A more general expression for the mobility which is valid for the two-band model is discussed in Appendix 2. The following average

$$\langle X\rangle = \frac{\int X\,\phi_2(K)\,K\,dK^2}{\int \phi_2(K)\,K\,dK^2} \qquad 2.5.5.$$

is used to obtain the average carrier energy ($X \equiv \varepsilon$), carrier lifetime ($X \equiv {}^1/\tau_{rec}$), etc.

2.6. DEPENDENCE OF THE DISTRIBUTION FUNCTION ON LIFETIME AND ε_{ph}

The distribution function depends on the lifetime, although results are not significantly affected by changes in the energy dependence of the lifetime. However the distribution function suffer important changes when the compensation density is increased. Thus for low N_D the distribution function is essentially the Maxwell-Boltzmann function (Figure 2.1). At higher compensation densities the form of the distribution function depends also on the value of the excitation energy. Thus for carrier lifetimes equal to or lower than the energy relaxation time and low values of ε_{ph} ($\sim$ 7 m.e.V), the distribution function is non-Maxwellian in form. In this case $\phi(K)$ is mainly determined by the competition between the excitation and the recombination rates, and reflects their forms. The distribution function rapidly reaches a maximum and then decreases equally rapidly. On the other hand, at greater values of ε_{ph} ($\sim$ 30 m.eV) and $\hbar \Delta\omega \sim \hbar \omega_{ac}$ the distribution function is to a first approximation a Maxwellian function with a carrier temperature much greater than T. The distribution function for this case is determined by the competition between excitation and the scattering rates. In all cases the form of the distribution function of energies greater than ε_{ph} is nearly a thermal Maxwellian function. Figures 2.4, 2.5 and 2.6 show the variation in the form of the distribution with ε_{ph} for a heavily compensated sample.

2.7. TRANSPORT AND TRAPPING PROPERTIES

The carrier lifetime can become comparable with the energy relaxation time in Ge at low temperatures. Under this condition photocarrier properties are expected to depend on the radiation

energy. Godik [5] has reported an experimental study of this kind in Cu-doped Ge at low temperature. In this study the low field photohall mobility of photoexcited holes is measured as a function of the photon energy. The model already developed is applied to this experimental study.

In the experiments of Godik [5] the applied electric field is 5 v/cm and is on the edge of the onset of non-ohmic behaviour; consequently the carriers receive neglegible amounts of energy from the field. Furthermore the Hall number is assigned the value r=1 corresponding to high magnetic fields (the classical limit). The sample under consideration is characterised by

$$N_A \text{ (Cu-impurities)} = 2 \times 10^{15} \text{ cm}^{-3}$$

$$N_D \text{ (Sb-impurities)} = 2 \times 10^{14} \text{ cm}^{-3}$$

and the measurements were done at T = 5^{O}K and 11^{O}K (one sample with Cu and compensation densities of 2×10^{16} and 1.6×10^{13} cm^{-3} respectively is not considered because it has been found [1] impurity conduction effects at such densities). In thermal conditions the mobility, in this sample, is dominated by ionised impurity scattering. However when illumination is applied to the sample, acoustic scattering plays a moderate role in the determination of the mobility. This scattering uses two deformation potentials (Section 2.5). One of which, the deformation parameter a is left as a fitting parameter. It is found that only one value is needed for the deformation parameter a in order to obtain good agreement with the experimental mobility data [5] as function of the excitation energy and at a given temperature. It is noted, however, that the calculated mobility remains nearly

constant at $\varepsilon_{ph} < 15$ meV. This is in disagreement with the experimental data which shows a reduction in the mobility as a consequence of dominant ionised impurity scattering. The disagreement may be caused by a recombination lifetime expression which needs modification. In Chapter V a model is proposed for the lifetime in order to give an explanation of this disagreement.

Calculation at two lattice temperatures give two values for the deformation potential a:

$$a = 18 \text{ eV at } 5^{o}K \quad \text{and} \quad a = 13 \text{ eV at } 11^{o}K.$$

It is found that the average carrier energy is nearly independent of the lattice temperature and is an increasing function of ε_{ph}. Its absolute values are much greater than the thermal energy. The average lifetime is nearly independent on ε_{ph} but has a stronger dependence on T. Table 2.2. presents a summary of these calculations.

2.8. CONCLUSIONS

A narrow spectrum of photoexcitation produces a distribution function which exhibits a series of equally spaced peaks at carriers wavevectors equal to and less than the photoexcitation wavevector K_{ph}. This regular spacing between peaks is related to the range of hole states which are in contact with a given carrier state K by the emission and absorption of acoustic phonons. It is also noted that the wavevector ΔK between peaks corresponds to the minimum momentum that a carrier should have in order to

emit an acoustic phonon. This suggests that the distribution function at K_{ph}, which is strongly peaked because of carriers being photoexcited into that state, will decay into the state K_{ph}-K A by emission of acoustic phonons with wavevector equal to the acoustic phonon threshold momentum. Similarly the distribution $\phi(K_{ph}$-K A) will decay at lower wavevectors values by an identical procedure. This process of generation of peaks in the distribution function resembles the similar effect caused by the emission of optical phonons with quantum energies equal to the optical threshold energy [12, 29]. The presence of equally spaced peaks in the distribution function, caused by the emission of acoustic phonons with wavevectors equal to the acoustic phonon threshold momentum, has not previously been seen.

It is found that the distribution function for pure samples is essentially a thermal Maxwellian function. The recombination lifetime for these samples is much greater than the acoustic relaxation time. Therefore holes have enough time to lose much of the energy excess received from the external source and come to a nearly thermal equilibrium with the lattice. On increasing the compensation density the recombination lifetime is reduced and holes will then have less time to lose their excess energy. Therefore the possibility of reaching thermal equilibrium with the lattice becomes increasingly remote. This effect is clearly reflected in the departure of the distribution function from the Maxwell-Boltzmann function as the compensation increases. However the form of the distribution function depends also on the photoexcitation energy. Thus for lifetimes of the order of $\tau_{ac}(k_B T)$

and low values of ε_{ph} the distribution function is non-Maxwellian. This is a consequence of the competition between the excitation and recombination rates. At higher values of ε_{ph} the distribution function resembles a Maxwellian function with a temperature parameter much greater than T. This form arises from the competition between the lattice scattering and the photoexcitation rates. The possibility of obtaining a Maxwellian function from laser-photoexcitation has not previously been considered.

The large values found for the average hole energy and its nearly independence on the lattice temperature suggest a strong carrier heating in the sample studied (Godik [6]). This result is consistent with the fact that the average carrier lifetime is of the same order of the acoustic energy relaxation time. Although the model of semiconductor is based on a parabolic heavy hole band, satisfactory agreement with the experimental mobility at a given temperature and various ε_{ph} is obtained. It is noted, however, that the deformation potential (which gives the inelastic scattering, in the one-deformation theory) changes with temperature when attempts are made to fit the experimental and calculated mobilities at two lattice temperatures. The values found for this parameter are about three times as large as those obtained from thermalised mobility calculations based on the one-parameter deformation theory of elastic scattering. These large values for the deformation potential may be a consequence either of unknown factors affecting the experiments or of weaknesses in the theory. It is possible that the deformation potential is forced to have large values in order to compensate any deficiency in the scattering mechanisms. In particular the conventional theory of acoustic lattice scattering uses only one-phonon processes. Evidence which supports the idea

of including two-acoustic phonon process will be discussed in Chapter V. In the same chapter is reported an attempt to explain the disagreement between experimental and calculated mobilities at radiation energies $\varepsilon_{ph} < 15$ m.eV. To this end a model is proposed for the recombination lifetime which removes the difficulty.

elastic constants ($77^{o}K$)	
C_{11} dyn/cm^2	1.2×10^{12}
C_{12} "	0.49×10^{12}
C_{44} "	0.68×10^{12}
Erginsoy's multiplicity factor (A)	4
mass density ρ (gr/cm^3)	5.323
average sound velocity (cm/sec)	
longitudinal (S_L)	5.36×10^{5}
transverse (S_T)	3.28×10^{5}
electron free mass m_e (Kgr)	9.11×10^{-31}
Effective mass	
heavy hole	$.33\ m_e$
light hole	$.045\ m_e$
capture cross-section (cm^2)	
shallow impurities ($4^{o}K$)	1.95×10^{-11}
Cu impurities ($5^{o}K$)	1.5×10^{-11}
" " ($11^{o}K$)	5.3×10^{-12}
sample S_1	
N_A cm^{-3}	2.7×10^{13}
N_D "	1.9×10^{11}
sample S_2	
N_A cm^{-3}	2.2×10^{15}
N_D "	1.7×10^{13}
sample S_3	
N_A cm^{-3}	3.0×10^{15}
N_D "	2.2×10^{14}

TABLE 2.1: Data for numerical calculations

elastic constants ($77^{o}K$)	
C_{11} dyn/cm^2	1.2×10^{12}
C_{12} "	0.49×10^{12}
C_{44} "	0.68×10^{12}
Erginsoy's multiplicity factor (A)	4
mass density ρ (gr/cm^3)	5.323
average sound velocity (cm/sec)	
longitudinal (S_L)	5.36×10^{5}
transverse (S_T)	3.28×10^{5}
electron free mass m_e (Kgr)	9.11×10^{-31}
Effective mass	
heavy hole	$.33\ m_e$
light hole	$.045\ m_e$
capture cross-section (cm^2)	
shallow impurities ($4^{o}K$)	1.95×10^{-11}
Cu impurities ($5^{o}K$)	1.5×10^{-11}
" " ($11^{o}K$)	5.3×10^{-12}
sample S_1	
N_A cm^{-3}	2.7×10^{13}
N_D "	1.9×10^{11}
sample S_2	
N_A cm^{-3}	2.2×10^{15}
N_D "	1.7×10^{13}
sample S_3	
N_A cm^{-3}	3.0×10^{15}
N_D "	2.2×10^{14}

TABLE 2.1: Data for numerical calculations

Lattice Temperature ^{o}K	Excitation Energy ϵ_{ph} (m.e.V)	Average Energy $k_B T$ units	Effective Carrier Temperature ^{o}K	Average Lifetime 10^{-10} sec
	15	9.2	46.0	2.95
5	20	10.14	51.0	3.08
	35	14.42	72.0	3.22
	15	5.0	54.8	4.0
11	20	5.3	58.2	4.1
	30	6.0	66.0	4.4
	35	6.3	69.0	4.0

TABLE 2.2. Summary of transport and trapping calculations

$$\langle \tau_{ac} \rangle_{11^{o}K} = 1.062 \times 10^{-10} \text{ sec.}$$

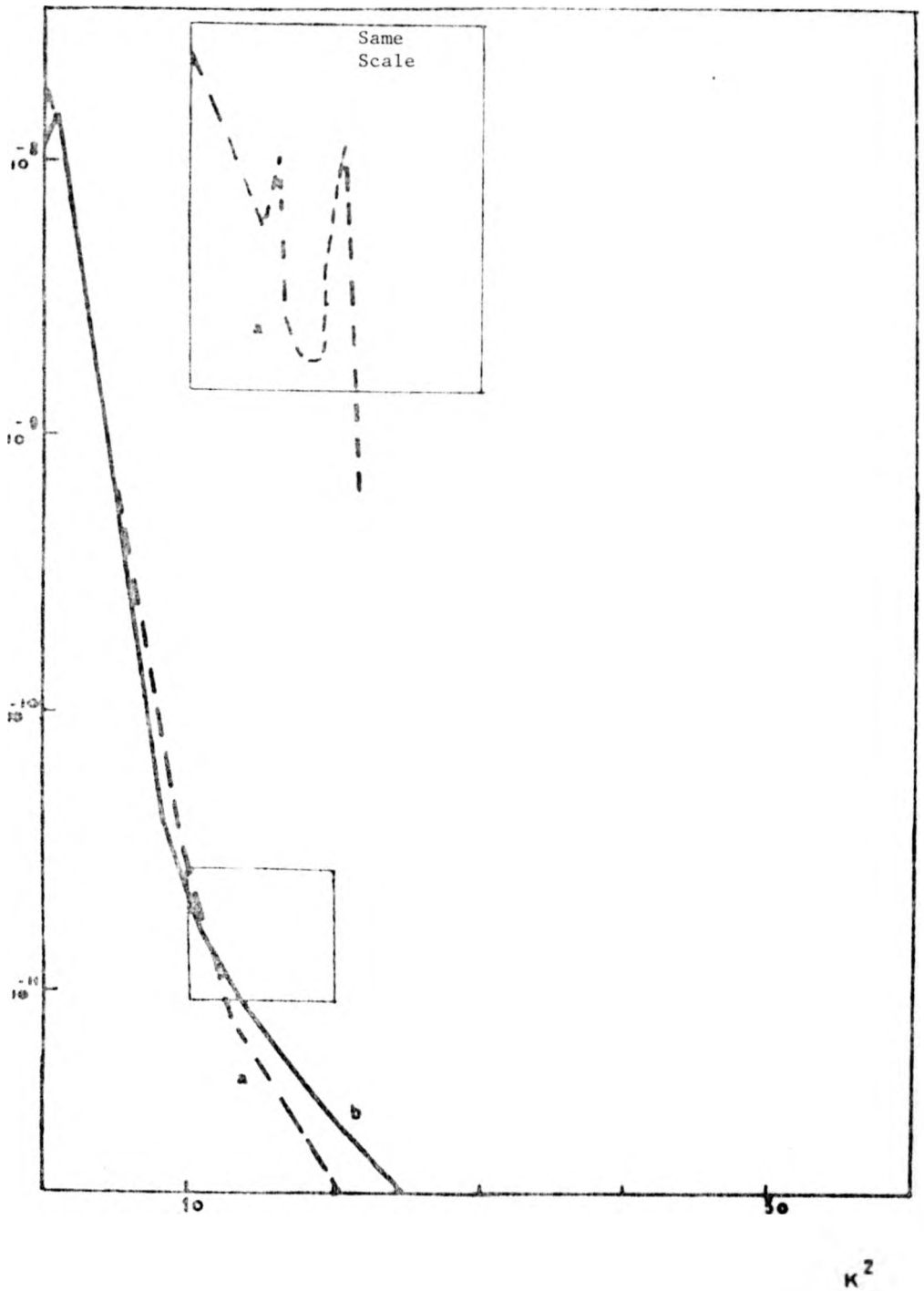

FIGURE 2.1: Comparison of the distribution function for two values of the bandwidth parameter ν in sample S_1 at $4^{o}K$. The broken line corresponds to $\nu=2$ and the continuous line to $\nu=.001$. The excitation energy is $\varepsilon_{ph}= 7meV$.

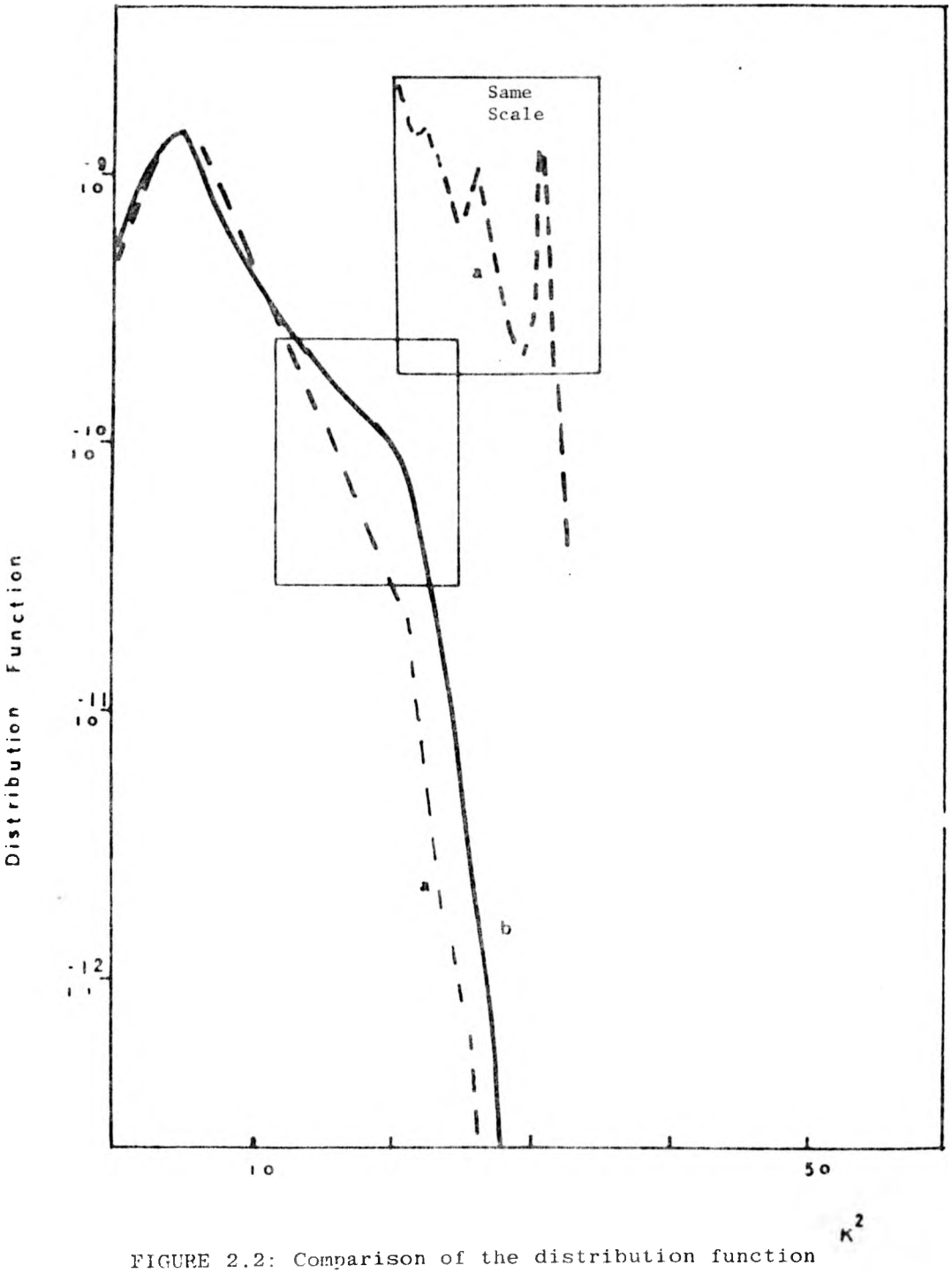

FIGURE 2.2: Comparison of the distribution function for two values of the bandwidth parameter ν in sample S_2 at $4^{O}K$. The broken line corresponds to $\nu=2$ and the continuous line to $\nu=.1$ ε_{ph} = 7 meV.

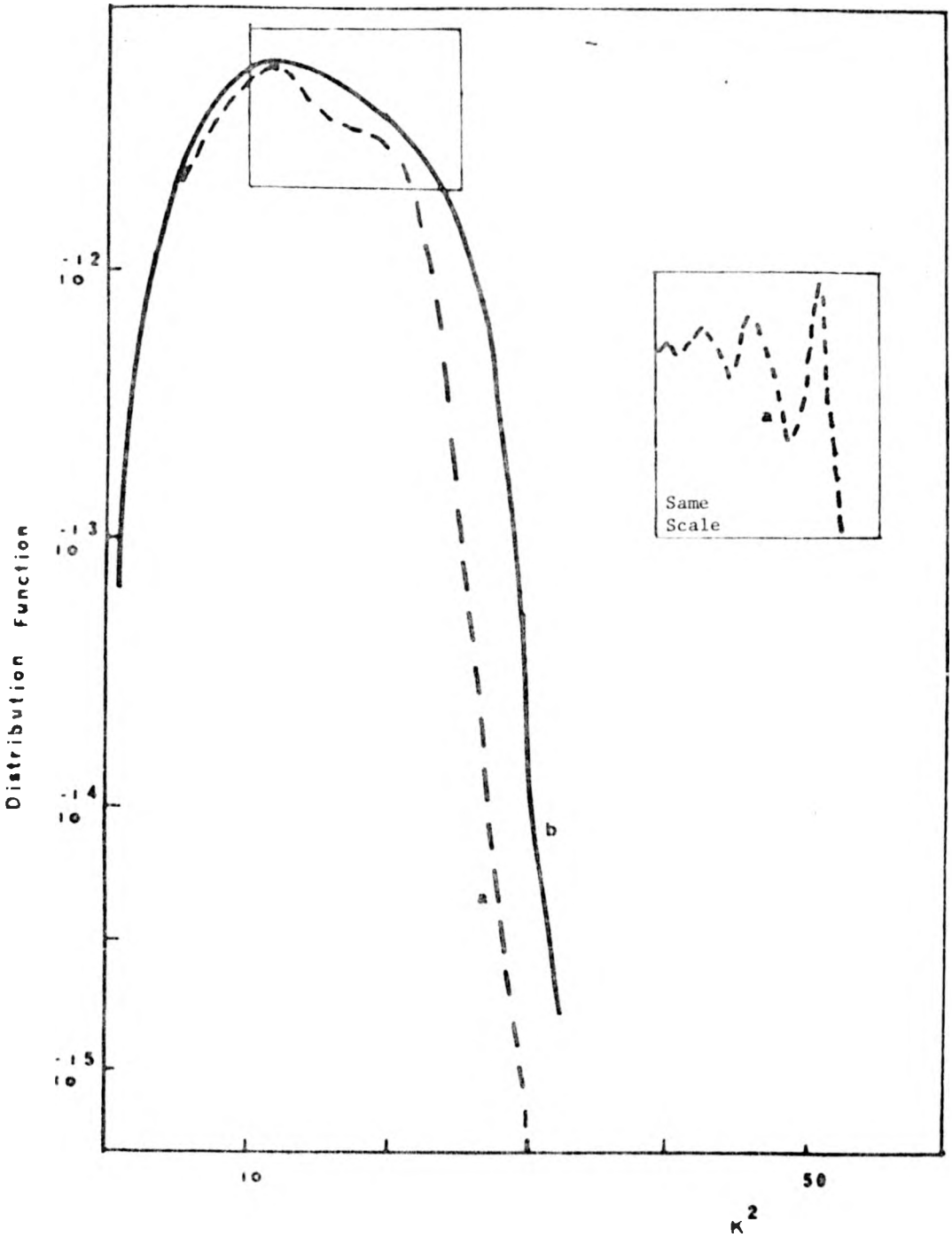

FIGURE 2.3: Comparison of the distribution function for two values of the bandwidth parameter ν in sample S_3 of $4^{O}K$. The broken line corresponds to $\nu=1$ and the continuous line $\nu=0.05$, $\varepsilon_{ph} = 7$ meV.

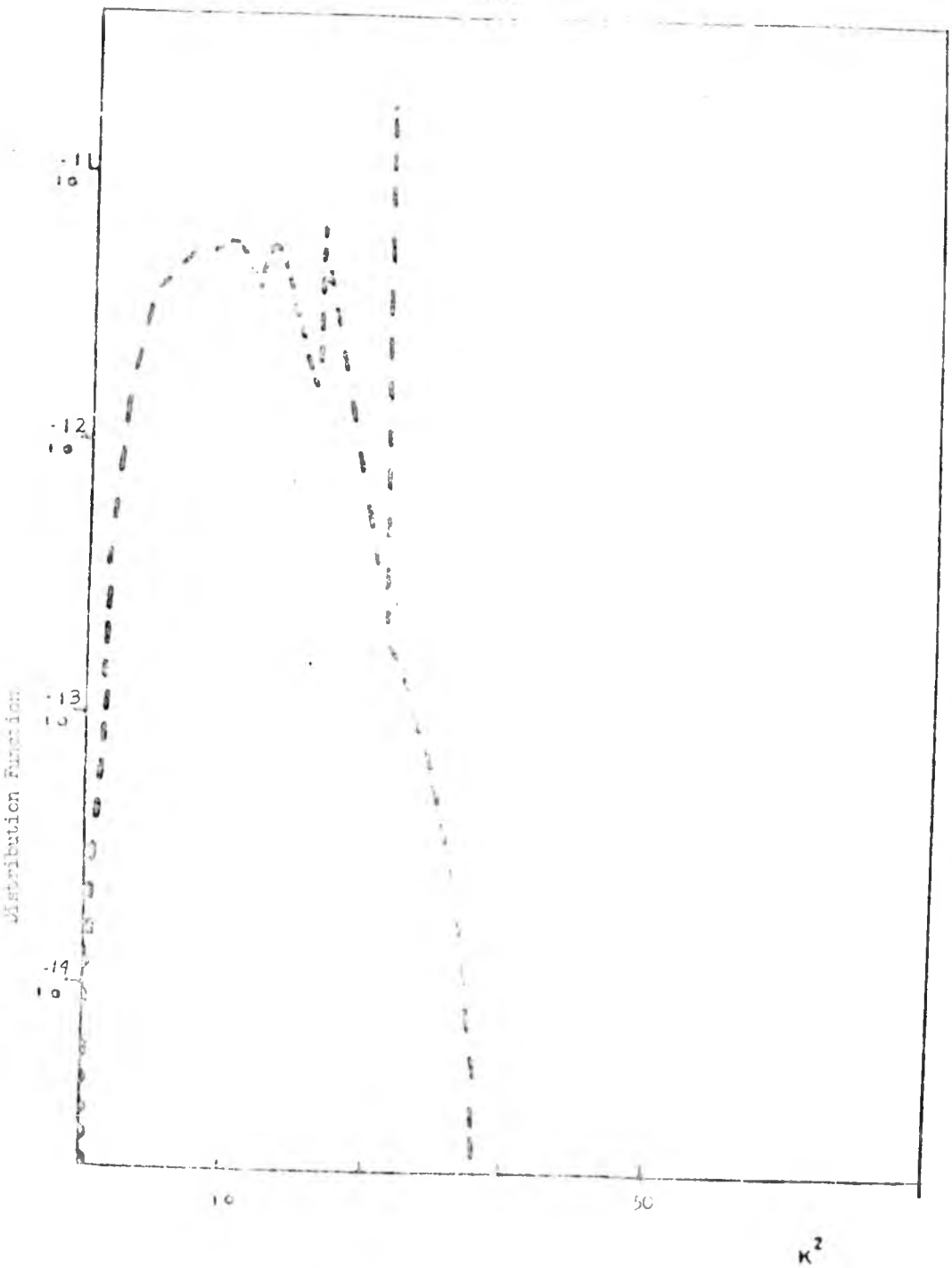

FIGURE 2.4: The distribution function for sample S_3 at $4^{\circ}K$ and $\epsilon_{ph} = 7$ meV. The value of bandwidth parameter is $\nu=2$.

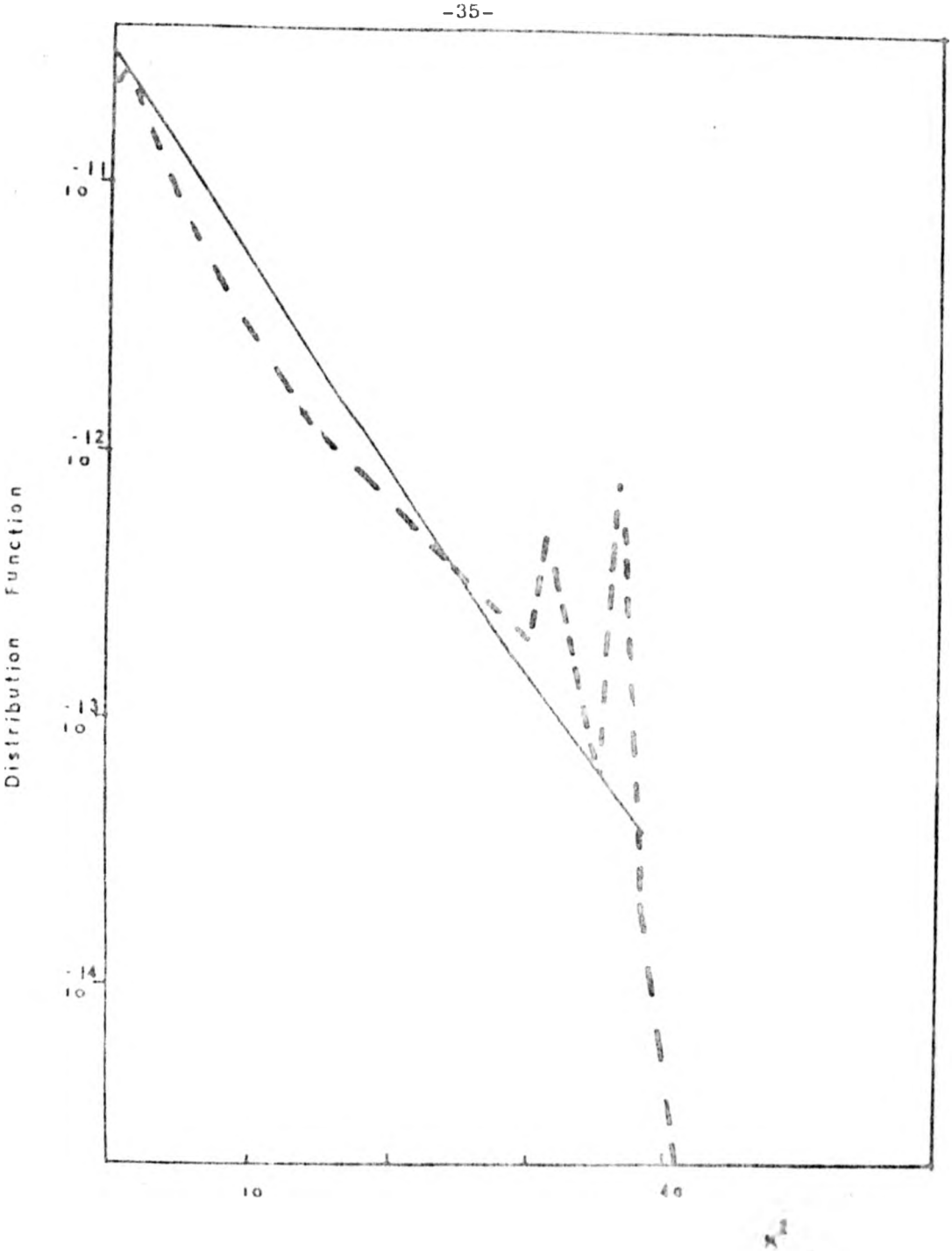

FIGURE 2.5: The distribution function for sample S_3 at $4^{O}K$, ϵ_{ph} = 15 meV and ν = 2.

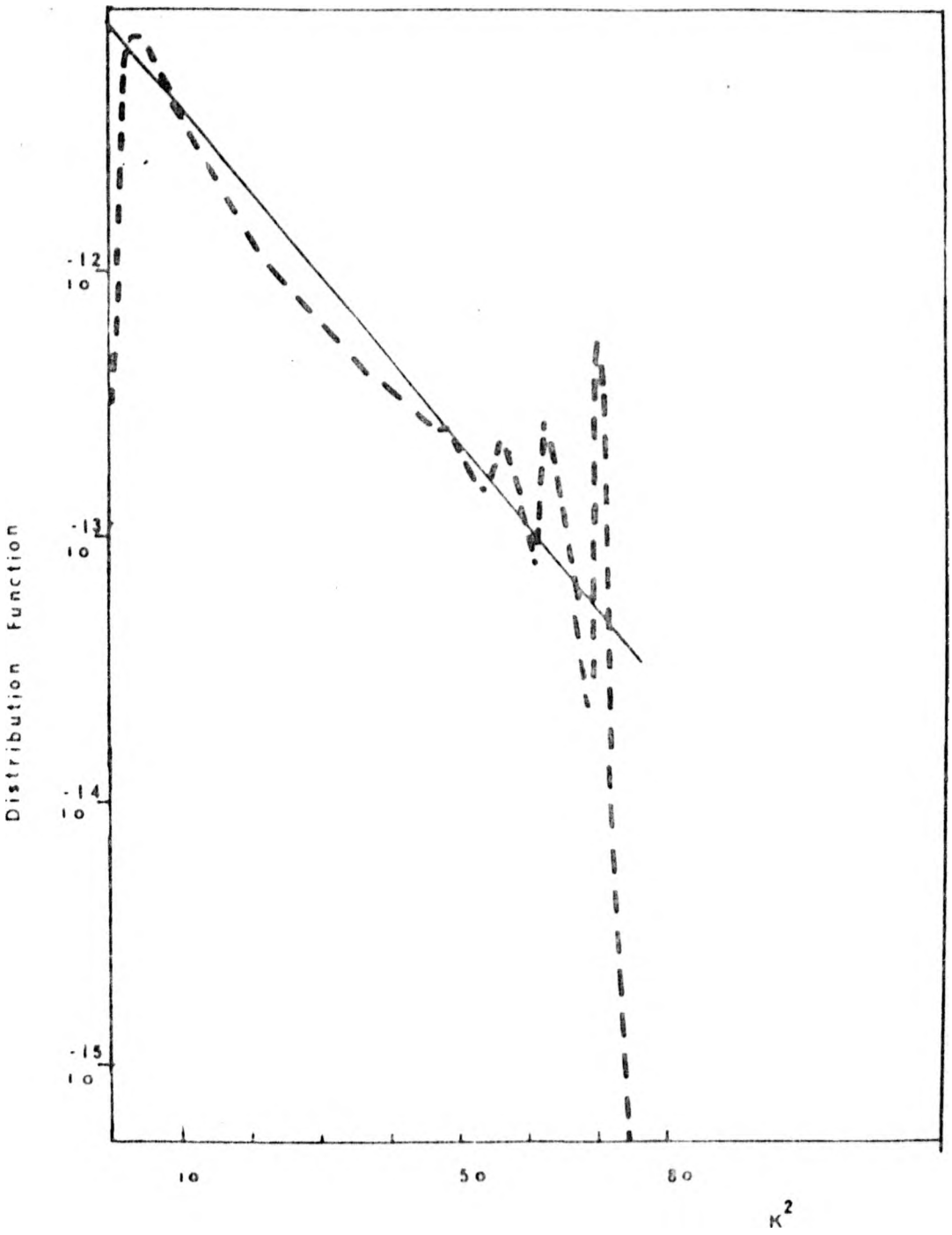

FIGURE 2.6: The distribution function for sample S_3 at $4^{O}K$, ε_{ph} = 30 meV and ν = 2.

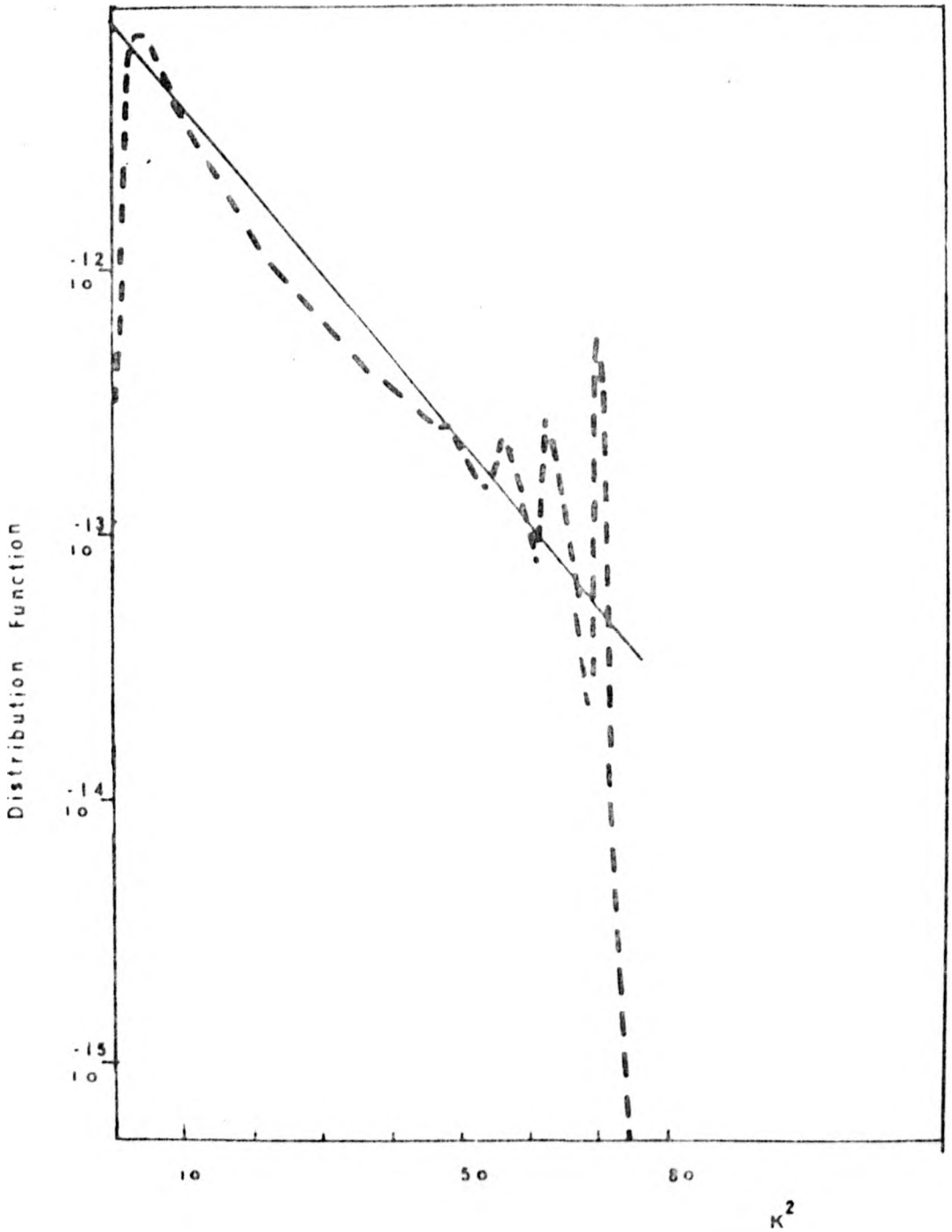

FIGURE 2.6: The distribution function for sample S_3 at $4^{o}K$, ε_{ph} = 30 meV and ν = 2.

CHAPTER III

THE ENERGY DISTRIBUTION FUNCTION OF PHOTOEXCITED HOLES IN P-TYPE GE ROOM TEMPERATURE BLACKBODY RADIATION

In this chapter we continue the study of the physics of photoexcited holes in the valence band of a simple model of semiconductor. In contrast with previous chapter holes are generated by a broad spectrum of photoexcitation of an approximately blackbody radiation at room temperature. The distribution function is derived from a rate equation involving photoexcitation, recombiantion and lattice scattering. The distribution function is compared with a Maxwellian distribution function with the carrier temperature parameter evaluated from an energy balance equation. Details of the model of photoexcitation rate and the energy balance equation are given in Section 3.2. Section 3.3. compares the distribution function obtained from both procedures for various donor compensations densities. The energy distribution function, for compensation densities lower than about 10^{13} cm^{-3}, is essentially a Maxwellian function with the carrier temperature calculated from the energy balance equation. At higher compensation densities the distribution function is non-Maxwellian over most of the range of energies available.

Photohall measurements by Norton and Levinstein [1] and Godik [5] at low temperatures, suggest that hot holes occur for compensation densities greater than about 10^{13} cm^{-3}. The average hole lifetime is, in such samples, shorter than the hole-lattice energy relaxation time ($\tau_{ac}(K_BT)$). Samples with densities near 10^{13} cm^{-3} seem to involve a carrier lifetime which is of the same

order as the energy relaxation time and warm carriers are observed [1]. In the experiments of Norton and Levinstein [1] holes were photoexcited by room temperature black-body radiation and so have initial energies much greater than the thermal energy (k_BT).

This report presents a theoretical study of the transport and trapping parameters of photoexcited carriers in Cu-doped Ge. These parameters are averaged over the isotropic distribution function occurring in the absence of an electric field. This work has direct relevance to the experimental measurements by Norton and Levinstein [1] of the mobility and carrier lifetime at low temperatures of a series of Cu-doped Ge samples with various compensating donor densities. The physical model gives good agreement with experimental data for samples with compensation densities less than or equal to 10^{13} cm^{-3}. At higher compensation densities valuable results are obtained.

3.2. THEORY

A simple parabolic band structure characterized by the heavy-hole effective mass m_2 is assumed. The isotropic nature of the radiation and the rapid momentum relaxation ensure that the zero-field distribution function $\phi(K)$ is dependent on the energy only. Effects of degeneracy, inter-carrier scattering and non-equilibrium of phonons are ignored. Furthermore, there is no effective change in the occupancy of the impurity levels. Thus the carrier distribution function, normalised to unit rate of photoexcitation, obeys a linear integral equation (Equation 2.2.4)

$$\bar{\omega}_{ph}(K) - \frac{\phi(K)\ K}{\tau_{rec}(K)} = J(\phi)$$

Where the recombination lifetime (τ_{rec}) has an energy dependence given by Equation 2.2.8 with n = 1. The capture cross section has been measured for a few low compensated samples by Norton and Levinstein [1] and the validity of these values is extended to all samples considered in this report. J represents the total intraband scattering rate out of state K. This involves the use of one-parameter deformation theory and that parameter is assigned the value 10 eV [1]. This implies that the deformation potential parameter denoted by a is equal to 8.2 eV (Equation 2.5.1). Incidentially Norton and Levinstein [28] have obtained a good fit of their experimental dark mobilities by assigning that value for the deformation potential a. The mathematical expression for J is given in Appendix 1.

The normalised rate of photoexcitation ($\bar{\omega}_{ph}$) produced by a flux of photons incident on the neutral acceptors is proportional to the concentration of neutral impurities, the photoexcitation cross-section and the intensity of radiation. This rate is poorly known experimentally. Barker and Hearn [10] and Barker [14] have proposed a model for $\bar{\omega}_{ph}$ based on a radiation field which approximates to blackbody radiation with temperature radiation Tr. (for a brief summary of the derivation of the expression for $\bar{\omega}_{ph}$ see Appendix 3).

$$\bar{\omega}_{ph}(K) \propto K^{2\ell+1} \exp(-K^2 T/Tr) \qquad 3.2.1.$$

where ℓ is a parameter determined by the matrix elements for the electron-photon interaction and the corresponding selection rules for the transition probabilities. A high frequency cut-off is incorporated to eliminate photoexcitation into the split-off band and second ionization of Cu-impurities. Our calculations have shown that the transport parameters do not depend critically on the value chosen for ℓ. Intrinsic blackbody radiation from the lattice is neglected as $k_B T$ ($\sim$ 0.0025 e.V) is much lower than $k_B Tr$ ($\sim$ 0.025 e.V)

Photoionization of neutral impurities requires a minimum photon energy of 42.86 m.eV. The average photon-energy from room temperature radiation is of the order of 100 m.eV. Thus the average carrier energy is about 60 m.eV immediately after the excitation. Since optical phonon emission takes place in about 10^{-12} sec, carriers will then emit one or more optical phonons until their average energy is less than the optical-phonon emission energy ε_{op} ($\sim$ 0.037 eV). We then assume that all carriers will have energies less than ε_{op} in a time very much smaller than any other physical time. This instantaneous optical emission generates an effective rate of photoexcitation of the form (details in Appendix 3)

$$\bar{\omega}_{ph}(K) \propto K \exp\left(-K^2 \frac{T}{Tr}\right) \left[\sum_{n=0}^{5} \left(K+n\sqrt{\frac{430}{Tr}}\right)^{2\ell} \exp\left(-n \frac{430}{Tr}\right)\right] \qquad 3.2.2.$$

$$K^2 = \frac{\varepsilon}{k_B T} \leq \frac{0.037}{k_B T}$$

We have included in this equation the fact that photon energies greater than 0.23 eV have been removed from the excitation spectrum, and n = 5 is the maximum number of optical phonons contained in that energy range. The radiation temperature Tr is equal to $300^{O}K$.

Instead of solving the rate equation, information about the distribution function and transport parameters can be obtained from "The Moment Balance Method". This method is a set of "moment balance equations" obtained by integration of some moment functions over the rate equation [30]. If the distribution function is assumed to have a fixed shape with a number of adjustable parameters equal to the number of moment balance equations, then the parameters may be determined through the condition of self consistency of the equations. Conservation of carriers, momentum and energy are among the moment balance equations. In this report only that energy balance equation which gives the carrier temperature (Te) in a Maxwellian carrier distribution function truncated at the optical phonon emission threshold is set up. The energy balance equation appropriate to our model is derived by multiplying Equation 2.2.4 by the carrier energy ϵ and summing over the band.

$$\sum_{\substack{K \\ \text{band}}} \epsilon\, \bar{\omega}_{ph}(K) - \sum_{\substack{K \\ \text{band}}} \epsilon\, \frac{\phi(K)\, K}{\tau_{rec}(K)} = \sum_{\substack{K \\ \text{band}}} \epsilon\, J(\phi) \qquad 3.2.3.$$

In (3.2.3) $W\Sigma\, \epsilon\, \bar{\omega}_{ph}(K)$ is the total rate of energy input into the band by external radiation measured relative to the bottom of the band, $W\Sigma\, \epsilon\, \frac{\phi(K)K}{\tau_{rec}(K)}$ is the total rate of energy loss relative to

bottom of the band due to recombination and - $W\Sigma \epsilon J(\phi)$ is the net rate of energy loss to the lattice due to either phonon emission or absorption. Details corresponding to the expressions for each one of these rates are given in Appendix 4. The polynomial equation (in Te) 3.2.3 is then solved by a standard iterative technique which gives the real root of that polynomial.

3.3. DISTRIBUTION FUNCTION

The distribution function has been obtained for five Cu-doped Ge samples at various compensation densities. The method of calculation has been described in Section 2.3. A list of the relevant data concerning such samples appears in Table 3.1. The compensation density goes from 10^{11} cm^{-3} to 10^{14} cm^{-3}, that is, the carrier lifetime is varied over three orders of magnitude. This change in the lifetime is consequently reflected in the form of the distribution function. Thus for our purest sample S_1 (and S_2), the lifetime is of the order of 10^{-7} (10^{-8}) sec and the distribution function shows a Maxwellian form with the carrier temperature calculated from the energy balance equation. However for lifetime of the order of 10^{-9} sec (sample S_3), which is comparable with the acoustic energy relaxation time τ_{ac} (k_BT), the distribution function deviates from a Maxwellian form for most of the range of energies available. Finally, for even lower values of τ_{rec}, the distribution function is non-Maxwellian throughout the whole range of energies. Figures 3.1, 3.2 and 3.3 present an illustration of the distribution function at three compensation densities.

3.4. TRANSPORT AND TRAPPING PARAMETERS

Solution of the rate equation gives mobilities which are very similar to those of the Maxwellian approximation; both sets are in good agreement with the experimental data of Norton and Levinstein [1] for the three low compensated samples. However, the Maxwellian mobility of sample S_3 is slightly higher than experimental data. This is because the distribution function for this sample, and for the more heavily compensated samples, is non-Maxwellian over most of the energy range. For the two heavily compensated samples S_4, S_5 both calculated mobilities are nearly identical and about 25% greater than the corresponding experimental values.

Numerical solutions of the energy balance equation 3.2.3. give the carrier temperature for a Maxwellian distribution function. The main features of the calculated carrier temperature (Te) are:

(i) at low compensation density, Te is very close to and strongly dependent on the lattice temperature. Carriers are nearly in thermal equilibrium as the distribtuion function is essentially a Maxwellian,

(ii) at intermediate compensation densities (sample S_3), the absolute value of Te has greatly increased while its temperature dependence has diminished. Carriers are warm,

(iii) finally for the heavily compensated samples S_4 and S_5, the absolute value of Te is very much greater than T and its dependence on the same parameter has nearly disappeared. This suggests that carriers are hot.

Table 3.2 summarises the mobility and carrier temperature calculations.

The ratio of the acoustic energy relaxation time to the carrier lifetime when $\varepsilon = k_B T$ replaces the carriers energy, gives a better characterization of the degree of carrier heating in the system. The average lifetime and acoustic relaxation time together give a ratio which although is satisfactory for the two low compensated samples (S_1, S_2) is rather small for those samples (S_3, S_4, S_5) with intermediate and heavy compensation densities. Carriers are in these cases warm and hot respectively.

A mild temperature dependence is seen for the average lifetime in the two heavily compensated samples (S_4, S_5). This dependence is in the range of $T^{.2}$ to $T^{.3}$. This temperature dependence is in close agreement with the behaviour of the experimental photocarrier density in sample S_4 as taken from photohall data [1]. However the same temperature dependence for sample S_5 is not observed in the experiments. On reducing the compensation density the temperature dependence of the average carrier lifetime gradually increases. The strongest temperature dependence occurs for the purest sample S_1 and is about $T^{.75}$ which is slightly lower than the experimental behaviour. In Table 3.3 the averages for the carrier lifetime, the acoustic energy relaxation time, the carrier energy and the ratio τ_{ac}/τ_{rec} with the energy equal to $k_B T$ are listed.

3.5. Conclusions

The solution of the rate equation and the energy balance equation, based on a one-band model for holes which are photoexcited by room temperature blackbody radiation, satisfactorily explains

the trapping and photo transport properties of Cu-doped Ge with compensation densities $N_D < 10^{13}$ cm^{-3}. The average hole lifetime in the low compensated samples ($N_D < 10^{13}$ cm^{-3}) is of the order of or greater than the acoustic energy relaxation time. Under this condition the energy distribution function can be approximated by a Maxwellian function with the carrier temperature very close to and strongly dependent on the lattice temperature. All these factors suggest that the holes are nearly in thermal equilibrium and this is agreement with the conclusions of Norton and Levinstein [1].

The value of the shape parameter ℓ which appears in the rate of photoexcitation is not critical in the present calculations and optimum agreement is obtained when ℓ is taken to be zero. The average acoustic energy relaxation time exhibits a mild dependence on the compensation density and this arises from the average over the distribution function (so as carrier heating) which depends on the recombination lifetime. It is noted that the degree of carrier heating is better characterised by the ratio of acoustic relaxation time to carrier lifetime when the energy is assigned the value k_BT. The ratio of their respective average times is too low for both warm and hot carriers.

The mild temperature dependence ($T^{\cdot 2}$) found for the average carrier lifetime in sample S_4 is in close agreement with experimental data. However this same temperature dependence for sample S_5 is not in agreement with experimental results which show no such dependence. It is hoped that a more realistic model of semiconductor based on two parabolic heavy and light hole bands will remove this difficulty.

The onset of non-Maxwellian behaviour occur at $N_D \sim 10^{13}$ cm^{-3}. However the Maxwellian approximation and the numerically derived distribution functions give identical mobilities in samples with $N_D > 10^{13}$ cm^{-3} and the mobilities are about 25% greater than experimental data. The carriers temperature associated with these samples are much greater than T and nearly independent of this parameter. This result indicates a strong carrier heating in those samples. The deformation potential in the one-parameter theory is taken arbitrarily to be 10 eV (i.e. a = 8.2 eV) and this gives satisfactory results for samples with compensation less than about 10^{13} cm^{-3}. It is noted that this value for the deformation potential is nearly twice as large as that obtained from thermalised mobility calculations based on a one-parameter theory of elastic scattering [22]. Chapter IV explores the possibility of deducing a value for the deformation potential a by fitting the calculated hot-hole mobilities to those of Norton and Levinstein [1] and Bannaya et.al. [2]. The physical model for those calculations assumes two parabolic heavy and light hole bands.

SAMPLE	DONOR DENSITY		ACCEPTOR DENSITY		NEUTRAL IMPURITY	CAPTURE CROSS SECTION	
NAME	N_D	cm^{-3}	N_A	cm^{-3}	Scat. Parameter A	Temp. ^oK	σ cm^2
S_1	1.9	10^{11}	2.7	10^{13}	3	4	2.0 10^{-11}
S_2	2.5	10^{12}	5.9	10^{13}	3	8	7.6 10^{-12}
S_3	1.7	10^{13}	2.2	10^{15}	5	15	3.0 10^{-12}
S_4	1.1	10^{14}	2.5	10^{15}	4.5		
S_5	2.2	10^{14}	3.0	10^{15}	4		

Table 3.1. Impurity concentrations, multiplicity factor of the Erginsoy neutral impurity scattering time [27] and the capture cross-section for Cu-doped Ge [17]

Sample	Lattice Temp (^{o}K)	Carrier Temperature TE (^{o}K)	Experimental Mobility	Rate Eq. Mobility	Energy B.E. Mobility
S_1	4	4.9	1.58×10^6	1.55×10^6	1.66×10^6
	8	8.5	1.08×10^6	1.12×10^6	1.12×10^6
	15	15.4	5.82×10^5	5.85×10^5	5.82×10^5
S_2	4	9	4.28×10^5	3.75×10^5	5.45×10^6
	8	11	4.0×10^5	4.02×10^5	4.42×10^5
	15	17	2.95×10^5	3.21×10^5	3.23×10^5
S_3	4	19	1.78×10^5	1.77×10^5	2.24×10^5
	8	19	1.55×10^5	1.56×10^5	1.86×10^5
	15	23	1.40×10^5	1.5×10^5	1.58×10^5
S_4	4	42	9.8×10^4	1.33×10^5	1.38×10^5
	8	38	8.7×10^4	1×10^5	1.07×10^5
	15	40	7.1×10^4	8.4×10^4	8.69×10^4
S_5	4	56	7.13×10^4	1.13×10^5	1.12×10^5
	8	51	6.6×10^4	8.65×10^4	8.62×10^4
	15	51	5.6×10^4	7.03×10^4	6.99×10^4

TABLE 3.2. Summary of the one-single band model mobility calculations, carrier temperature taken from the energy balance equation, experimental mobility taken from Norton and Levinstein [1].

Lattice Temperature ^{o}K	Average Lifetime sec	Average Acoustic Energy Relaxation Time (sec)	$\frac{\tau_{ac}(k_BT)}{\tau_{rec}(k_BT)}$	Sample Name
4	1.00×10^{-7}	6.23×10^{-10}	.008	
8	1.68×10^{-7}	4.73×10^{-10}	.003	S_1
15	3.00×10^{-7}	3.49×10^{-10}	.001	
4	1.00×10^{-8}	4.6×10^{-10}	.1	
8	1.45×10^{-8}	4.16×10^{-10}	.04	S_2
15	1.98×10^{-8}	3.32×10^{-10}	.02	
4	2.14×10^{-9}	3.1×10^{-10}	.7	
8	2.87×10^{-9}	3.1×10^{-10}	.26	S_3
15	3.40×10^{-9}	2.86×10^{-10}	.13	
4	4.83×10^{-10}	2.0×10^{-10}	4.52	
8	6.00×10^{-10}	2.23×10^{-10}	1.73	S_4
15	7.15×10^{-10}	2.17×10^{-10}	.835	
4	3.00×10^{-10}	1.90×10^{-10}	9	
8	3.63×10^{-10}	2.0×10^{-10}	3.5	S_5
15	4.60×10^{-10}	2.0×10^{-10}	1.7	

TABLE 3.3. Summary of some carriers properties.

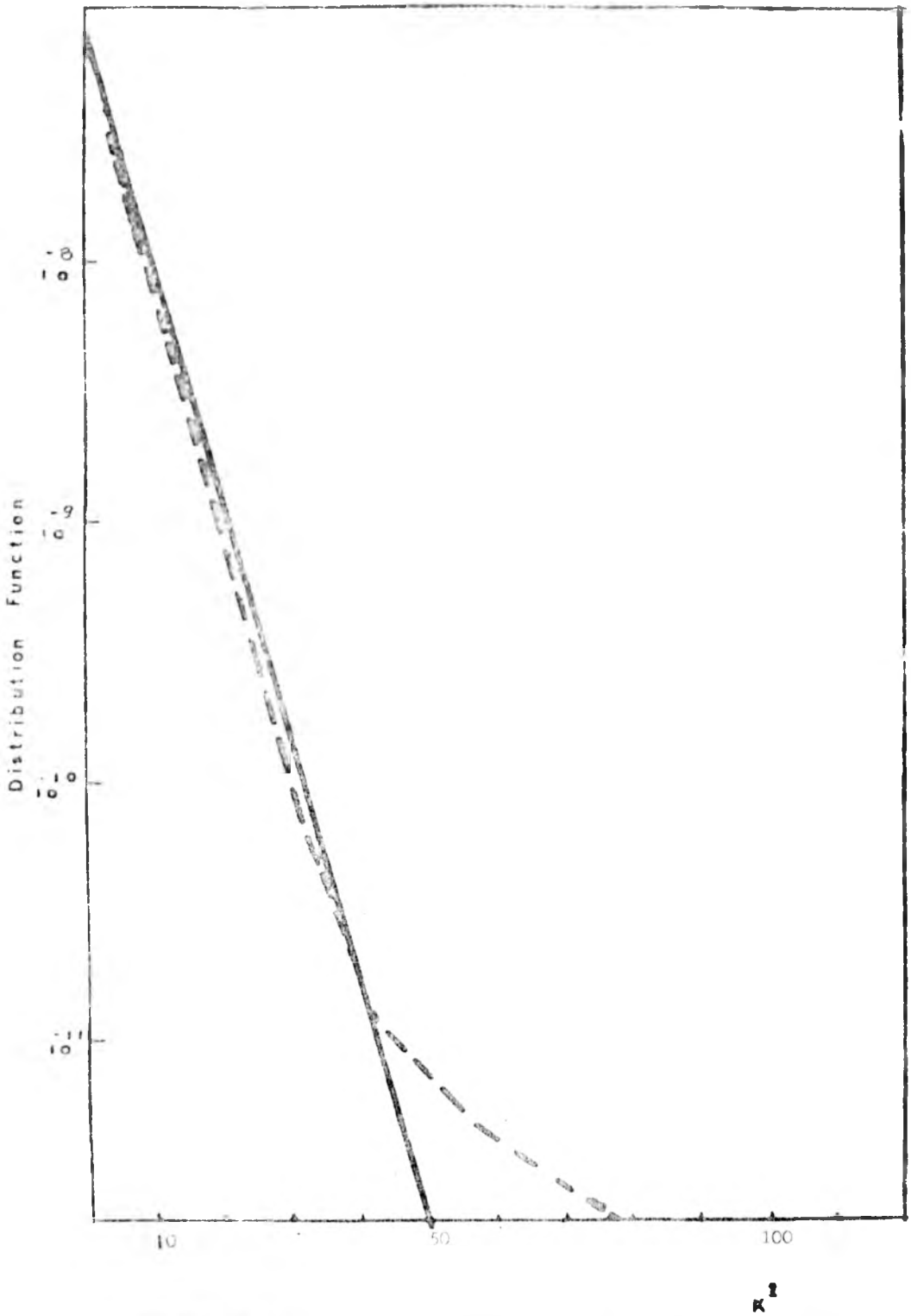

FIGURE 3.1: Comparison between the numerical (broken line and the Maxwellian (continuous line) distribution functions for sample S_1 at 1°K and carrier temperature Te=4.90K.

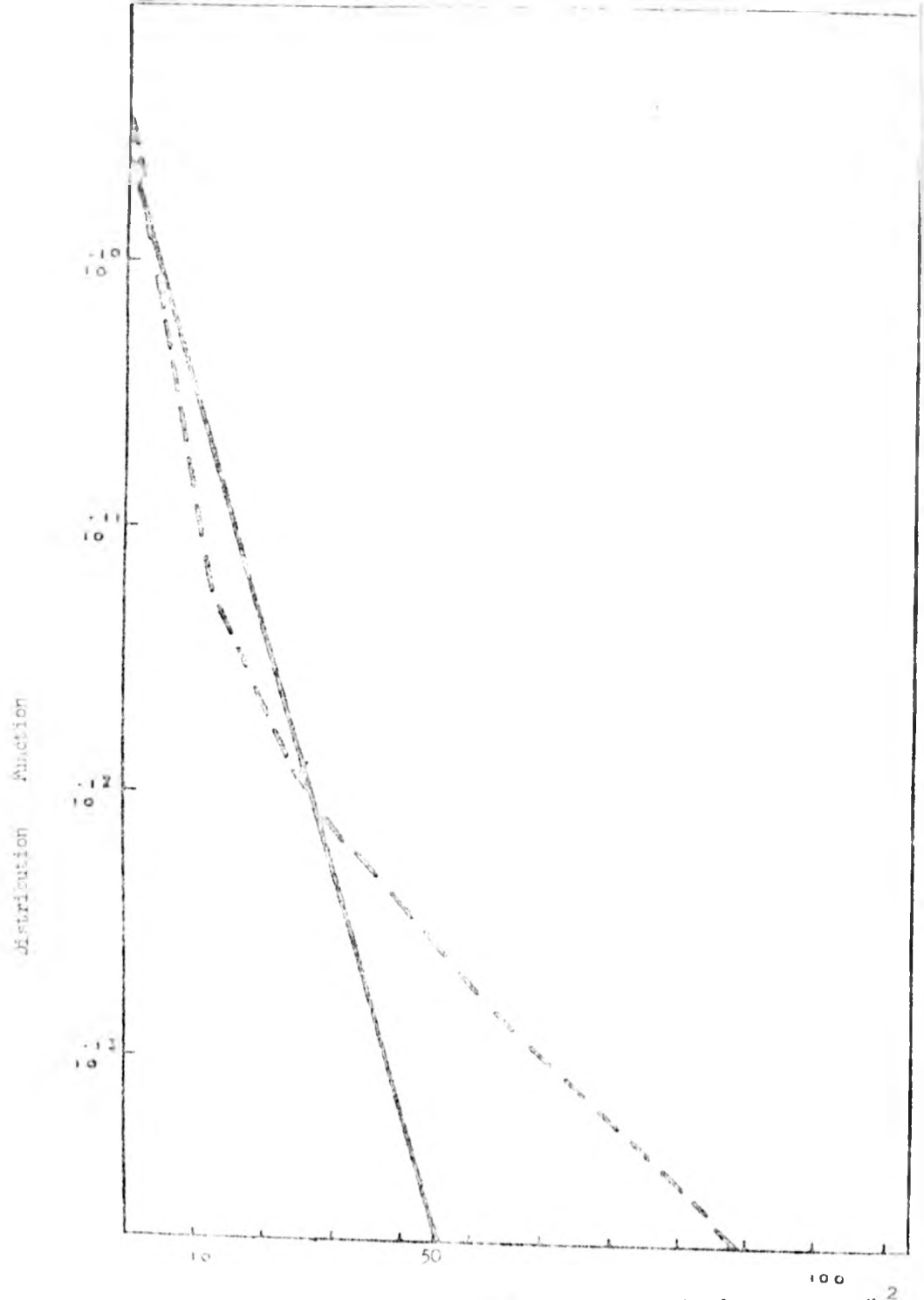

FIGURE 3.2: Comparison between the numerical (broken line) and the Maxwellian (continuous line) distribution functions for sample S_3 at 4°K and carrier temperature Te = 19°K.

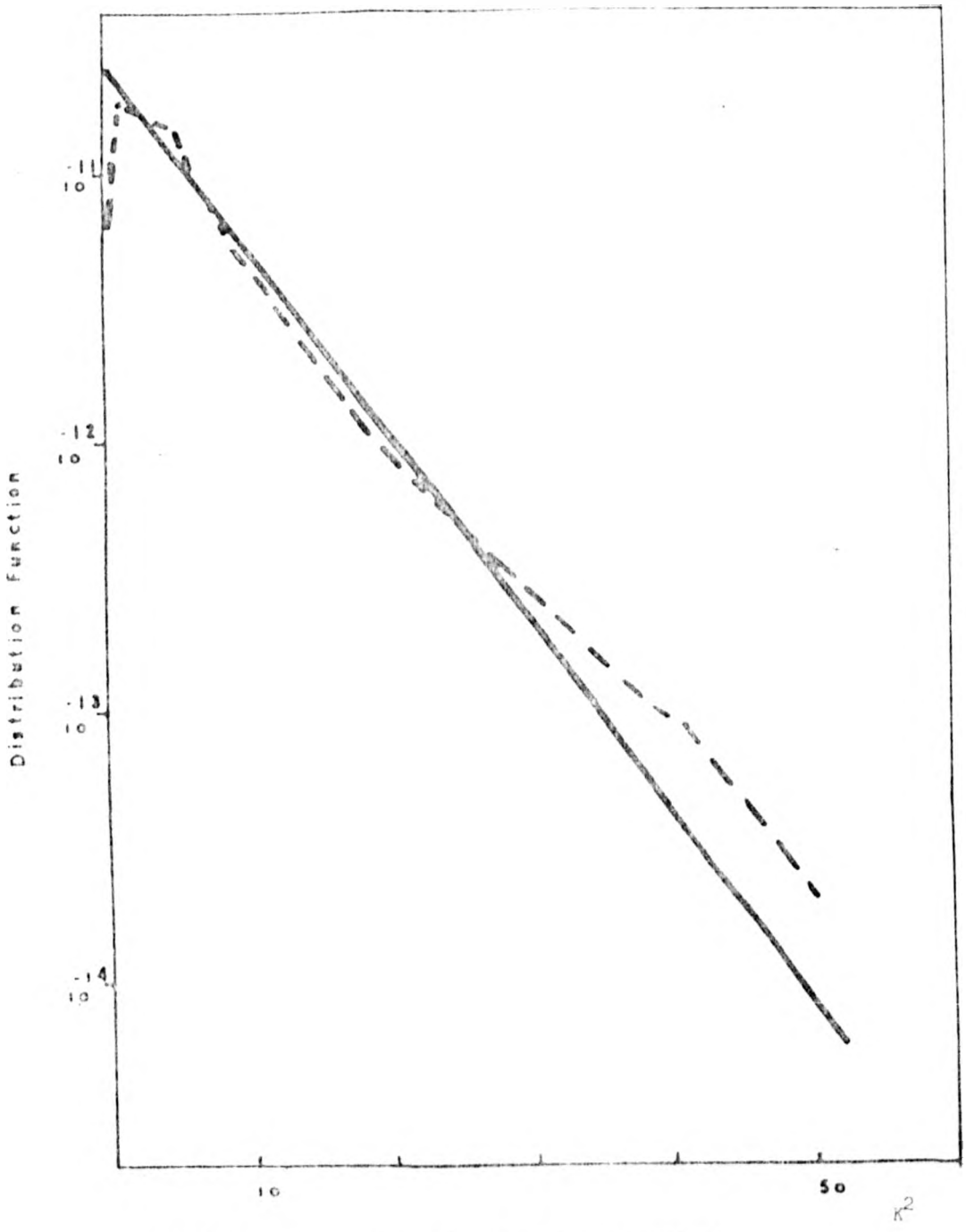

FIGURE 3.3: Comparison between the numerical (broken line) and the Maxwellian (continuous line) distribution functions for sample S_5 at $4^{O}K$ and carrier temperature Te = $56^{O}K$.

CHAPTER IV

DEFORMATION POTENTIALS

Photoexcitation produces a wide class of distribution functions and this offers new possibilities of studying the carrier - acoustic phonon coupling constants in p-type Ge. In order to pursue this end a model of semiconductor is proposed which includes the parabolic heavy and light hole bands. Details of the theoretical model are given in Section 4.2. The energy distribution function of holes which are generated by a broad spectrum of photoexcitation is derived from a rate equation involving photoexcitation, recombination and lattice scattering. Transport and trapping parameters are obtained as suitable averages over the zero field distribution function and subsequently compare with experimental data [1,2]relevant to p-type Ge doped with either deep or shallow impurities. The photohall mobilities and the carrier lifetimes appropriate to Cu-doped and Ga-doped Germanium have been measured by Norton and Levinstein [1,17] and Bannaya et.al [2] respectively at low temperatures and various compensating densities. In both cases carriers were photoexcited by room temperature blackbody radiation. The salient features of the heavy-and light-hole distribution functions are presented in Section 4.3.

Under thermal conditions the mobility for samples with high compensation densities, such as those of Bannaya et al. [2] and the two heavily compensated samples of Norton and Levinstein [1], is essentially determined by ionised impurity scattering. However

on increasing the carrier heating the acoustic deformation scattering can become important and plays a moderately important role in the determination of the mobility. Bir and Pikus [20] have developed a theory of acoustic deformation scattering which is applicable to p-type Ge. The carrier-long wavelength acoustic phonon scattering cross section is characterised by three deformation potential parameters which also give the variation of the band under homogeneous deformation. Hence these parameters can be determined from experiments such as those of the variation of the conductivity under homogeneous deformation. Hensel and Suzuki [23] have accurately determined the two shear deformation potentials from a study of the quantum resonance spectroscopy in the valence band of Ge under uniaxial stress at $4.2^{o}K$. Experiments based on different techniques at other temperatures (Pollak and Cardona [31], Balslev [32], etc) have given values for the shear deformation potentials which agree within experimental error with those of Hensel and Suzuki. On the other hand, the dilatational deformation potential is poorly known. This parameter can only be determined indirectly from experiments. Such a determination requires an accurate knowledge of the shear and dilatational deformation potentials related to the conduction band, however the latter potential is itself poorly known. A brief review of the status of the three deformation potential parameters related to the valence band of Ge is given in Section 4.3. It is hoped that the value of the dilatational deformation potential parameter can be deduced by fitting the calculated hot-hole mobilities to those measured by Norton and Levinstein [1] and Bannaya et.al [2]. Results corresponding to carrier lifetimes

and mobility calculations are given in Section 4.5 and an analysis of these results in Section 4.6. Two different values for the dilatational deformation potential parameter are obtained from these results. In one case hot-carrier mobilities for Ga-doped Ge samples give a value 2 eV for the deformation potential a, which is in agreement with some of the experimental values for this parameter. Similar result is obtained from mobilities for Cu-doped Ge with low compensation densities. In the other case the hot-carrier mobilities for Cu-doped Germaniam samples with high compensation densities give a deformation parameter of approximately 8 which is much greater than any of the experimental values already available. In addition, this parameter is also found to depend on the lattice temperature.

4.2. THEORETICAL MODEL

The valence band of Ge consists of three bands, two of which are degenerate at the centre of the Brillouin zone ($\bar{k} = 0$). The third one is separated by 0.29 eV at $\bar{k} = 0$ from the two upper bands by spin-orbit interaction. According to Kane's description of the valence band structure of Ge near $\bar{k} = 0$ [33] the heavy hole band is parabolic along the main crystallographic axes. However for the light-hole and the split-off effective masses increases and decreases with energy respectively. Pinson and Bray [34] have shown that the light hole band is parabolic to energies about the optical phonon emission threshold, $\varepsilon_{op} = 0.037$ eV. Thus for small values of $\bar{k}$ the heavy-and-light-hole effective masses can be set equal to their respective experimental values, that is, 0.33 and 0.045 m_e respectively.

In the experiments of Norton and Levinstein [1] and Bannaya et. al. [2] carriers were photoexcited by room temperature blackbody radiation (with a high frequency cut-off filter incorporated to eliminate photoexcitation into the split-off band and second ionization of Cu impurities). Furthermore carriers intially photoexcited at energies greater than the optical phonon threshold energy (ε_{op}) will instantaneously emit one or more optical phonons. Thus in a very short time ($\sim 10^{-12}$ sec) all carriers will have energies less than ε_{op}. All these factors lead us to propose a model of semiconductor which uses both the parabolic heavy and light hole bands. The energy dispersion relation for each band is given by

$$\varepsilon_i(\underset{\sim}{k}) = \frac{\hbar^2 k^2}{2 m_i} \qquad i = 1,2 \qquad 4.2.1.$$

where m_1 and m_2 correspond to the light- and heavy-hole effective mass respectively and $\underset{\sim}{k}$ is the hole wavevector.

As in previous chapters, free carrier absorption and change in the occupancy of the impurity levels are neglected, as are the effects of degeneracy, intercarrier scattering and non-equilibrium of phonons. The isotropic nature of the radiation and the rapid momentum relaxation time ensure that the zero-electric field distribution function is dependent only on energy. The rate equation (2.2.4) transforms, in the two-band model, into two coupled integral equations

$$\bar{\omega}_{ph_i}(K) - \frac{\phi_i(K)\ K}{\tau_{rec_i}(K)} = J_i(\phi_i, \phi_j) \qquad 4.2.2.$$

where i, j = 1,2. The recombination lifetimes (τ_{rec_i}) are assumed to have the same form, Equation 2.2.8, but the average velocities differ because of the different effective masses. The shape parameter ℓ in the excitation spectrum Equation 3.2.2, is set equal to zero in the two band model largely as a consequence of the insensitivity of the results of the one-band model to its value. This is also consistent with the use of an integrating cavity in the experimental measurements. The reduced rate of photoexcitation into each band is given by the same equation (3.2.2) with an appropriate density-of-states weighting factors (Appendix 3).

The inter-and intra-band hole transition probabilities from state $\underset{\sim}{k}$ to state $\underset{\sim}{k}'$, $W_{ij}(\underset{\sim}{k},\underset{\sim}{k}')$ due to either emission or absorption of a long wavelength acoustic phonon has been given by Bir and Pikus [20]. This three deformation-parameter theory can be, by use of some approximations, reduced to a two-deformation-parameter theory [19]. Within the spirit of the model of semiconductor the solid can be assumed as elastically isotropic [35]. This means that the longitudinal and transverse sound velocities are independent of the direction although not necessarily equals. The values for the sound velocities can be obtained as suitable weighted averages over the crystallographic directions. The longitudinal (S_L) and transverse (S_T) sound velocities are then given by

$$S_L^2 = \frac{1}{\rho} C_\ell \qquad \text{and} \qquad S_T^2 = \frac{1}{\rho} C_t \qquad 4.2.3.$$

where C_ℓ, C_t are the average longitudinal and transverse elastic constants defined in equation (2.5.1) and ρ is the mass density. This assumption is identical, in spirit, to that involved in the Equation 4.2.1 which uses an average (with respect to the crystallographic axes) for the effective masses [35]. This implies that the constants B and $D/\sqrt{3}$, which determine the effective masses, are equal. Within the same order of ideas, Bir, Normantas and Pikus [19] have assumed that the transition probabilities $W_{ij}(\underset{\sim}{k},\underset{\sim}{k}')$ depend only on the energies $\varepsilon(k)$, $\varepsilon(k')$ and the angle Θ between the wavevectors $\underset{\sim}{k}$ and $\underset{\sim}{k}$

$$W_{ij}(\underset{\sim}{k},\underset{\sim}{k}') = P_{ij}\ (\varepsilon(k),\ \varepsilon(k'),\Theta)\ \ \delta(\varepsilon_i(k) - \varepsilon_j(k')) \qquad 4.2.4.$$

This assumption requires the shear deformation potentials, b and $d/\sqrt{3}$ to be equal. If in the emission or absorption of an acoustic phonon i.e. inelastic scattering, is allowed the transition probabilities P_{ij} in Equation 4.2.4 become [21]

$$p^L_{ii} = \frac{a^2\pi}{4\rho S_L}\left[\bar{n}_q + \tfrac{1}{2} \pm \tfrac{1}{2}\right] q\ \ \{(1\pm\eta)^2 + \frac{9}{4}\eta^2 - 6\eta\cos\Theta(\tfrac{\eta}{4} \pm 1) + 3(1-\frac{\eta^2}{4})\cos\Theta\} \qquad 4.2.5.$$

$$p^L_{12} = p^L_{21} = \frac{3a^2\pi q}{4\rho S_L}\left[\bar{n}_q \pm \tfrac{1}{2} + \tfrac{1}{2}\right] \sin^2\Theta\ \{1 - \frac{\eta^2}{4} + 2\eta(\delta_1 + \frac{\eta}{4}\delta_2) +$$

$$+ \frac{3}{4}(\delta_1^2\,\eta^2\} \qquad 4.2.6.$$

$$p^T_{ii} = \frac{9a^2\pi q}{16\rho S_T}\left[\bar{n}_q + \tfrac{1}{2} \pm \tfrac{1}{2}\right]\ \eta^2 \sin^2\Theta \qquad 4.2.7.$$

$$P_{12}^{T} = P_{21}^{T} = \frac{3a^2 \pi q \eta^2}{2\rho S_T} \left[\bar{n}_q + \tfrac{1}{2} \pm \tfrac{1}{2}\right] \times \{1 - \frac{3}{8} \sin^2\theta \, (1+\delta_1^2)\} \qquad 4.2.8.$$

where $\eta = b/a$, $\bar{n}_q$ is the average phonon density equal to

$$\bar{n}_q = \frac{1}{\exp(hSq/k_B T)-1} \quad , \quad S = S_L, \; S_T,$$

$$\delta_{1'2} = \frac{1 \mp \gamma^2 \, \varepsilon/\varepsilon'}{1 + \gamma^2 \, \varepsilon/\varepsilon' - 2\gamma\sqrt{\varepsilon/\varepsilon'} \cos\theta}$$

$\gamma^2 = m_1/m_2 = .13$ and ε/ε' is the ratio of initial to final hole energies. In calculations of $\delta_{1,2}$ this ratio has been set equal to 1. The sign + (-) in the first parenthesis of 4.2.5 to 4.2.8 is realted to emission (absorption) of phonons. The sign + (-) in the second parenthesis is for light (heavy) holes. With these transition probabilities the general expression for $J(\phi_i, \phi_j)$ is easily obtained. This is presented in Appendix 1.

4.3. DEFORMATION POTENTIALS IN GE: EXPERIMENTAL STATUS

The shear deformation potentials b and d are related to the lifting of the degenerate valence-band edge at $\underset{\sim}{k} = 0$ under <100> and <111> uniaxial stress respectively. As a consequence of the degeneracy of the valence band of Ge the low lying Landau levels are anomolously spaced. Therefore the cyclotron resonance of holes under quantum conditions exhibits complex line spectrum.

$$P_{12}^{T} = P_{21}^{T} = \frac{3a^2\,\pi q \eta^2}{2\rho\, S_T} \left[\bar{n}_q + \tfrac{1}{2} \pm \tfrac{1}{2}\right] \times \{1 - \frac{3}{8}\sin^2\theta\,(1+\delta_1^2)\} \qquad 4.2.8.$$

where $\eta = b/a$, $\bar{n}_q$ is the average phonon density equal to

$$\bar{n}_q = \frac{1}{\exp(h\mathrm{S}q/k_B T)-1}, \qquad S = S_L,\ S_T,$$

$$\delta_{1'2} = \frac{1 \mp \gamma^2\ \varepsilon/\varepsilon'}{1 + \gamma^2\ \varepsilon/\varepsilon' - 2\gamma\sqrt{\varepsilon/\varepsilon'}\cos\theta}$$

$\gamma^2 = m_1/m_2 = .13$ and ε/ε' is the ratio of initial to final hole energies. In calculations of $\delta_{1,2}$ this ratio has been set equal to 1. The sign + (-) in the first parenthesis of 4.2.5 to 4.2.8 is realted to emission (absorption) of phonons. The sign + (-) in the second parenthesis is for light (heavy) holes. With these transition probabilities the general expression for $J(\phi_i,\phi_j)$ is easily obtained. This is presented in Appendix 1.

4.3. DEFORMATION POTENTIALS IN GE: EXPERIMENTAL STATUS

The shear deformation potentials b and d are related to the lifting of the degenerate valence-band edge at $\underset{\sim}{k} = 0$ under <100> and <111> uniaxial stress respectively. As a consequence of the degeneracy of the valence band of Ge the low lying Landau levels are anomolously spaced. Therefore the cyclotron resonance of holes under quantum conditions exhibits complex line spectrum.

Uniaxial stress applied to the sample removes the degeneracy of the bands and the quantum resonance spectroscopy can be successfully studied. Hensel and Suzuki have used this method to derive the two shear deformation potentials at 4.2 ^{O}K [23]. The value for the shear deformation potentials obtained from these very accurate measurements are: b = -2.18 eV and d = 4.5 eV. Other experimental techniques have been used to obtain a reliable value for each one of the shear deformation potentials. Amongst these techniques are the optical reflactance combined with static and oscillatory stress [36], piezo-electroreflactance [37], modulated piezo-reflactance [38], cyclotron resonance [39], Sckottky barrier electroreflactance [40]. The values for the shear deformation potentials obtained from these techniques agree within experimental error with those of Hensel and Suzuki. Table 4.1 compares the values for shear deformation parameters as obtained from these experimental techniques at various temperatures.

The effective shear deformation potential $\bar{b}$ which appears in the two-deformation-parameter theory is evaluated by using the values reported by Hensel and Suzuki [23]. According to Bir, Normantas and Pikus [19] the effective shear deformation potential depends linearly on the b and d as follows

$$\bar{b} = \frac{1}{5} \frac{2bB + \sqrt{3B^2 + C^2}\, d}{\bar{B}} \qquad 4.3.1.$$

where B and C are constants which are determined by the structure of the Valence band at low values of $\underset{\sim}{k}$; and $\bar{B} \equiv \frac{B}{|B|}\left[B^2 + \frac{C^2}{5}\right]^{\frac{1}{2}}$.

The two constants B and C have also been determined very precisely by, among others, Hensel and Suzuki [23]. Their values are: B = -8.48 and C^2 = 172.782. These data give consequently $\bar{b}$= -2.4eV .The dilatational deformation potential $\underline{a}$ is related to the shift of the valence band edge under hydrostatic pressure. This parameter cannot be determined directly from experiments. This is because they give only the relative shift between the valence and conduction bands. The conduction band of Ge has a local minimum at the centre of the Brillouin zone ($\underset{\sim}{k}$ = O). This minimum is only shifted under stress and the deformation parameter associated with this shift is experimentally unknown. On the other hand, the deformation potentials related to the true minimum of the conduction band are partially known. Various experimental techniques have been used to measure these parameters. These attempts show that the shear deformation potential Ξ_u has a value about 19 eV at temperatures in the range from 70^{O}K to 300^{O}K. However, this value decreases to about 16 eV at low temperatures. This discrepancy in values cannot be explained on the basis of the experimental errors. It is likely that Ξ_u changes slowly with the lattice temperature. The techniques so far used to measure the conduction-band dilatational deformation parameters Ξ_d require the ratio κ of the parallel and perpendicular momentum relaxation times which are related to the carrier scattering in the conduction band. This anisotropic momentum relaxation time arises because the conduction band edge has a spheroidalenergy surface orientated along the <111> crystal axis [41]. No agreement has been found from all experimental attemps so far made to give a definite value for Ξ_d. A list of

values for Ξ_u and Ξ_d a various temperature appears in Table 4.2.

On studying the indirect absorption in Ge under combined static and oscillatory stress, Balslev [32] derived the following expression which relates the deformation potentials (Ξ_u, Ξ_d) of the conduction band with the dilatational deformation potential of the valence band:

$$\Xi_d + \frac{1}{3}\ \Xi_u - a = E_{1g} \qquad 4.3.2.$$

where E_{1g} is the shift of the energy gap with dilatation i.e.

$$E_{1g} = V \frac{\partial E_g}{\partial V}$$

In this study Balslev reported a value for E_{1g} = 2.9 eV at 300^{o}K and 77^{o}K. Paul [42] has also measured E_{1g} from variation of electrical conductivity with stress and has obtained E_{1g} = -3.9 eV at room temperature. Therefore the value of a to be obtained from all these experimental information will be spread over a wide range of values. Wiley [22] has reported a value for the deformation potential a equal to 2eV.This value was obtained from a model based on the dielectric band theory [51]. A list of values for the deformation potential a appears in Table 4.3. Because of this chaotic situation the deformation potential a is retained as a fitting parameter in mobility calculations.

4.4. DISTRIBUTION FUNCTIONS

The energy distribution functions for the heavy and light hole bands are obtained by a numerical solution of the rate equation 4.2.2. The numerical technique and the criterion of convergency

described in section 2.3 are again used in here. The number of iterations needed to reach satisfactory convergence in the solution of the two coupled integral equations 4.2.2 is about 130 at $15^{O}K$. This number of iterations reduces to about 100 at $4^{O}K$. The heavy and light hole distribution functions exhibit non-Maxwellian behaviour over most of the range of energies available. Moreover our calculations indicate that the light hole distribution function ϕ_1 can satisfactorily be obtained from the heavy hole one by the use of the following relationship

$$\phi_1 \sim \left(\frac{m_1}{m_2}\right)^{3/2} \phi_2 \qquad 4.4.1.$$

It should be noted that an identical formula was used in Section 2.5 to obtain the light hole distribution function.

In Figure 4.1 the heavy and light hole distribution functions for one Cu-doped Germaniam sample (S_5) are compared with two Maxwellian functions with carrier temperature Te deduced from the energy balance equation 3.2.3. The data for Te appear in Table 3.2. The light hole Maxwellian function is derived from equation 4.4.1.

Figures 4.2. and 4.3 show the heavy and light hole distribution functions for two Ga-doped Ge samples. Hypothetical Maxwellian functions are also shown in order to make clear the departure of the distribution function from the simple Maxwellian form. Data relevant to these calculations appear in Tables 2.1 and 3.1.

4.5. DERIVATION OF THE DEFORMATION POTENTIAL a FROM TRANSPORT DATA CU IMPURITIES:

The experimental mobilities for the two heavily compensated samples S_4, S_5 (Table 3.1) of Norton and Levinstein [1] are used to deduce a value for the deformation potential a. The total momentum relaxation time for each band is obtained as the harmonic sum of the acoustic deformation -, ionised - and neutral-impurity-scattering times (see Section 2.5) and is then appropriately averaged over the corresponding distribution function to give the mobility in that band. The appropriate procedure required to obtain the total mobility is derived in Appendix 2. The final expression for the mobility is a generalization of the equation 2.5.3. The dominant momentum relaxation mechanism in the two S_4, S_5 samples is the ionised impurity scattering.

A sample with negligible ionised impurity scattering but with dominant acoustic scattering, for example sample S_1, gives values for the deformation a which are in the range between 2 and 3 eV. These values agree with some of the experimental results and in particular they are close to the value 2eV reported by Wiley [22] These values for the deformation potential a could not be confirmed by using dark mobility data [28] (a better fit is obtained by using a = 8.2 eV).

It is noted that, for the two heavily compensated samples, changes in the energy dependence of the recombination lifetime strongly affect the resultant values for the deformation potential a. Thus the energy dependence of the recombination lifetime mentioned earlier (equation 2.2.8) with n = 1 gives rise to a temperature dependence of the average lifetime of the order of $T^{\frac{1}{16}}$

for sample S_5. This result is a very significant improvement over the results of the one band model and is in good agreement with the temperature behaviour of the experimental photo-carrier density [1]. On the other hand, it is found that the deformation potential a decreases rapidly with the lattice temperature. This strongly decreasing dependence on temperature is substantially reduced by choosing the strong energy dependence of the type derived by Lax [15] for recombination into shallow traps. However the average recombination lifetime now becomes strongly dependent on T. Table 4.4 summarises the calculation of the apparent dependence of the deformation potential on the energy dependence of the carrier lifetime. The deformation potential a is also affected by the multiplicity factor for the Erginsoy neutral impurity scattering time. This factor cannot be satisfactorily determined by fitting the experimental thermal mobilities in those samples with high compensation densities as this is controlled by the ionised impurity scattering. Calculations indicate that the neutral impurity and acoustic scattering play a moderately important role in determining the photohall mobilities, and it is found that the deformation potential a changes by about 1 eV when A is varied by a factor of two.

It has not been possible to remove the apparent dependence of a on T and N_D by adjustment of other parameters. However the capture cross-section used in this study is related to measurements on samples with low compensation densities and is probably incorrect for highly compensated samples. Further study of the cross-section

for these samples is clearly required before any explanation can be offered for the anomaly in the fitting procedure for the value of a.

Shallow Impurities:

Bannaya et. al [2] have measured the mobility for various Ga-doped Germanium samples at 4.2^{o}K. The experimental mobility data suggest that the ionised impurity scattering is the dominant momentum relaxation mechanism. Although the role of the acoustic deformation scattering in the determination of the mobility is therefore small, it is however sufficient to enable us to deduce a value for the deformation potential a by fitting the calculated hole mobilities to those of Bannaya et.al [2]. A list of relevant data concerning the samples is given in Table 4.5. We have chosen eight of the samples studied by Bannaya et.al. The experimental mobilities are reported for only four of the eight samples considered; for the rest of the samples the mobilities can be roughly estimated from Figure 1 in the paper of Bannaya et.al [2].

In order to evaluate the mobility in Ga-doped Germanium samples the procedure already used in connection with Cu impurities is again employed in here. It is noted however that Ga is a hydrogenic impurity and therefore the Erginsoy formula for neutral impurity scattering time is used. The recombination of carriers into shallow impurities occurs via attractive cascade mechanism [15], and n = 3 for the energy dependence of the lifetime (equation 2.2.8) is adopted. Stannard [17] has measured the capture cross-section for shallow acceptor impurities in pure p-type Ge samples at low temperatures. We use these data in our calculations.

The value 2eV for the deformation potential a used in the calculation of the average hole mobility gives rise to an optimal fit with experimental data. The agreement with experimental mobilities is very good for three of the samples (Sa2, Sa4, Sa8) and is too low for the fourth (Sa5). The calculated mobilities for the other group of samples are rather small compared with the estimated values. However for sample Sa3 the agreement is good. The value 2 eV for the deformation potential a could not be confirmed by using non-illuminated mobility data because the Brooks-Herring-Dingle formula for ionised impurity scattering is no longer valid at $4^{o}K$. This formula is based on the Born approximation which needs $|ka| >> 1$, where k is the carrier momentum, and a is the scattering length. This condition is not satisfied at $4.2^{o}K$ in dark conditions. A summary of the mobility calculations appears in Table 4.6.

In the same study Bannaya et.al. [2] has evaluated the averaged carrier lifetime for each of the eight samples considered in this study. In that work, the density of photoexcited carriers is obtained from photohall measurements and the total generation rate is then calculated from a theoretical model of generation. This procedure has been used to obtain the capture cross section into shallow impurities and gives values which are comparable with those of generation and recombination noise [52].

The main characteristics of the carrier lifetime as obtained from photohall measurements are:

i) It is inversely proportional to the compensation density N_D up to values of about 10^{14} cm^{-3}.

ii) It is also dependent on the degree of compensation $R = N_D/N_A$. Two broad regions can be distinguished, one for $R > .1$ and the other for $R < .1$. Thus the carrier lifetime for samples in the first region is considerably greater than that for samples in the second one.

iii) At compensation densities greater than 10^{14} cm^{-3} the average lifetime deviates from the inverse dependence on N_D and tends to level off. On the other hand, our calculated carrier lifetime presents the following characteristics.

i) It is inversely dependent on the compensation density N_D.

ii) It is independent of the relative value of the ratio R. (see figure 4.4).

iii) Two samples with $N_D > 10^{14}$ cm^{-3} are considered; for one of them the carrier lifetime deviates from the inverse dependence on N_D and indicates a tendency to level off. The carrier lifetime for the other sample (Sa5) is again dependent on N_D^{-1}. This latter result is not reliable because it is not possible to fit the experimental mobility for that sample.

iv) Our calculated absolute values for the average lifetime are in reasonably good agreement with those reported by Bannaya et.al [2]. However for samples Sa6 and Sa7 the calculated average lifetime values are about one order of magnitude greater than the reported ones.

ii) It is also dependent on the degree of compensation $R = N_D/N_A$. Two broad regions can be distinguished, one for $R > .1$ and the other for $R < .1$. Thus the carrier lifetime for samples in the first region is considerably greater than that for samples in the second one.

iii) At compensation densities greater than 10^{14} cm^{-3} the average lifetime deviates from the inverse dependence on N_D and tends to level off. On the other hand, our calculated carrier lifetime presents the following characteristics.

i) It is inversely dependent on the compensation density N_D.

ii) It is independent of the relative value of the ratio R. (see figure 4.4).

iii) Two samples with $N_D > 10^{14}$ cm^{-3} are considered; for one of them the carrier lifetime deviates from the inverse dependence on N_D and indicates a tendency to level off. The carrier lifetime for the other sample (Sa5) is again dependent on N_D^{-1}. This latter result is not reliable because it is not possible to fit the experimental mobility for that sample.

iv) Our calculated absolute values for the average lifetime are in reasonably good agreement with those reported by Bannaya et.al [2]. However for samples Sa6 and Sa7 the calculated average lifetime values are about one order of magnitude greater than the reported ones.

The degree of carrier heating in the system is better described in terms of the ratio $\tau_{ac}(k_BT/\tau_{rec}(k_BT)$ (The acoustic energy relaxation time to carrier lifetime at $\varepsilon = k_BT$) rather than by the ratio of their respective average values. This latter ratio is too low for both warm and hot carriers. In the evaluation of the acoustic energy relaxation time the value D = 6.5 eV [22] for the deformation potential in one-parameter theory is assumed. This value for D is consistent with a = 2 eV. The calculated acoustic relaxation time is 1.827×10^{-9} sec and is comparable with the value 1.4×10^{-9} sec (quoted by Bannaya et. al. [2]). It is also noted that the average carriers energy is much greater than the thermal energy. Combining this information with that coming from the ratio $\tau_{ac}(k_Bt)/\tau_{rec}(k_BT)$ we can say that the carriers in samples Sa4, Sa8, Sa5, Sa3 and Sa7 are hot and in samples Sa2, Sa1, Sa6 they are warm. A list of the average carrier lifetime, average energy, average acoustic relaxation time and the ratio $\tau_{ac}(k_BT)/\tau_{re}(k_BT)$ appears in Table 4.7.

4.6. CONCLUSIONS

The energy dependence of the hole lifetime corresponding to n = 1 (equation 2.2.8), in Cu-doped Ge with high compensation densities, gives an average lifetime which is in close agreement with the photohall measurements in those samples. The temperature dependence of the average lifetime of about $T^{.06}$ for the heavily compensated sample S_5 represents a very significant improvement with respect to the result previously obtained from a one-band model.

The Lax cascade mechanism correctly characterises the recombination into shallow impurities and this corresponds to n = 3 (equation 2.2.8) in the energy dependence of the hole lifetime. Our average absolute values for the carrier lifetime in Ga-doped Germanium are in reasonable agreement with those reported by Bannaya et.al. [2]. Our calculations reveal no dependence of the average lifetime on the compensation ratio; and this is contrary to photohall measurements. However the average lifetime changes with the inverse of N_D as in experimental data. The lack of dependence of the average lifetime on the compensation ratio may be a consequence of the value used for the recombination cross section. Firstly, this value was measured in pure samples so that the use of this value in samples with higher compensation could be an oversimplification. The use of only one value for the cross section in all samples considered there could be a further oversimplification. This point is open to discussion until new sets of data are available.

The ratio $\tau_{ac}(k_BT)/\tau_{rec}(k_BT)$ is found, once more, to give a better description of the degree of carrier heating in the system in both hot and warm carriers. The average acoustic relaxation time and the carrier lifetime together give a ratio which can decrease either by increasing the heating in the system of holes or by increasing the compensation density N_D. Thus a low value in the latter ratio does not necessarily imply that carriers are thermalised. However a low value in the former ratio means that the lifetime is large and carriers are likely to be in nearly thermal equilibrium with the lattice.

Photohall mobilities for Ga-doped Ge samples give a value for the deformation potential a equal to 2eV. This value corresponds to the value reported by Wiley [22] obtained from a model based on the dielectric band theory [52]. The experimental Hall mobility data for Cu-doped Ge samples with low compensation densities generate values for the deformation potential a between 2 and 3 eV in agreement with the experimental values for this parameter (Table 4.3). However non-illuminated data, for the same low compensated Cu-doped Ge samples, give for the same parameter a value of about 8.2eV. These different results in the value of a can be explained as follows: the photohole energy distribution function in samples with low compensation densities is approximated by the Maxwell-Boltzmann function for much of the energy range (fig.4.5). Nevertheless the calculated distribution function presents a tail at higher energies which gives rise to an increase in the average energy. Precisely at these energies the acoustic momentum relaxation time dominates all the other scattering mechanisms. These two factors make the average acoustic scattering stronger and consequently causes deformation potential to diminish in value. It is noted that the use of values for the deformation potential around 2eV in the calculation of non-illuminated Hall mobilities forces the ionised impurity scattering to be the dominant mechanism. This artificial result suggests that either the Brooks-Herring-Dingle formula overestimates the ionised impurity scattering in Cu-doped Ge at low temperature or, perhaps, an extra scattering mechanism should be included in the total momentum relaxation time. The good fit of the non-illuminated mobility data in Cu-doped Ge samples with various

compensation densities at low temperatures suggests that the Brooks-Herring-Dingle formula is satisfactory for these kind of samples. An entirely new scattering mechanism that can be tested out is the two-acoustic phonon processes. However there is no expression for the two-acoustic phonon momentum relaxation time that can be tested. On the other hand, photohall mobilities for Cu-doped Ge samples with high compensation densities give values for the deformation potential $\underline{a}$ of about or greater than 8 eV. These values although closer to those obtained from non-illuminated data are nevertheless much greater than any experimental value for $\underline{a}$. There is an indication that the average carrier energy in these samples is greater than it should be. This indicates that energy relaxation mechanisms included in the theory are not enough to account for the total energy relaxation time. In the next chapter the effect of two-phonon processes as energy relaxation mechanisms will be explored.

The dependence of the deformation potential $\underline{a}$ on the compensation density and lattice temperature may also have arisen from the recombination mechanism. The use of an average cross section measured under low-compensation conditions seems to become incorrect in samples with high compensation densities. Measurements [17] of the cross section indicate that its temperature dependence diminishes as the compensation density is increased. Thus a new temperature dependence for the cross section may give a different temperature dependence for the deformation potential. Finally the use of an unique energy dependence for τ_{rec} may be an oversimplification. Further study of the recombination process in Cu-doped Germanium is clearly needed before any explanation can be offered for the anomaly in the fitting procedure for the value of $\underline{a}$.

It should be pointed out that the deformation potential $\underline{a}$ may have a real dependence on the lattice temperature. This possibility arises from the fact that at least the shear deformation potential Ξ_μ for the conduction band of Ge has been found to depend in a very mild way on the temperature. However much more experimental data are required at various temperatures in order to find out the temperature dependence of that parameter (Ξ_μ).

The energy distribution function for the heavily compensated Cu-doped Germanium samples is non-Maxwellian over the whole range of energies. In these samples the neutral and acoustic scattering play an important role in the evaluation of the hot carrier mobility. Recognition of this fact opens up the possibility of using the fitting of the hot carrier mobilities to determine the multiplicity factor for the Erginsoy neutral impurity scattering time or even to test other models for this scattering mechanism. In the next chapter a new model for this scattering mechanism is stated. We will show that the new expression for the neutral scattering time which depends on carriers energy gives results similar to those obtained from the modified Erginsoy formula.

The wide class of energy distribution functions that photoexcitation brings about opens up the opportunity of deducing new important information about the energy and momentum relaxation mechanisms, in the valence band of Ge, that otherwise cannot be derived from equilibrium transport measurements. In the next chapter this is used to explore the effects of two-phonon process as energy relaxation mechanism. New formulae for the recombination lifetime and the neutral impurity scattering time are also studied.

It should be pointed out that the deformation potential $\underline{a}$ may have a real dependence on the lattice temperature. This possibility arises from the fact that at least the shear deformation potential Ξ_μ for the conduction band of Ge has been found to depend in a very mild way on the temperature. However much more experimental data are required at various temperatures in order to find out the temperature dependence of that parameter (Ξ_μ).

The energy distribution function for the heavily compensated Cu-doped Germanium samples is non-Maxwellian over the whole range of energies. In these samples the neutral and acoustic scattering play an important role in the evaluation of the hot carrier mobility. Recognition of this fact opens up the possibility of using the fitting of the hot carrier mobilities to determine the multiplicity factor for the Erginsoy neutral impurity scattering time or even to test other models for this scattering mechanism. In the next chapter a new model for this scattering mechanism is stated. We will show that the new expression for the neutral scattering time which depends on carriers energy gives results similar to those obtained from the modified Erginsoy formula.

The wide class of energy distribution functions that photoexcitation brings about opens up the opportunity of deducing new important information about the energy and momentum relaxation mechanisms, in the valence band of Ge, that otherwise cannot be derived from equilibrium transport measurements. In the next chapter this is used to explore the effects of two-phonon process as energy relaxation mechanism. New formulae for the recombination lifetime and the neutral impurity scattering time are also studied.

b eV	d eV	Lattice Temperature °K
$-2.18^{(a)}$	-4.5	4.2
$-2.6^{(b)}$	-4.7	300
$-2.4^{(c)}$	-4.1	80,297
$-2.8^{(d)}$	-4.95	300
$-2.86^{(e)}$	-5.28	70,300
$-2.4^{(f)}$	-7	4.2

TABLE 4.1. Shear deformation potentials b,d of Ge.

(a) Quantum cyclotron resonance [23]

(b) Piezo-electroeflactance [31]

(c) Indirect optical piezo-absorption [32]

(d) Intrinsic piezo-briefringence [38]

(e) Electroeflactance [40]

(f) Dependence of the acceptor ground state [50].

Ξ_u e.V.	Ξ_d e.V.	Lattice Temperature ^oK
16.2[a]		77 → 300
16.7[b]	-3.84	∿ 100
16.6[c]	-11.3	
18.7[d]	-9.8	4
19.2[e]	-9.07	∿ 6.12
16.3[f]	-10.0	∿ 77
16.9[g]	-6.40	77
19.3[h]	-12.3	4.2
18.7[i]	-10.5	4.2
	-9.8[k]	4.2

TABLE 4.2. Experimental values for the conduction-band deformation potentials.

(a) Indirect piezo-absorption [32]

(b) Magnetoresistence [43]

(c) Cyclotron resonance and piezo-reflactance [44]

(d) Electron energy relaxation rates [49]

(e) Piezoresistence [45]

(f) Minority carrier mobility [46]

(g) Piezoresistence, relative population in the valleys [47]

(h) Electron cyclotron resonance, classical limit [39]

(i) Anisotropic phonon scattering and cyclotron resonance [48]

Ξ_u e.V.	Ξ_d e.V.	a E_{1G}=-3.8eV	e.V. E_{1G}=-2.9eV	Lattice Temperature ^oK
19.2	-9.07	1.13	.23	6.1
18.7	-9.8	0.23	-.66	4
19.3	-12.3	-2.1	-2.97	4.2
19.3	-6.4	3.83	2.93	
19.3	-4.4	5.8	4.9	
16.2	-10.0	-0.8	-1.7	77
16.3	-11.3	-2.0	-3.0	20 → 100^o
16.3	-4.4	-4.8	3.9	100
16.3	-6.4	-2.8	1.9	77

TABLE 4.3. Experimental values for the deformation potential a. Values for Ξ_d and Ξ_u taken from Table 4.2.

Lattice Temperature ^{o}K	Energy Exponent of the Lifetime (n)	Deformation Potential a eV
4		13
8	1	9
15		7
4		6.2
	3	
15		4.9

TABLE 4.4. Summary of calculations of the dependence of the deformation potential parameter on the energy exponent of the carrier lifetime.

Donor Density cm^{-3}	Acceptor Density cm^{-3}	Sample Name
1.7×10^{13}	4.8×10^{13}	Sa1 (3)
2.6×10^{13}	2.0×10^{14}	Sa2 (4)
3.6×10^{13}	5.8×10^{13}	Sa3 (5)
2.4×10^{14}	3.0×10^{14}	Sa4 (9)
4.9×10^{14}	7.0×10^{14}	Sa5 (11)
1.4×10^{13}	2.3×10^{14}	Sa6 (13)
3.4×10^{13}	5.7×10^{14}	Sa7 (15)
5.3×10^{13}	2.3×10^{14}	Sa8 (6)

TABLE 4.5. Summary of samples properties. The number in brackets corresponds to the identification number used by Bannaya et. al. [2].

Sample Name	Experimental Mobility	Calculated Mobility
Sa2	3.0×10^5	3.0×10^5
Sa4	1.2×10^5	1.2×10^5
Sa8	1.5×10^5	1.4×10^5
Sa5	1.0×10^5	5.7×10^4
Sa1	4.6×10^5	2.6×10^5
Sa3	2.2×10^5	1.9×10^5
Sa6	4.6×10^5	2.2×10^5
Sa7	2.3×10^5	1.3×10^5

TABLE 4.6. Summary of mobility calculations. Experimental data from Bannaya et. al. [2].

Sample Name	Average Carrier Lifetime $\overline{\tau}_{rec}$ sec	Experimental τ_{rec} sec	Average Carrier Energy in k_BT units	$\frac{\tau_{ac}(k_BT)}{\tau_{rec}(k_BT)}$	Average Acoustic Relaxation Time $\overline{\tau}_{ac}$ sec
Sa2	4.5×10^{-8}	1.3×10^{-8}	13.2	.8	5.6×10^{-10}
Sa4	6.7×10^{-9}	5.7×10^{-9}	17.7	7	4.7×10^{-10}
Sa8	1.7×10^{-8}	8.0×10^{-9}	10	1.6	6.3×10^{-10}
Sa5	2.3×10^{-9}	4.0×10^{-9}	13	14.4	4.7×10^{-10}
Sa1	9.2×10^{-8}	4.8×10^{-9}	9.2	.5	6.5×10^{-10}
Sa3	2.5×10^{-8}	1.4×10^{-8}	9.75	1	6.3×10^{-10}
Sa6	6.36×10^{-8}	5.4×10^{-9}	9.25	.4	6.3×10^{-10}
Sa7	2.65×10^{-8}	2.5×10^{-9}	9.85	1	6.3×10^{-10}

TABLE 4.7. Summary of carriers properties in Ga-Doped Ge samples. The experimental recombination lifetime from Bannaya et.al. [2].

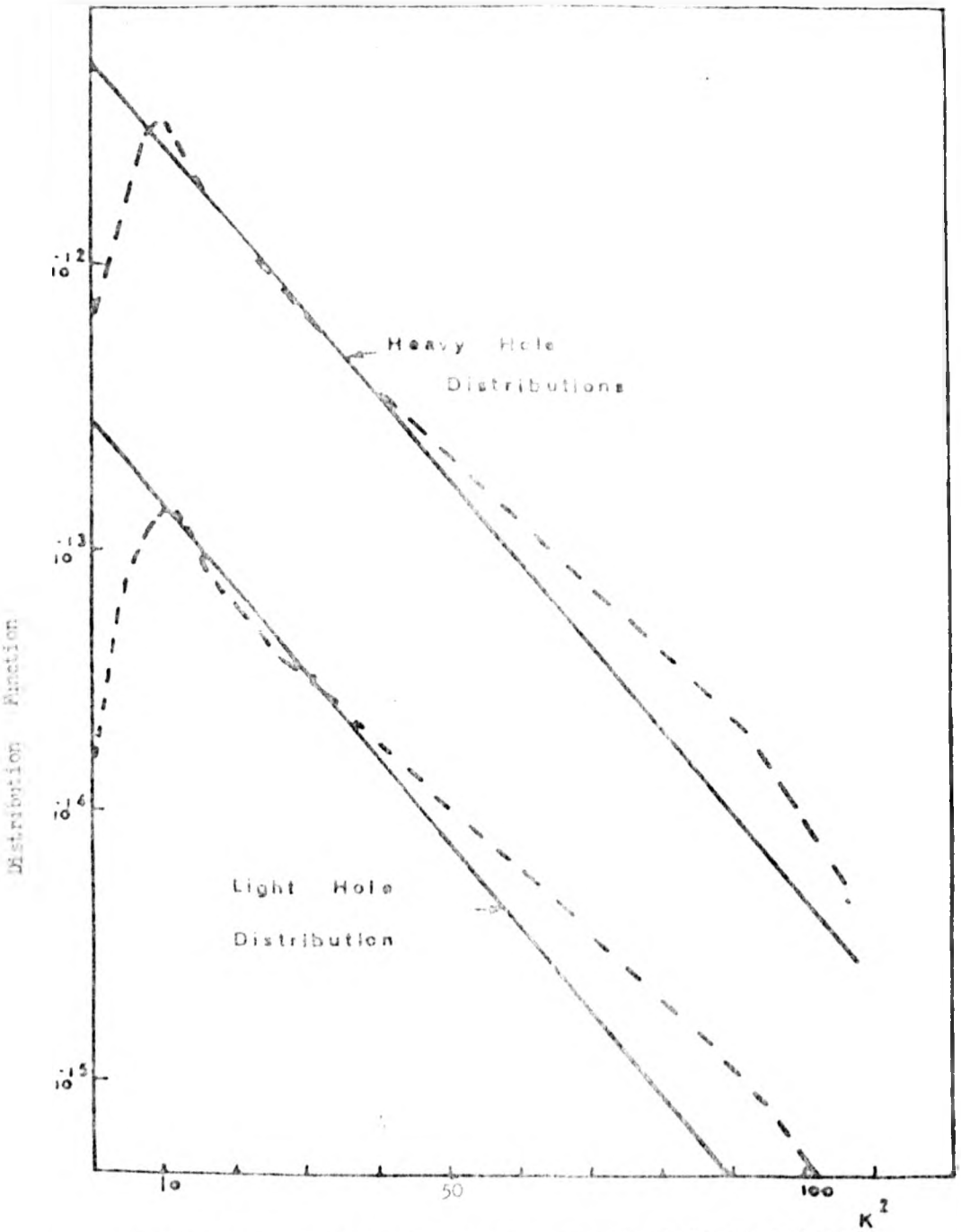

FIGURE 4.1: Comparison at the numerical (broken line) and the Maxwellian (continuous line) distribution functions for both bands in a Cu-doped Ge sample (S_5) at $4^{0}K$ and carrier temperature Te = $56^{0}K$.

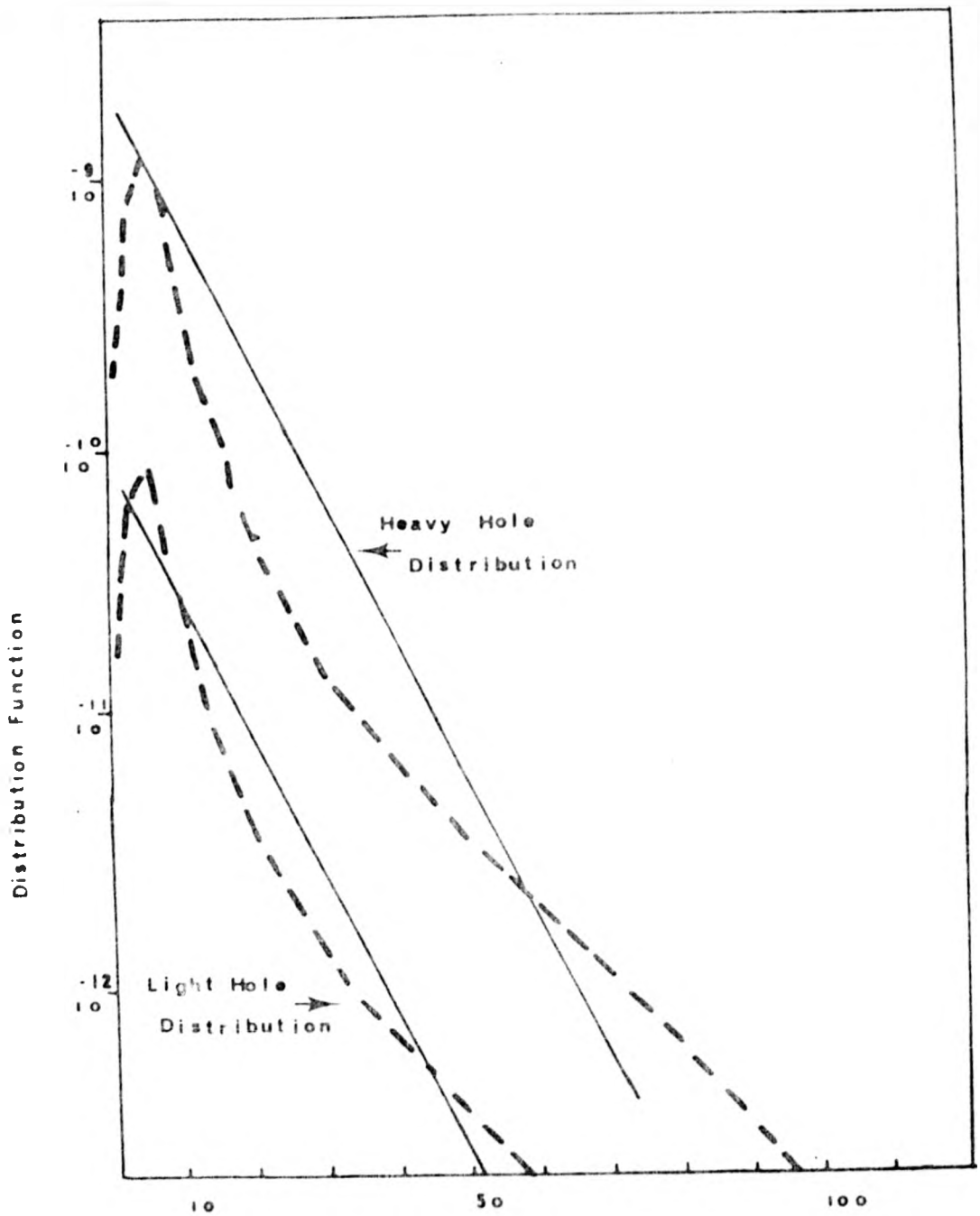

FIGURE 4.2: The distribution function (broken line) for both bands in a Ga-doped Germanium sample (Sa2) at $4^{O}K$. The continuous lines are hypothetical Maxwellians with carrier temperature Te = $44^{O}K$.

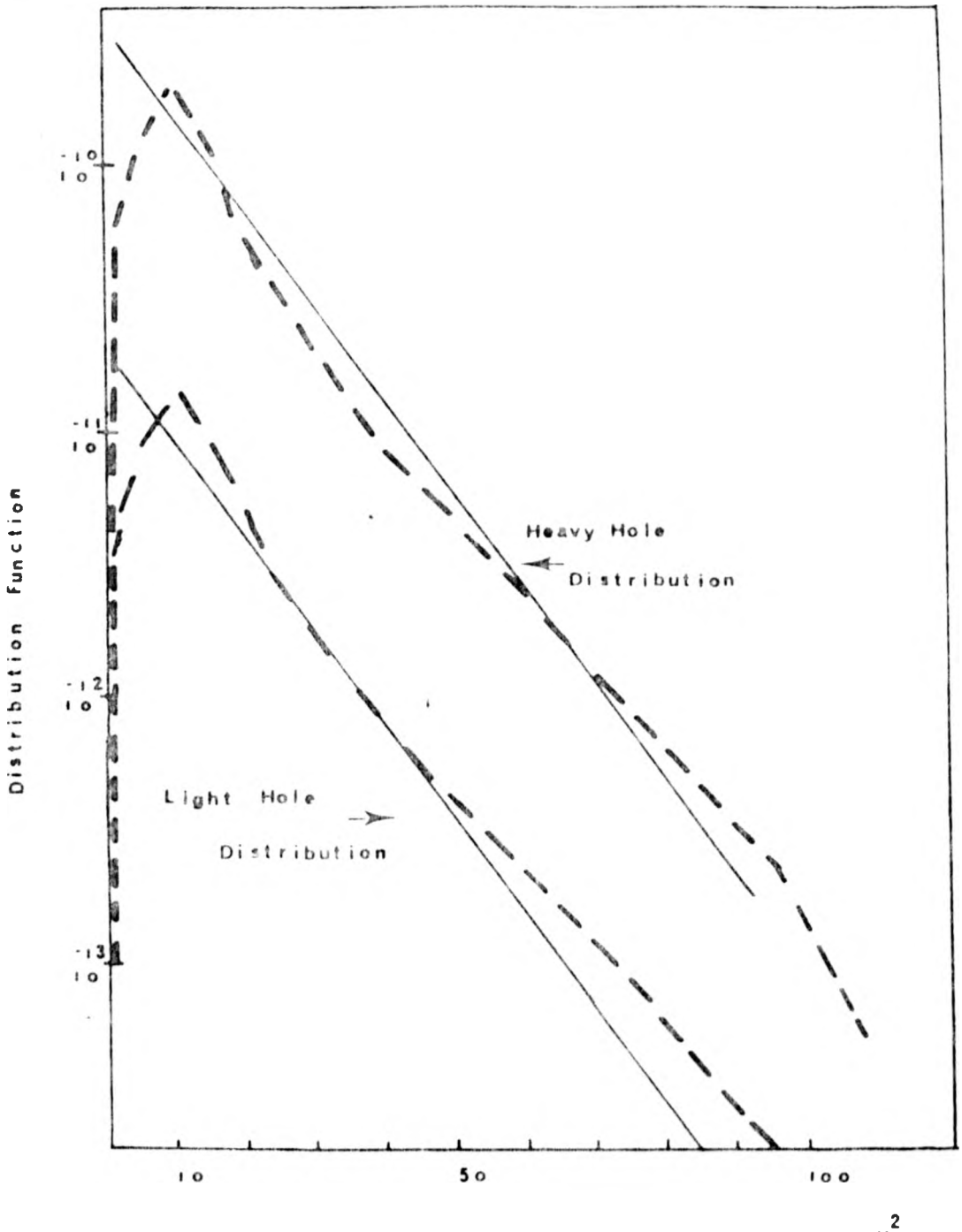

FIGURE 4.3: The distribution function (broken line) for both bands in a Ga-doped Germanium sample (Sa4) at $4^{O}K$. The continuous lines are hypothetical Maxwellians with carrier temperature Te = $55^{O}K$.

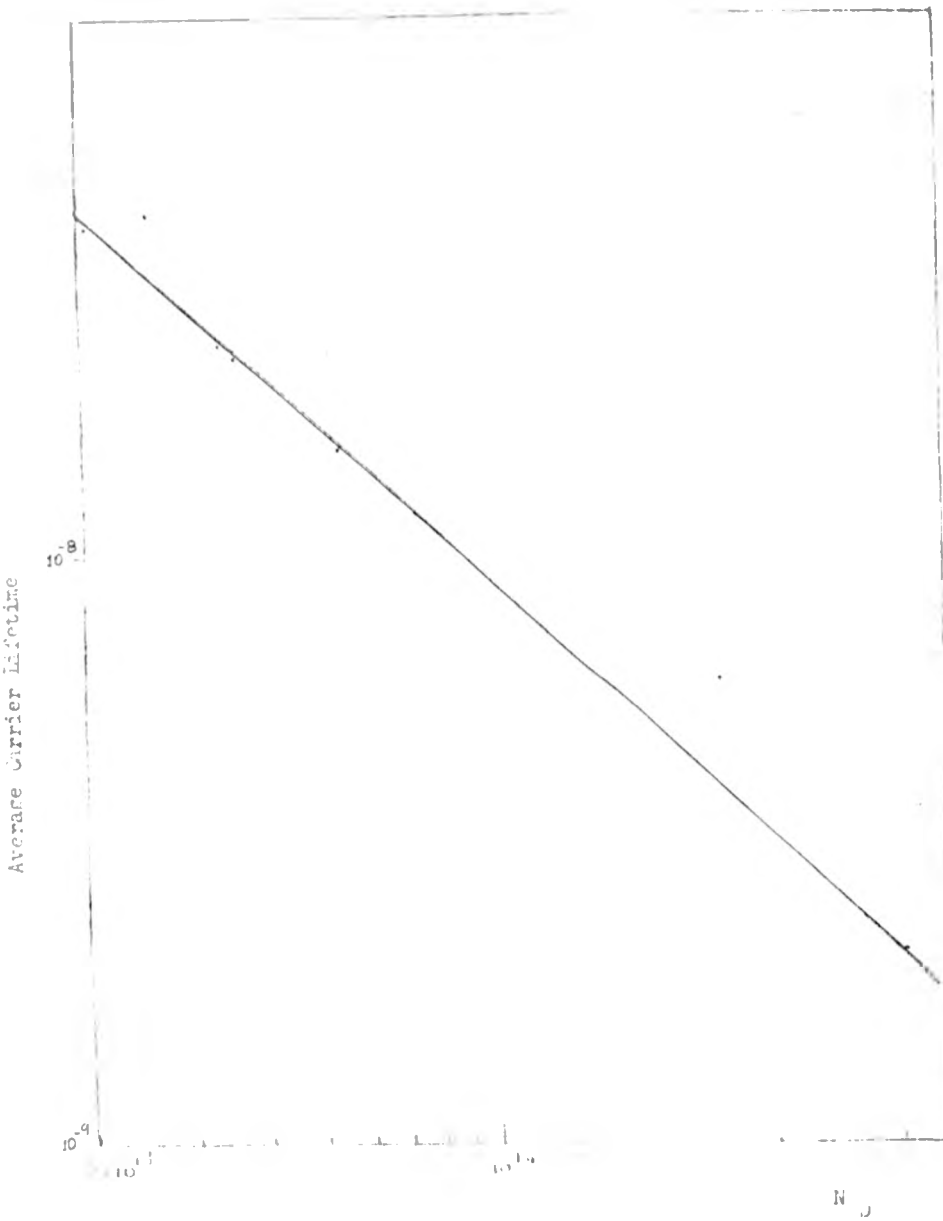

FIGURE 4.4: The average carrier lifetime for various Ga-doped Germanium samples at $4^{o}K$.

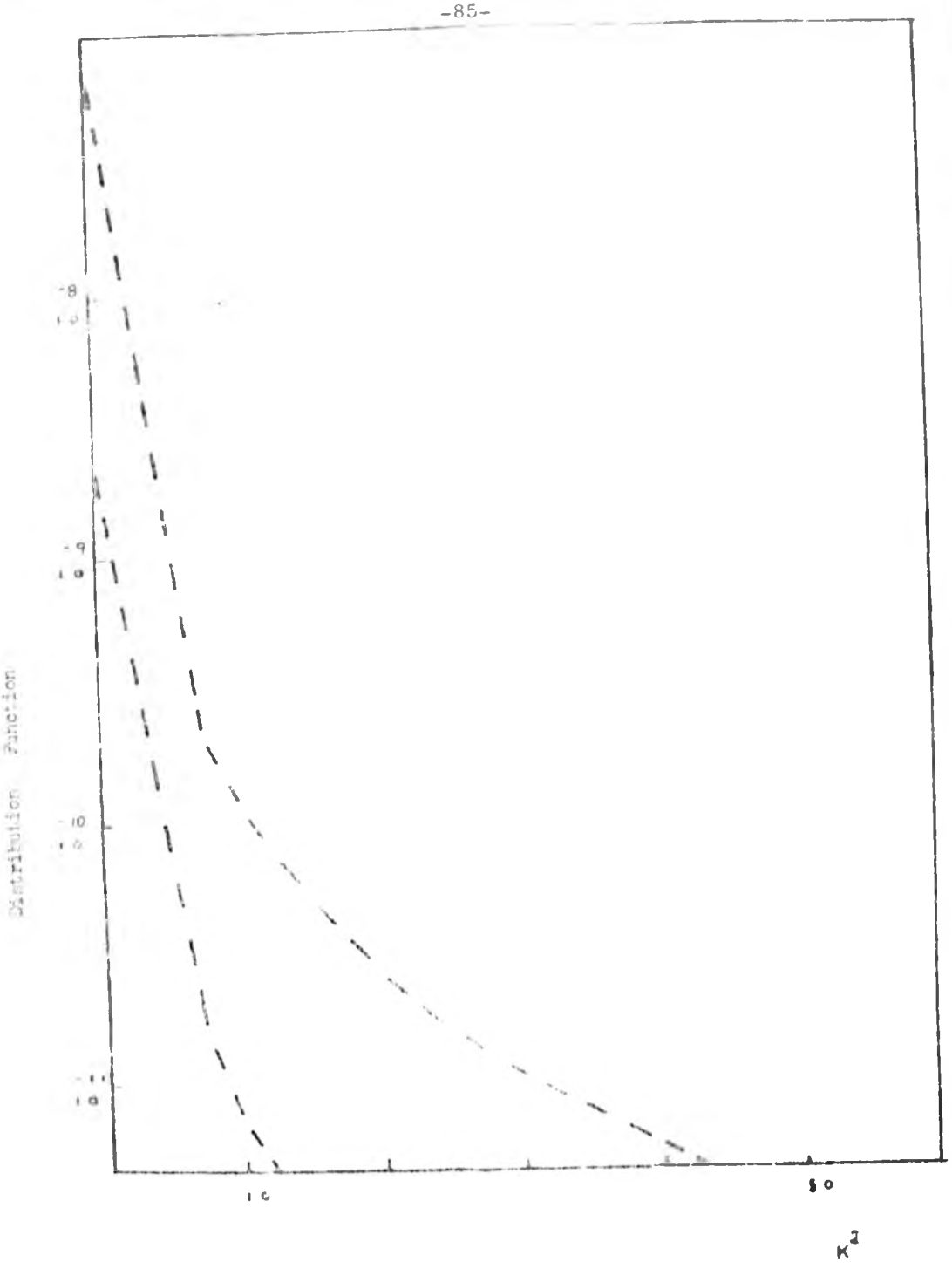

FIGURE 4.5: The distribution function for both bands in a Cu-doped Ge sample (S_1) at $4^{\circ}K$.

CHAPTER V

DISCUSSION

5.1. INTRODUCTION

This chapter is envisaged as a summary of some of the consequences of non-equilibrium distribution of carriers with regard to carriers properties (Section 5.2). In order to bring some light on some of the difficulties found during the course of this study, factors not included in the model are briefly discussed in connection with their possible consequences (Section 5.3). Some of those factors are roughly included in the original theoretical model and a new set of results is presented which partially explains the difficulties found in our study (Section 5.4). These new results suggest how the theoretical model can be improved and where further experimental research is needed.

5.2. SUMMARY OF RESULTS

Hot carrier distribution functions occur in semiconductors for carrier lifetimes smaller than the acoustic relaxation time. When both times are of the same order the carriers are warm and for greater values of the carrier lifetime the holes are in near thermal equilibrium. The form of the distribution function for both warm and hot carriers depends on the kind of photoexciation used. Thus for a narrow excitation spectrum and for low values of the initial photoexcitation energy ($\varepsilon_{ph} \sim 10$ meV) the distribution function has a non-Maxwellian form. However at higher excitation energies the distribution function resembles a Maxwellian function

with carrier temperature much greater than the lattice temperature T. This latter result is found for a low density system of carriers in which the inter-carrier scattering is ignored. Such a possibility of obtaining a Maxwellian function from a laser-type of radiation, has not been considered before.

A very narrow spectrum of photoexcitation also generates a series of equally spaced peaks at carriers wavevector equal to and less than the initial momentum K_{ph}. The appearance of these peaks is likened to the carriers emission of acoustic phonons with wavevectors equal to the threshold momentum. Such emission of phonons with quantum wavevectors has not previously been noted. Because the carrier lifetime and the mobility are averaged over the entire distribution function the presence of the peaks is hidden in those parameters. This suggests that the acoustic emission of phonons with quantum wavevector can only be seen in experiments in which the parameters are not automatically averaged over the distribution of carriers.

For the isotropic room temperature blackbody radiation and the one-band model the mobility and carrier lifetime in Cu-doped Ge samples with compensation densities less than 10^{13} cm^{-3} are successfully explained. The distribution function is, in this case, a Maxwellian function with carrier temperature correctly obtained from the energy balance equation. The holes are, for these samples, nearly in thermal equilibrium. At higher compensation densities the distribution function deviates from the Maxwellian form for most of the energy range. At $N_D > 10^{13}$ cm^{-3} the Maxwellian function and the solution of the rate equation give

identical mobilities but about 25% greater than the experimental data. For the two heavily compensated samples (S_4, S_5) the two-band model produces a significant improvement of the temperature dependence of the average lifetime as compared with the one-band model. The new dependence on the lattice temperature is in good agreement with the behaviour of the excess carrier density with temperature for those two samples.

Optimal fit of the photohall mobility data for Ga-doped Ge samples with compensation densities greater than 10^{13} cm^{-3} is obtained on assigning the value 2 for the deformation potential a. This value is in agreement with the one reported by Wiley. A similar value is also obtained from photohall data for a pure Cu-doped Ge sample. However the non-illuminated mobility data for this sample requires a much greater value for the deformation parameter (8.2 eV). The photohall mobility data for the heavily compensated samples give a value for the deformation potential which depends on the lattice temperature and is much greater than any of the experimental values for this parameter. It is thought that this anomaly in the fitting procedure for the value of a is partially due to the use of incorrect values of the capture cross-section and to weaknesses in the theoretical model. In this respect, we will discuss in Section 5.4 three possible improvements of the theoretical model. These improvements are connected with three physical situations for which the theory has failed to provide a satisfactory explanation of the experimental data. Our calculations do not reproduce the mobility dependence on the excitation energy at $\varepsilon_{ph} < 15$ meV. This difficulty arises as a consequence of the model of recombination which considers only an effective capture cross-section at all carrier energies. We shall

see that in order to remove this difficulty is required at least two effective capture cross sections. We shall also see that the experimental hot mobility data for the heavily compensated Cu-doped Germaniam samples can be fitted by averaging the calculated mobilities over a Maxwellian distribution function but with carrier temperature parameters much lower than those obtained from the energy balance equation. This result indicates that the carrier heating in the system is much less than that calculated. This failure suggests that the energy relaxation mechanisms considered in the theoretical model are not sufficient to give a correct account of the entire energy relaxation processes in the system under consideration. This difficulty can be partially removed by taking into account two-phonon processes. Finally because the inferred value of the deformation potential is affected by changes in the multiplicity factor of the Erginsoy's formula for the neutral impurity scattering time, we believe that temperature dependence of the deformation parameter can partially be due to an energy dependence of the scattering of holes by neutral impurities. A new formula is explored which reduces the temperature dependence of the deformation parameter slightly.

5.3. Revision of some factors not included in the theory

Instantaneous optical phonon emission is an assumption used throughout this study. Such an assumption leads us to consider that all carriers are in the range of energies below the optical phonon energy. This picture is, however, not far from the real

physical situation. The optical phonon emission occur in a very short, but finite time; this means that the majority (not all) of the carriers are in a range of energies below 0.037 eV. The presence of carriers outside this range of energies generates distributions of carriers at multiples of the optical phonon energy. The distribution function at each multiple is a rapidly decreasing function. The net effect of these distribution functions on the average transport parameters is thought to be negligible. However experimental mobility data as a function of the excitation energy at ε_{ph} close to ε_{op} could be used to obtain information about the carrier-lattice interaction via optical phonons. In this respect the theory of Lawaetz for this kind of scattering may be of interest. In this theory effects of long range forces of the quadruple and optupole type are included.

Since most of the carriers are in the range of energies below 37 meV the effect of non-parobolicity will be very small. It should be noted that at those energies the heavy and light hole bands are parabolic. Lawaetz has found in calculation of mobility and galvanomagnetic parameters in p-type Ge at room temperature that this effect produces changes of about 4%. At lower temperatures this effect is less important.

The conventional theory of acoustic deformation scattering is based on short range forces. Lawaetz [53] has included effects of long range forces for this scattering mechanism. A displacement of an atom in a crystal with a diamond type of lattice produces a disturbance in the surrounding change distribution which gives rise to moments of quadrupole and optupole nature.

Because in the experiments of Norton and Levinstein the samples were put in an integrating spherical cavity, the radiation on the crystal is isotropic and therefore the crystal can be considered isotropically homogeneous. For this kind of physical situation the net effect of the generalization of the scattering theory is one of reducing the value of the deformation potential by about 0.7 eV. Incidentally, measurements of the quadrupole and optupole coupling constants could lead to a better derivation of the deformation potentials Ξ_u and Ξ_d of the conduction band of Germaniam [56]. This consequently leads to a better determination of the deformation potential $\underline{a}$.

The applied magnetic field in the experiments of Norton and Levinstein [1] and Bannaya et.al. [2] is high. High magnetic fields may alter the density of states in the band due to the presence of Landau levels. It can also affect the Hall coefficient by the so-called "magnetic freeze out". This effect is basically the increasing in the impurity ionization energy due to quantization of the bound state wave function in the magnetic field. Of the data reported by Norton and Levinstein [1] we used only those in which the effects of the magnetic field are negligible. However the second effect could be significant [57] in the data for Ga-doped Ge reported by Bannaya et.al. These authors did not discuss this problem in that paper.

Norton [54] has found that the carrier lifetime (obtained from a model of decay of excess holes when the photon beam is switched off) presents dip at about 5 V/cm when the electrical field is changed. On the other hand the average lifetime from photohall

measurements does not show such a dip. The explanation of Norton for this experiment is based on the following elements.

i) Carriers recombine via acoustic and optical phonon emission.
ii) The cross section for the optical phonon emission shows a singularity at about the optical phonon energy (0.037 eV). Therefore the holes are able to gain energy from the electric field and reach energies about 0.037 eV which gives rise to the dip in the carrier lifetime as a function of the electric field.
iii) The magnetic field affect, present in the photohall measurements, this ability to gain energy from the electric field.

This experiment suggests that a generalization of the theoretical model to include the electric and magnetic fields will give new important information about the recombination processes. However a direct measurement of the time constant as a magnetic field is applied is needed to resolve this question.

5.4. ADDITIONAL RESULTS

5.4.1. Two Phonon Processes

The experimental photohall mobility data for the heavily compensated Cu-doped Ge samples (S_4, S_5) can be fitted by averaging the calculated mobilities over a Maxwellian distribution function but with carrier temperatures much lower than those obtained from the energy balance equation. The following table compares the new carrier temperatures with those of the energy balance equation.

Lattice Temperature ^{o}K	Sample Name	CARRIER TEMPERATURE TE(^{o}K) E.B.E.	Mobility Fitting
4		42	22
8	S_4	39	26
15		40	28
4		56	26
8	S_5	51	30
15		52	32

The fact that hot mobility data can be fitted with much lower values of the carrier temperature parameter indicates that the heating in the system of carriers is lower than calculated. This suggests the necessity of an extra energy relaxation mechanism to be included in order to account for the excess of energy still present in the system. Further support for this idea arises from the study of the experiments of Godik. The sample used in that study is very similar to the sample S_5 of Norton and Levinstein. For such a sample the ionised impurity scattering is the dominant scattering mechanism. The stronger the carrier heating is in that sample, the more the mobility is increased. It is noted that the mobilities of Norton and Levinstein are greater than those of Godik, therefore the carrier heating in the former case must be greater than in the second one.

Our calculations give average energies very close to each other.(Table 2.2 This suggests, again that the total energy relaxation is not correctly described in our model.

Alldredge and Blatt[58] have studied the role of the two-phonon processes in the energy relaxation of a heated-carrier distribution function. Their calculations showed that:

i) Either the direct two-phonon process and the interference of this process with the intermediate state process contribute very little to the energy relaxation time. The intermediate state process means that the carrier emit on an acoustic phonon and goes to a virtual state, to emit a second phonon almost immediately.

(ii) The intermediate state process is about the same order of magnitude of the one-single phonon process.

Their calculation is applicable to n-type Ge with a Maxwellian distribution of carriers and various carrier temperature parameters. The values of this parameter range from $5^{O}K$ to $115^{O}K$. The deformation parameter in the one-parameter theory is set equal to 10 eV as in the present calculations. Another basic assumption is that the lattice is at $T = 0^{O}K$. Our calculation with a one phonon process suggests that the inclusion of finite density of phonons produces only very mild changes. Under these conditions Alldredge and Blatt found that the average energy loss due to the intermediate states process is about twice that of the one-phonon.

Although the heavy-hole effective mass is about three times as large as the electron effective one, this deficiency is partially compensated by the values of Te used by Alldredge and

Blatt. Their results are not critically dependent on Te. We feel that the results found by them are also valid for p-type Germaniam.

An estimated value for the carrier temperature Te, in sample S_5, can be obtained by putting T = O in the expression for energy loss via one-phonon process (see Appendix 4), and using an average lifetime equal to 5×10^{-10} sec and the results of Alldredge and Blatt. The energy balance equation now becomes $314.22 - Te = .644\ Te^{3/2} + P_{two\text{-}phonon}$, where the term proportional to $Te^{3/2}$ is the rate of energy loss via one-phonon processes. $P_{two\text{-}phonon}$ is the rate of energy loss via two-phonon process. According to Alldredge and Blatt this rate is about twice the one-phonon term. The following table gives the values of the parameter Te for three values of the ratio R defined as the ratio of $P_{two\text{-}phonon}$ to $P_{one\text{-}phonon}$.

	R = O	R = 1	R = 2
Te	55	35	27

$Te = 55^{O}K$ is in good agreement with the value for this parameter obtained from the general expression for the energy balance equation, that is, $T \neq O$. The values of Te at R = 1 and R = 2 are much closer to those of the fitting mobility mentioned above. It is hoped that the inclusion of a finite density of phonon's ($T \neq O$) would give the correct temperature dependence of Te.

What this rough calculation shows is that the two-phonon processes are important in the calculation of hot mobilities in Cu-doped Ge samples. However more rigorous calculations are clearly needed in order to establish how the effect of two-phonon process affects the evaluation of other parameters such as the deformation potential. It is possible that the energy and momentum relaxation via two-phonon emission will be needed in order to bring the values of the deformation potential down to the experimental values.

5.4.2. Neutral Impurity Scattering Time

We think that dependence of the deformation potential parameter on temperature is partially due to a temperature dependence of the neutral scattering time. There is experimental evidence which suggests that this is the case. In an early study of the acoustic electric effect on n-type Germanium, Weinreich et.al. [58] found that the average neutral impurity scattering depends on T. More recently Blagosklonskaya et.al. [59] and Norton et.al. [60] have also arrived at the same conclusion. The usual model for this kind of scattering mechanism was given by Erginsoy [27]. This model gives constant neutral impurity scattering. Erginsoy derived this formula, for the scattering of electrons by neutral donors in semiconductors, on the assumption that this scattering is equivalent to that produced by hydrogen atoms and based its expression on the results of Massey and Moiseiwitsch [62]. Subsequent studies of the scattering of electrons by hydrogen atoms indicate that the polarization

produced on the neutral atom by the electric field arising from the scattered electron has not been correctly accounted for [59]. In particular it is noted that the Erginsoy model gives a cross section $\sigma = (20\ a_o)/K$ (where a_o is the Bohr radius and K is the electron wavevector) which diverges at K = 0, whereas according to Temkin [63] $\sigma \rightarrow$ constant at K = 0.

Blagonklonskaya et.al. [59] have derived an expression for the scattering of electrons by neutral atoms based on experimental data of Temkin [62] for scattering of electrons by hydrogen atoms. This new formula gives neutral impurity scattering times which varies with T and are in reasonable agreement with experimental data [59]. The new model takes into consideration the following factors:

i) The strong interaction of an electron with an unperturbed hydrogen atom, the exchange interaction and the polarization of the atom by the electric field of the scattered electron. The net potential is an attractive one.

ii) The zero phase δ_o is used for carrier energy less than $\varepsilon_{a/4}$ (ε_a is the activation energy). At higher energies the first (δ_1) and second (δ_2) phase shifts are also used.

The final expression for the neutral impurity scattering time takes the following form:

$$\tau_N^{-1} = \frac{F(\varepsilon/\varepsilon_a)h\ a_o^*}{m^*} N_N$$

where $F(\varepsilon/\varepsilon_a)$ is a function of that ratio, a_o^* the effective Bohr radius, m^* the effective mass and N_N the neutral impurity density. In our calculations we use an approximation expression for τ_N^{-1} [59] given by

$$\tau_N^{-1} = \frac{N_N \sqrt{2} \Pi a_o^{*2}}{\sqrt{m^*}} \left[\frac{1}{0.0275 + \frac{K^2}{K_a^2}} + 10 \right] K$$

where $K_a^2 = \frac{\varepsilon_a}{k_B T}$, this equation is consistent with figure 1 in the paper of Temkin [62]. This formula is in principle only valid for $\varepsilon/\varepsilon_a < \frac{1}{2}$. We however assumed that it is still valid up to $\varepsilon = 37$ meV.

The use of the new formula for the neutral impurity scattering time in the study of the mobility data of Godik [6] produces no changes in the calculated values for the deformation potentials (Chapter II). On the other hand, the new formula slightly reduces the variation of the deformation potential on the lattice temperature when applied to the study of the measurements of Norton and Levinstein [1] . The following table compares the new set of values of the deformation potential for sample S_5 with those previously obtained when the modified Erginsoy's formula was used (Chapter IV, Table 4.4).

Lattice Temperature ^{o}K	DEFORMATION POTENTIAL a (eV)	
	New values	Previous values
4	11	13
8	8.5	9
15	7	7.5

Finally, the new formula and the modified Erginsoy's expression give nearly identical values for the dark mobilities. Both calculated mobilities agree with the experimental data of Norton and Levinstein [28] if a $\sim$ 8.2 eV.

The small reduction in the temperature dependence of the calculated deformation potential obtained from the fitting of the hot mobility data of Norton and Levinstein certainly indicates that the neutral impurity scattering depends on the carriers energy as proposed.

How to take into account the fact that Cu impurities in Ge are non-hydrogenic is a problem which is not well understood. Further theoretical study is clearly needed in order to answer that question. The problems arise because the potential seen by the incident carrier at short distances (close to the atoms) is different from that of the hydrogen atom. This difference in the form of the potential at short distances affects the wave function within that potential and therefore the phase shifts may also be changed.

5.4.3. Recombination Lifetime

It was found in Chapter II that our calculations do not reproduce the dependence of the mobility on the excitation energy at $\varepsilon_{ph} < 15$ eV. We attempt to remove this difficulty by setting up a model of recombination which uses two effective capture cross sections. The background for this model goes as follows:

i). In order to describe the decay of excess carriers produced by CO_2 laser when the light pulse is switched off, Norton [54] needed a model of decay of the form

$$\frac{\Delta p}{\Delta p_{max}} = (1-b)\exp((t_o-t)/\tau_{fast}) + b\exp((t_o-t)/\tau_{slow})$$

where b is the relative percentage of the lower decay component, Δp_{max} is the excess carrier concentration at t_o when the light pulse is turned off, τ_{slow} and τ_{fast} are the two time constants required to fit the experimental data. The average time is then given by

$$\langle\tau\rangle = (1-b)\,\tau_{fast} + b\,\tau_{slow}$$

In all cases studied by Norton τ_{fast} is about one order of magnitude lower than τ_{slow} and $b \sim 39\%$.

(ii) The CO_2-laser photoexcitation energy is 0.117 eV and in our model this is equivalent to an effective photoexcitation of carriers at 7 m.eV. The distribution function for the sample under consideration (sample studied in Section 2.7) shows the

following characteristics: a). it is non-Maxwellian in form and b) it rapidly reaches a maximum and then decreases equally rapidly. The rapidly decreasing function can be approximated by a thermal Maxwellian function. Because of the striking difference between the two functions we can think of the system of carriers as being formed by two groups of carriers. Those below the maximum of the distribution function form one group. Carriers in this region (region I) are much more effective recombined than those carriers outside it, (region II). We then propose a model of recombination in which it is assumed that the capture cross section for carriers in the region one is much greater than that of the second group. Carriers in the first region will give rise to a τ_{fast} while the second one will give rise to τ_{slow}.

The calculated mobility at ε_{ph} = 10 meV agrees with experimental data of Godik [6] if the capture cross-section is given by:

$$\sigma \sim 15\sigma_o \quad \text{at } \varepsilon < \varepsilon_{ph}$$

$$\sigma = \sigma_o \quad \text{otherwise}$$

where σ_o is the experimental cross-section [17].

At other photoexcitation energies $10 < \varepsilon_{ph} < 15$ meV the capture cross section for the first region must gradually diminish until finally disappear any distinction between them.

This model of recombination suggests that the two constant lifetimes observed, for the decay of excess carriers, by Norton, is a consequence of the narrow type of photoexcitation used in the experiments and the photoexcitation energy associated with

that radiation source. Further study, at theoretical and experimental levels, of the decay of excess of carriers at other values of the excitation energy is clearly required to obtain a better understanding of the physics of this process.

REFERENCES

1. NORTON, P. and LEVINSTEIN, H. Phys. Rev. BC.478 (1973).
2. BANNAYA, V.F. LADYZHINSKII, Yu,P. and FULKS T.G., Soviet Physics. Semiconductors 7, 1319 (1974).
3. STOKER, H.J. and KAPLAN, N., Phys. Rev. 150, 619 (1966)
4. BESFAMILNAYA, V., KUROVA, I. ORMONT, N. and OSTROBORODOVA, V. Soveit Physics JETP 21, 1065 (1965).
5. GODIK, E.E., Phys. Stat. Solid 30, K127 (1968).
6. MATTIS, D.C., Phys. Rev. 120, 52 (1960).
7. HEARN, C.J., Proc. Phys. Soc. 86, 881 (1965).
8. HEARN, C.J., Proc. Phys. Soc. 88, 407 (1966).
9. LADYZHINSKII, Yu.P., Soviet Physics. Solid State 11, 1842 (1970).
10. BARKER, J.R. and HEARN, C.J., J. Phys. C. Solid State Phys. 6, 3097 (1973).
11. ROLLIN, B.V. and ROWELL, J.M., Proc. Phys. Soc. 76, 1001 (1960).
12. RIDLEY, B.K. and HARRIS, J.J., J. Phys. C. Solid State 9, 991 (1976).
13. CONWELL, E.M., Solid State Phys. Suppl. 9. High Field Transport in Semiconductors. New York Academic Press.
14. BARKER, J.R., Ph.D. Thesis. University of Warwick 1969.
15. LAX, M., Phys. Rev. 119, 1502 (1960).
16. KATSITADZE, A.P. KACHLISKRILI Z.S. and MOROZOVA, V.A., Soviet Phys. Semiconductors 4, 1486 (1971).
17. NORTON, P. and LEVINSTEIN, H., Phys. Rev. 86, 489 (1973).
18. ZIMAN, J.M. Electrons and Phonons. 1960. Oxford Univ. Press.
19. BIR, G.L., NORMANTAS, E and PIKUS, G.E. Soviet Physics Solid State 4, 869 (1962)
20. BIR, G.L., and PIKUS, G.E. Soviet Physics Solid State 2, 2039 (1960).

21. LAWAETZ, P., Phys. Rev. 174. 867 (1968).

22. WILEY, J.D., Solid State Comm. 8, 1865 (1970).

23. HENSEL, J.C. and SUZUKI, K., Phys. Rev. B9, 4219 (1974).

24. BROOKS, H. Adv. in Electronics and Electron Phys. Volume VII Edited by L. Marton, p. 161, Academic Press (1955).

25. FISHER, P. and FAN, H.Y., Phys. Rev. Letters 5, 195 (1960).

26. PAJOT, P. and DARVIOT, Y., Phys. Letters 21, 512 (1966).

27. ERGINSOY, C., Phys. Rev. 79, 1013 (1950).

28. NORTON, P. and LEVINSTEIN, H., Phys. Rev. B6, 470 (1973).

29. FOLLAND, N.O., Phys. Rev. B 2, 418 (1970).

30. CHEUNG, P.S.Y., Ph.D. Thesis, University of Warwick (1972).

31. POLLAK, F. and GARDONA, M. Phys. Rev. 172, 816 (1962).

32. BALSLEV, I. Solid State Communications 5, 315 (1967).

33. KANE, E.O. Phys. Chem. Solids 1, 82 (1956).

34. PINSON, W.E. and BRAY, R. Phys. Rev. 136, A 1449 (1964).

35. EHRENREICH, H. and OVERHAUSER, A.W. Phys. Rev. 104, 331 (1956).

36. BALSLEV, I. Phys. Letters 24A, 113 (1967).

37. POLLAK, E. and CARDONA, M. Phys. Rev. 172, 816 (1968).

38. GAVINI, A. and CARDONA, M. Phys. Rev. B1, 672 (1970).

39. MURASE, K. ENJOUJI, K. and OTSUKA, E. J. Phys. Soc. Japan 29, 1248 (1970).

40. POLLAK, F. and CHANDRASEKHAR, M. Phys. Rev. B15, 2127 (1977).

41. KITTEL, Ch., Introduction to Solid State Physics. J. Wiley and Sons 5th edition (1976).

42. PAUL, W. J. Appl. Phys. 32, 2082 (1961).

43. HERRING, C. and VOGHT, E. Phys. Rev. 101, 944 (1956).

44. BAGGULEY, D.M.S., FLAXEN, D.W. and STRADLING, R.A. Phys. Letters 1, 111 (1962). J. Phys. Soc. Japan 29, 685 (1970).

21. LAWAETZ, P., Phys. Rev. 174. 867 (1968).

22. WILEY, J.D., Solid State Comm. 8, 1865 (1970).

23. HENSEL, J.C. and SUZUKI, K., Phys. Rev. B9, 4219 (1974).

24. BROOKS, H. Adv. in Electronics and Electron Phys. Volume VII Edited by L. Marton, p. 161, Academic Press (1955).

25. FISHER, P. and FAN, H.Y., Phys. Rev. Letters 5, 195 (1960).

26. PAJOT, P. and DARVIOT, Y., Phys. Letters 21, 512 (1966).

27. ERGINSOY, C., Phys. Rev. 79, 1013 (1950).

28. NORTON, P. and LEVINSTEIN, H., Phys. Rev. B6, 470 (1973).

29. FOLLAND, N.O., Phys. Rev. B 2, 418 (1970).

30. CHEUNG, P.S.Y., Ph.D. Thesis, University of Warwick (1972).

31. POLLAK, F. and GARDONA, M. Phys. Rev. 172, 816 (1962).

32. BALSLEV, I. Solid State Communications 5, 315 (1967).

33. KANE, E.O. Phys. Chem. Solids 1, 82 (1956).

34. PINSON, W.E. and BRAY, R. Phys. Rev. 136, A 1449 (1964).

35. EHRENREICH, H. and OVERHAUSER, A.W. Phys. Rev. 104, 331 (1956).

36. BALSLEV, I. Phys. Letters 24A, 113 (1967).

37. POLLAK, E. and CARDONA, M. Phys. Rev. 172, 816 (1968).

38. GAVINI, A. and CARDONA, M. Phys. Rev. B1, 672 (1970).

39. MURASE, K. ENJOUJI, K. and OTSUKA, E. J. Phys. Soc. Japan 29, 1248 (1970).

40. POLLAK, F. and CHANDRASEKHAR, M. Phys. Rev. B15, 2127 (1977).

41. KITTEL, Ch., Introduction to Solid State Physics. J. Wiley and Sons 5th edition (1976).

42. PAUL, W. J. Appl. Phys. 32, 2082 (1961).

43. HERRING, C. and VOGHT, E. Phys. Rev. 101, 944 (1956).

44. BAGGULEY, D.M.S., FLAXEN, D.W. and STRADLING, R.A. Phys. Letters 1, 111 (1962). J. Phys. Soc. Japan 29, 685 (1970).

45. FRITZSCHE, H.,Phys. Rev. 115, 336 (1959)

46. SCHETZINA, J.F. and MEKELVEY, J.P., Phys. Rev. 181, 1191 (1969).

47. BARANSKII, P.I. and KOLOMOETZ, V.V.,Phy. States Solid (b) 45, K55 (1971).

48. ITO, R, KAWAMURA, H. and FURAI, M., Phys. Letters 13, 26 (1964).

49. ZYLBERSTEJN, A.,Proc. Tenth Conf. Sem. p. 134 (1970).

50. HALL, J.J., Phys. Rev. 128, 68 (1962).

51. VAN VECHTEN, J.A., Phys. Rev. 187, 1007 (1969).

52. GODIK, E.E. and POKROVSKII, Ya.E.,Soviet Physics Solid State 6, 1870 (1965).

53. LAWAETZ, P., Phys. Rev. 183, 730 (1969).

54. NORTON, P., Ph.D. Thesis Syracuse University (1970).

55. MYCIELSKI,J., NEGRETE, P. and NOGUERA B, A. Solid State Comm. 11, 113, (1972).

56. GALLAGHER, J., Phys. Rev. 171, 987 (1968).

57. ALLDREDGE, G.P. and BLATT, F.J., Annals of Physics 45, 191 (1967).

58. WEIREICH, G, SANDERS, T.M. Jr. and WHITE, H.,Phys. Rev. 114, 33 (1959).

59. BLAGOSKLONSKAYA, L.E., GERSHENZON, E.M., LADYZHINSKII, Yu. P. and POPOVA, A.P. , Soviet Physics Solid State 11,2402 (1970).

60. NORTON, P. BRAGGINS, J. and LEVINSTEIN, H.,Phys. Rev. B 8, 5632 (1973).

61. MASSEY, H. J. and MOISEIWITSCH, B.L.,Proc. Roy. Soc. 205A, 483 (1951).

62. TEMKIN, A., Phys. Rev. 121, 788 (1961).

63. BARDEEN, J. and SCHOCKLEY, W.,Phys. Rev. 80, 72 (1950).

APPENDIX 1

THE ACOUSTIC SCATTERING RATE (J)

We give here expressions for the inelastic rate, $J_i(\underset{\sim}{k})$, out of state $\underset{\sim}{k}$ in band i via the emission of acoustic phonons. The distribution function $f_i(\underset{\sim}{k})$ is a function of the energy only. For a non-degenerate semiconductor $f_i(\underset{\sim}{k}) << 1$ so that we can ignore the restrictions due to the Pauli principle.

The rate of change of $f_i(\underset{\sim}{k})$ with time due to the scattering may be written as

$$\frac{\partial f_i(\underset{\sim}{k})}{\partial t} = - J_i(\underset{\sim}{k}) =$$

$$= - \frac{1}{(2\pi)^3} \sum_{j=1,2} \left(f_i(\underset{\sim}{k}) \int W_{ij}(\underset{\sim}{k},\underset{\sim}{k}') \, d^3k' \right. \qquad (1)$$

$$\left. - \int f_i(\underset{\sim}{k}') \, W_{ji}(k',k) \, d^3k' \right)$$

where $W_j(\underset{\sim}{k},\underset{\sim}{k}')$ are the transition probabilities averaged over the two degenerate (spin degeneracy) initial states of the band i with wavevector $\underset{\sim}{k}$ and summed over the final degenerate states of the band j with wavevector $\underset{\sim}{k}'$. The first terms in (1) describe the intraband scattering in the band i (=j) and interband transition into the band $j(\neq i)$, whereas the second term describes the arrival from both bands. In the more general theory of acoustic deformation scattering [20], the transition probabilities depend not only on the scattering angle θ but also on the direction of $\underset{\sim}{k}$ and $\underset{\sim}{k}'$ relative

to the crystal axes. In order to simplify the calculations based on the solution of the rate equations (eq. 4.2.7) the following assumptions are made [19]:

i). The two bands are parabolic, and isotropic, that is, the constant energy surfaces are spheres (eq. 4.2.1).

ii). The transition probabilities depend only on the scattering angle θ, the initial and the final energies.

$$W_{ij} = P_{ij}(\varepsilon_i, \varepsilon_j, \theta)\ \delta(\varepsilon_i, - \varepsilon_j + \hbar\omega_q) \tag{2}$$

where the transition probabilities P_{ij} are given by

$$p^L_{ii} = \frac{a^2 \Pi q}{4\rho S_L} \left[\bar{n}_q + \frac{1}{2} \pm \frac{1}{2}\right]\{(1\pm\eta)^2 + \frac{9}{4}\eta^2 - 6\eta(\frac{\eta}{4} \pm 1)\cos\theta + 3(1-\frac{\eta^2}{4})\cos^2\theta\} \tag{3}$$

$$p^L_{12} = p^L_{21} = \frac{3a^2 \Pi q}{4\rho S_L} \left[\bar{n}_q + \frac{1}{2} \pm \frac{1}{2}\right]\{\sin^2\theta[1-\frac{\eta^2}{4} + 2\eta[\delta_1 + \frac{\eta}{4}\delta_2] + \frac{3}{4}\eta^2\delta_1^2]\} \tag{4}$$

$$p^T_{ii} = \frac{9a^2 \Pi q}{16\rho S_T} \left[\bar{n}_q + \frac{1}{2} \pm \frac{1}{2}\right]\{\eta^2 \sin^2\theta\} \tag{5}$$

$$p^T_{12} = p^T_{21} = \frac{3a^2 \Pi q \eta^2}{2\rho S_T} \left[\bar{n}_q + \frac{1}{2} \pm \frac{1}{2}\right]\{1 - \frac{3}{8}\sin^2\theta(1 + \delta_1)\}$$

where $\eta = \frac{\bar{b}}{a}$ (The shear and dilatational deformation potentials), $\bar{n}_q$ is the average phonon density equal to the Bose-Einstein distribution

$$\bar{n}_q = \frac{1}{\exp(hSq/k_BT) - 1}, \qquad S = S_L,\ S_T$$

$$\delta_{1,2} = \frac{1 \mp \gamma^2 \frac{\varepsilon}{\varepsilon'}}{1 + \gamma^2 \frac{\varepsilon}{\varepsilon'} - 2\gamma\sqrt{\varepsilon/\varepsilon'}\cos\theta}$$

$\gamma^2 = m_1/m_2 = .13$ and ε/ε' is the ratio of initial to final hole energies. In calculations of $\delta_{1,2}$ this ratio has been set equal to 1. The sign + (-) in the first parenthesis of equations 3 to 6 are related to emission (absorption) of phonons. The sign + (-) in the second parenthesis is for light (heavy) holes.

In thermal equilibrium $f_i(\underset{\sim}{k})$ is proportional to $\exp(-\varepsilon_i/k_BT)$, where ε_i is the carrier energy in the band i and the total scattering rate (1) vanishes identically. The principle of detail balance gives

$$W_{ii}(\underset{\sim}{k},\underset{\sim}{k}') \exp(-\varepsilon_i/k_BT) = W_{ii}(\underset{\sim}{k}'k) \exp(-\varepsilon_i'/k_BT) \tag{7}$$

and

$$W_{ij}(\underset{\sim}{k},\underset{\sim}{k}') \exp(-\varepsilon_i/k_BT) = W_{ji}(\underset{\sim}{k}',\underset{\sim}{k}) \exp(-\varepsilon_j/k_BT) \tag{8}$$

An equation similar to (7) can be used to give an expression for the scattering rate J in the one-band model [14]

$$J(\underset{\sim}{k}) = -\frac{1}{(2\pi)^3}\int d^3k' G(\underset{\sim}{k},\underset{\sim}{k}') [f(\underset{\sim}{k}') \exp(\varepsilon'/k_BT) - f(k)\exp(\varepsilon/k_BT)] \tag{9}$$

where $G(\underset{\sim}{k},\underset{\sim}{k}') = W(\underset{\sim}{k},\underset{\sim}{k}') \exp(-\varepsilon/k_BT)$ and $W(\underset{\sim}{k},\underset{\sim}{k}')$ is given by

$$W(\underset{\sim}{k},\underset{\sim}{k}') = \sum_{q} \frac{2\pi}{\hbar} \{ | < \underset{\sim}{k}', n_q | H' | \underset{\sim}{k}, n_q + 1 > |^2 \delta(\varepsilon' - \varepsilon - \hbar\omega_q)$$

$$+ | <k', n_q | H' | k, n_q - 1> |^2 \delta(\varepsilon' - \varepsilon + \hbar\omega_q) \} \qquad (10)$$

where $\hbar\omega_q$ is the energy of a phonon with wavevector $\underline{q}$. The state $| k, n_q)$ describes an electron with wavevector $\underset{\sim}{k}$ and n_q phonons with wavevector $\underset{\sim}{q}$. The first term in (10) represents scattering with emission of a phonon, whereas the second one involves phonon absorption. H' is the perturbation Hamiltonian due to the electron-acoustic interaction. This Hamiltonian has been studied, in the one band model, by Shockley et.al [64]. H' is locally equivalent to the energy shift in the band edge produced by a homogeneous strain equal in magnitude to the local strain induced by the lattice vibration. The matrix elements in (10) can be written in the form [13]

$$| < \underset{\sim}{k}', n_q | H' | \underset{\sim}{k}, n_q \pm 1 > |^2 = \frac{D^2 \hbar\omega_q}{2\rho S_L^2} [\bar{n}_q + \frac{1}{2} \pm \frac{1}{2}] \delta \underset{\sim}{k}', \underset{\sim}{k} \pm \underset{\sim}{q} \qquad (11)$$

where D is the deformation potential, ρ is the mass density and $\bar{n}_q$ is the thermal distribution of phonons. With (11) and (10) into (9), the final expression for $J(\underset{\sim}{k})$, in the one-band case, is [14]

$$J(K) = - Y(f(K)) + Z(K)\, f(K) \qquad (12)$$

$$= -\frac{D_o}{K}\left[\int_a^b - \int_c^d \frac{K'(K^2-K'^2)^2 f(K')\,dK'}{1-\exp(K^2-K'^2)}\right.$$

$$+\frac{D_o}{K} f(K)\left[\int_a^b - \int_c^d \frac{K'(K^2-K'^2)^2\,dK'}{\exp(K'^2-K^2)-1}\right.$$

where

$$D_o = \frac{(k_B T)^{5/2}\, m_2 1/2\, D^2}{\pi 2\sqrt{2}\,\rho\,(hS_L)^4}$$

and the range of integration is defined as follows:

$$\begin{aligned}
a &= K && K > K_\alpha/2\\
&= K_\alpha - K && K < K_\alpha/2\\
b &= K + K_\alpha && \text{all } K\\
c &= K && K < K_\alpha/2\\
&= K_\alpha - K && K_\alpha/2 < K < K_\alpha\\
&= K - K_\alpha && K > K\\
d &= K && \text{all } K
\end{aligned} \qquad (13)$$

where $K_\alpha = 2\left(\frac{m_2 S_L^2}{k_B T}\right)^{\frac{1}{2}}$

It should be noted that the conservation of carriers follows immediately from equation (9)

$$\sum_{\underset{\sim}{k}} J(\underset{\sim}{k}) = 0$$

This latter condition in the two-band model becomes

$$\sum_{\underset{\sim}{k}} (J_1(\underset{\sim}{k}) + J_2(\underset{\sim}{k})) = 0$$

The scattering rate J_i out of state K can be written in a similar way to equation 2.3.1, that is

$$J_i(f_i,f_j) = [Z_{ii}(K) + Z_{ij}(K)]f_i(K) - \{Y_{ii}(f_i) + Y_{ij}(f_j)\} \qquad (14)$$

then a formal solution of the rate equation 4.2.2. is given as follows:

$$f_i(K) = \frac{\bar{\omega}_{ph_i}(K) + Y_{ii}(f_i) + Y_{ji}(f_j)}{\frac{K}{\tau_{rec_i}(K)} + Z_{ii}(K) + Z_{ij}(K)}$$

where $\bar{\omega}_{ph_i}(K)$ and $\tau_{rec_i}(K)$ are the excitation rate and recombination lifetime for the band i. The mathematical form for each one of the terms in (14) are as follows.

$$Z_{ii}(K) = \frac{D_{o_i}}{K}\left\{\int_\alpha^\beta + \int_\gamma^\delta\right\}\frac{(K'^2 - K^2)^2}{|\exp(K'^2-K^2) - 1|}\left[\psi_{ii}^{L} + \frac{9}{4}\left(\frac{S_L}{S_T}\right)^4 \psi_{ii}^{T}\right] K'dK' \qquad (16)$$

$$Z_{ij}(K) = 3\left(\frac{m_j}{m_i}\right)\frac{D_{o_i}}{K}\left\{\int_\alpha^\beta + \int_\gamma^\delta\right\}\frac{(K'^2-K^2)^2}{|\exp(K'^2-K^2) -1|}\left[\psi_{ij}^{L} + 2\left(\frac{S_L}{S_T}\right)^4 \psi_{ij}^{T}\right] K'dK' \qquad (17$$

$$Y_{ii}(K) = \frac{D_{o_i}}{K}\left\{\int_\alpha^\beta + \int_\gamma^\delta\right\}\frac{(K'^2-K^2)^2 f_i(K')}{|\exp(K^2-K'^2)-1|}\left[\psi_{ii}^{L} + \frac{9}{4}\left(\frac{S_L}{S_T}\right)^4 \psi_{ii}^{T}\right] K'dK' \qquad (18)$$

$$Y_{ij}(K)=3\left(\frac{m_i}{m_j}\right)\frac{1}{2}D_{o_i}\left\{\int_\alpha^\beta + \int_\gamma^\delta\right\}\frac{(K'^2-K^2)^2 f_i(K')}{|\exp(K^2-K'^2)-1|}\left[\psi_{ij}^{L} + 2\left(\frac{S_L}{S_T}\right)^4 \psi_{ij}^{T}\right] K'dK' \qquad (19)$$

where the integrand functions $\psi_{ij}^{L,T}$ are the terms in the second brackets ({}) of equations (3) to (6), that is

$$\psi_{ii}^{L} = (1\pm\eta)^2 + \frac{9}{4}\eta^2 - 6\eta(\eta/4 \pm 1)\cos\theta_{ii}^{L} + 3\cos\theta_{ii}^{L}(1-\eta^2/4)$$

$$\psi_{ii}^{T} = \eta^2 \sin^2\theta_{ii}^{T}$$

$$\psi_{ij}^{L} = \sin^2\theta_{ij}^{L}\left[1 - \frac{\eta^2}{4} + 2\eta(\delta_1 + \delta_2\eta/4) + \frac{3}{4}\eta^2\delta_1^2\right]$$

$$\psi_{ij}^{T} = 1 - \frac{3}{8}\sin^2\theta_{ij}^{T}(1 + \delta_1^2)$$

where $\dfrac{(K^2 - K'^2)^2}{(L,T)}$

$$\cos\theta_{ii}^{(L,T)} = \frac{K^2 + K'^2 - 4KA_i^2}{2KK'}$$

$$\cos\theta_{ij}^{(L_1T)} = \frac{\sqrt{\frac{m_i}{m_j}}K^2 + \sqrt{\frac{m_j}{m_i}}K'^2 - 4KA_i^{(L,T)}\dfrac{(K^2 - K'^2)^2}{KA_1^{L,T}}}{2KK'}$$

$$KA_i^{(L,T)} = \left[\frac{m_i S_{(L,T)}^2}{2k_BT}\right]^{\frac{1}{2}} \quad \text{and} \quad D_{o_i} = \frac{a^2(k_BT)^{5/2}m_i^{\frac{1}{2}}}{8\sqrt{2}\,\Pi\,(hS_L)^4\rho}$$

The range of integration in equations (16) to (19), when i = j is identical to that defined in (13) but $K_\alpha/2$ now becomes either KA_i^L or KA_i^T according to what type of function $\psi_{ij}^{L,T}$ is in the integrand of those integral equations.

For i = 1 and j = 2, the range of integration for K' is

$$\psi_{ii}^{L} = (1\pm\eta)^2 + \frac{9}{4}\eta^2 - 6\eta(\eta/4 \pm 1)\cos\theta_{ii}^{L} + 3\cos\theta_{ii}^{L}(1-\eta^2/4)$$

$$\psi_{ii}^{T} = \eta^2 \sin^2\theta_{ii}^{T}$$

$$\psi_{ij}^{L} = \sin^2\theta_{ij}^{L}\left[1 - \frac{\eta^2}{4} + 2\eta\left(\delta_1 + \delta_2\,\eta/4\right) + \frac{3}{4}\eta^2\delta_1^2\right]$$

$$\psi_{ij}^{T} = 1 - \frac{3}{8}\sin^2\theta_{ij}^{T}\left(1 + \delta_1^2\right)$$

where

$$\cos\theta_{ii}^{(L,T)} = \frac{K^2 + K'^2 - 4\,KA_i^2}{2\,KK'}$$

$$\cos\theta_{ij}^{(L_1T)} = \frac{\sqrt{\frac{m_i}{m_j}}\,K^2 + \sqrt{\frac{m_j}{m_i}}\,K'^2 - 4\,KA_i^{(L,T)}\,KA_1^{L,T}}{2\,K\,K'}$$

$$KA_i^{(L,T)} = \left[\frac{m_i\,S_{(L,T)}^2}{2\,k_BT}\right]^{\frac{1}{2}}, \quad \text{and} \quad D_{o_i} = \frac{a^2\,(k_BT)^{5/2}m_i^{\frac{1}{2}}}{8\sqrt{2}\,\Pi\,(hS_L)^4\rho}$$

The range of integration in equations (16) to (19), when i = j is identical to that defined in (13) but $K_\alpha/2$ now becomes either KA_i^L or KA_i^T according to what type of function $\psi_{ij}^{L,T}$ is in the integrand of those integral equations.

For i = 1 and j = 2, the range of integration for K' is

$$\alpha = KA_2 + (K^2 + KA_2^2 - 2K\,KA_1)^{\frac{1}{2}} \qquad \text{all } K$$

$$\beta = KA_2 + (K^2 + KA_2^2 - 2K\,KA_1)^{\frac{1}{2}} \qquad \text{all } K$$

$$\gamma = KA_2 - (KA_2^2 + K^2 - 2K\,KA_1)^{\frac{1}{2}} \qquad K < 2\,KA_1$$

$$= -KA_2 + (K^2 + KA_2^2 - 2K\,KA_1)^{\frac{1}{2}} \qquad K > 2\,KA_1$$

$$\delta = -KA_2 + (K^2 + KA_2^2 + 2K\,KA_1)^{\frac{1}{2}} \qquad \text{all } K$$

It should be noted that sound velocity in either KA_1 or KA_2 should correspond to whatkind of integrand function $\psi_{ij}^{L,T}$ is in the integral equation.

The limits of integration for K' when i = 2 and j = 1 are

$$\alpha = KA_1 + (K^2 + KA_1^2 - 2\,KA_2K)^{\frac{1}{2}} \qquad K \leq \frac{KA_2}{\sqrt{200}}$$

$$= -KA_1 + (K^2 + KA_1^2 + 2K\,KA_2)^{\frac{1}{2}}$$

$$= -KA_1 + (K^2 + KA_1^2 + 2K\,KA_2)^{2} \qquad K > \frac{KA_2}{\sqrt{200}}$$

$$\beta = KA_1 + (K^2 + KA_1^2 + 2K\,KA_2)^{\frac{1}{2}} \qquad K \leq \frac{KA_2}{\sqrt{200}}$$

$$= KA_1 - (K^2 + KA_1^2 - 2K\,KA_2)^{\frac{1}{2}}$$

$$= KA_1 + (K^2 + KA_1^2 + 2K\,KA_2)^{\frac{1}{2}} \qquad K > \frac{KA_2}{\sqrt{200}}$$

$$\gamma = KA_1 - (KA_1^2 + K^2 - 2K\,KA_2)^{\frac{1}{2}} \qquad 1.93KA_2 \leq K \leq 2\,KA_2$$

$$= -KA_1 + (KA_1^2 + K^2 - 2K\,KA_2)^{\frac{1}{2}} \qquad K > 2\,KA_2$$

$$\delta = -KA_1 + (K^2 + KA_1^2 + 2K\,KA_2)^{\frac{1}{2}} \qquad K > 1.93\,KA_2$$

In order to remove any confusion from the range of integration of K', this can be drawn for each case as follows:

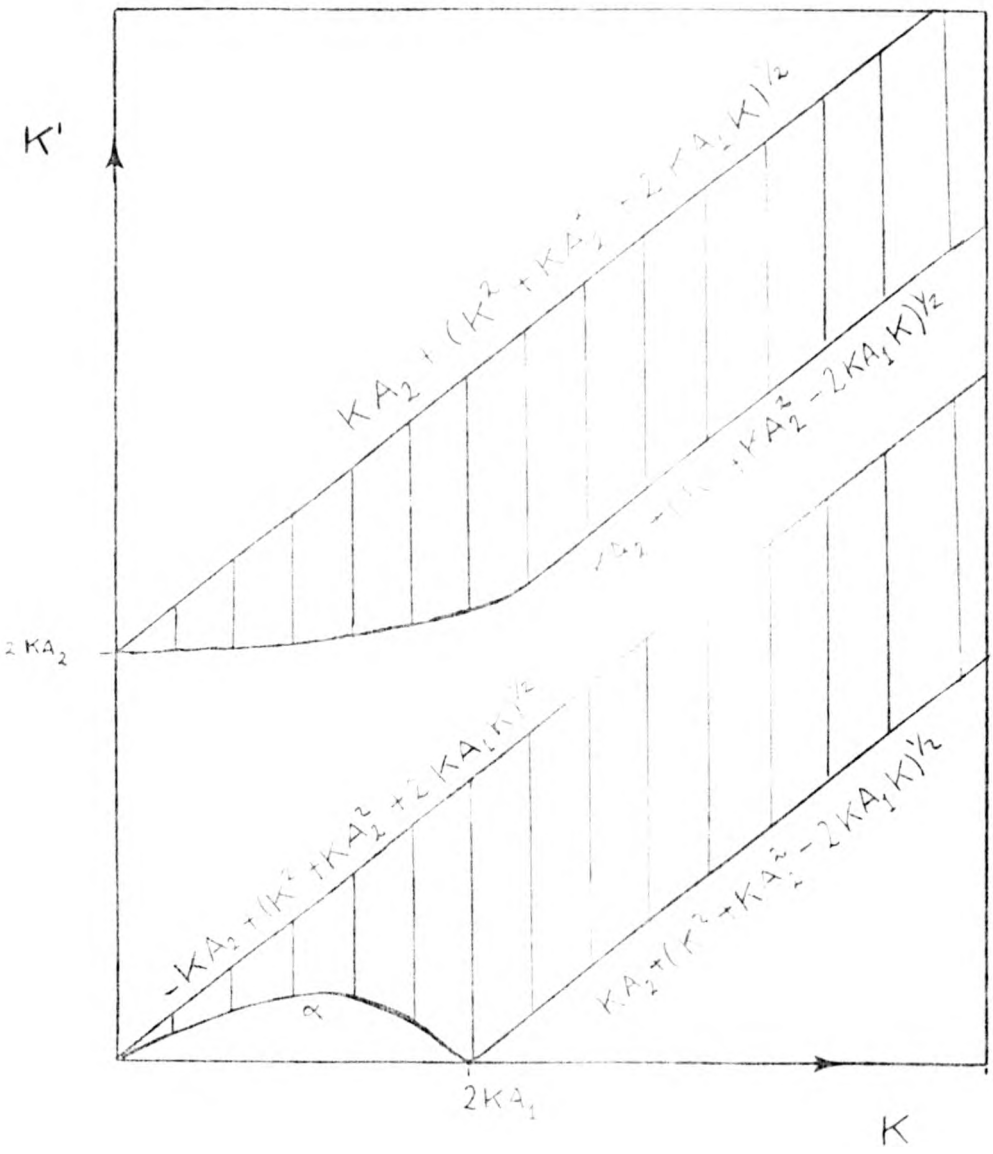

Range of integration of K' for case i=1, j=2.

$\alpha = KA_2 - (KA_2^2 + K^2 - 2\,KA_1K)^{\frac{1}{2}}$

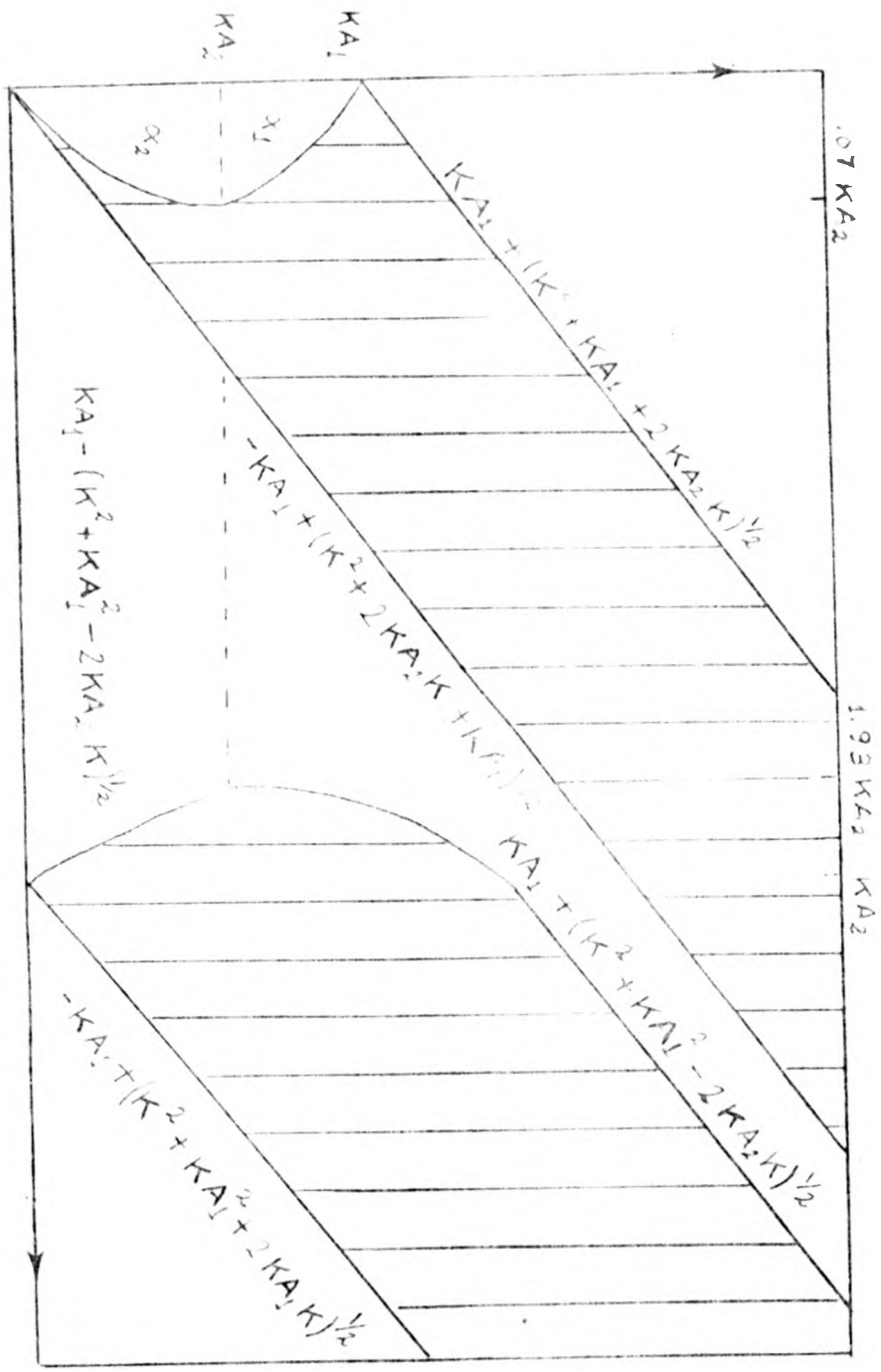

Range of integration of K' for case i=2, j=1.

$$\alpha_1 = KA_1 + (KA_1^2 + K^2 - 2\,KA_2K)^{\frac{1}{2}}$$

$$\alpha_2 = KA_1 + (KA_1^2 + K^2 + 2\,KA_2K)^{\frac{1}{2}}$$

APPENDIX 2

DETAILS OF THE SCATTERING MECHANISMS

Details of the three scattering mechanisms used in the calculations of the average mobility are given here, so as a more general expression for the latter quantity which is valid for the two-band model.

Acoustic Deformation Scatterings:

This scattering mechanism can be written:

$$\tau_{acoustic} = (\text{constant})\ T^{-3/2}\ K^{-1} \tag{1}$$

According to Bir, Normantas and Pikus [19] the inter-and intra-band acoustic scattering times are given by

$$\tau_{11} = \tau_o^L\ T^{-3/2} K^{-1}\ (1.0504 - 0.7628\ \eta + 5.193\ \eta^2)^{-1} \tag{2}$$

$$\tau_{22} = \tau_o^L\ T^{-3/2} K^{-1}\ (1.0504 - 2.0435\ \eta + 3.6\ \eta^2)^{-1} \tag{3}$$

$$\tau_{12} = -\tau_o^L\ T^{-3/2} K^{-1}\ (.567\ \eta^2 + .6632\ \eta)^{-1} \tag{4}$$

The minus sign in τ_{12} indicates that the band 2 was used as the reference, η = b/a (The ratio of the shear to dilatational deformation potentials). τ_o^L is a constant parameter given by [19]

$$\tau_o^L = \frac{\sqrt{2}\ \pi\ h^4\ \rho\ S_L^2}{a^2\ m_2^{3/2}\ k_B^{3/2}} \tag{5}$$

Norton [54] has found that in order to fit the dark mobility data τ_o must be equal to 5.77×10^{-9}. This value is equivalent to the use of a = 8.2 eV in the expression for τ_o^L. Since a is left as a fitting parameter in our calculations, the expressions (2) to (5) are consequently chosen.

Neutral Impurity Scattering:

The Erginsoy's formula [27] for the scattering of electrons by neutral donors is

$$\frac{1}{\tau_N} = \left(\frac{\kappa \, h^2}{m_o \, e^2}\right) \frac{20h}{m} N_N \qquad (6)$$

where the term inside the brackets is the scaled Bohr radius, m_o is the geometric mean mass which is taken to be equal to the density of states effective mass and m is the conductivity effective mass. N_N is the number of neutral impurities. In the case of neutral Cu impurities in Ge, Norton and Levinstein [28] have introduced a multiplicative factor A such that the neutral impurity scattering time in each band becomes

$$\tau_{N_i} = \frac{1.8758 \times 10^5 \, m_i^*}{N_N} A \qquad (7)$$

where $N_N = N_A - N_D - P$ (P is the density of free carriers) and $m_i^* = \frac{m_i}{m_e}$ (m_e is the free electron mass). A is subsequently used as a fitting parameter.

Ionised Impurity Scattering:

The Brooks-Herring-Dingle formula [24] was used to calculate the momentum relaxation τ_{I_i} for this scattering mechanism in band i, and it is given by

$$\frac{1}{\tau_{I_i}} = \frac{N_I \pi e^4 k_B^{-3/2}}{\kappa^2 (2m_i)^{\frac{1}{2}} K^3} T^{-3/2} \left[\ln(b_i+1) - \frac{b_i}{b_i + 1}\right] \quad (8)$$

where κ is the dielectric constant, N_I is the concentration of ionised centers equal to $P + 2N_D$

$$b_i = \frac{2 \kappa m_i k_B^2 T^2 K^2}{\pi h^2 e^2 P'} \quad ; \quad P' = P + (P + N_D)\left(1 - \frac{P + N_D}{N_A}\right) \text{ and}$$

$$K^2 = \frac{\varepsilon}{k_B T}$$

For ionised Cu impurities in Ge the equation (8) becomes

$$\frac{1}{\tau_{I_i}} = \frac{9.334 \times 10^{-3} N_I}{m_i^{1/2} K^3 T^{3/2}} \left[\ln (b_i + 1) - \frac{b_i}{b_i + 1}\right] \quad (9)$$

where b_i is now given by

$$b_i = \frac{6.9366 \times 10^{14} T^2 m_i^* K^2}{P'}$$

and m_i^* is the ratio m_i/m_e.

The Total Scattering Time and Mobility:

The total intra- and inter-band momentum relaxation times are obtained as the harmonic sum over the three scattering processes, that is

$$\tau_{ij} = \frac{1}{\sum_{\alpha} (\frac{1}{\tau_{ij}})_{\alpha}} \qquad i,j = 1,2 \tag{10}$$

where α represents the scattering process considered and $\tau_{12} = \gamma^5 \tau_{21}$.

If the carriers receive negligible amounts of energy from the applied electric field, the current density j is then given as

$$j = \frac{2e}{(2\pi)^3} \left[\int \tilde{f}_1 \, v_1 \, d^3k + \int \tilde{f}_2 \, v_2 \, d^3k \right] \tag{11}$$

where $\tilde{f}_i$ is the non-equilibrium distribution of carriers in the band i produced by the electric field, v_i is the carrier velocity in the same band, $\tilde{f}_i$ is given by

$$\tilde{f}_i = - \frac{e}{h} \underset{\sim}{E} \cdot \frac{\partial \phi_{oi}}{\partial \underset{\sim}{k}} \tau_{fi} \, p^i(\varepsilon) \tag{12}$$

where $\underset{\sim}{E}$ is the applied electric field, τ_{ii} is the total momentum relaxation time in the band i and ϕ_{oi} is the zero-field distribution function in the same band i,

$$p^i = \frac{1}{\delta_1} (1 + \gamma_{ij} \frac{\tau_{jj}}{\tau_{ij}})$$

where $\gamma_{ij} = \frac{m_i}{m_j}$ and $\delta_1 = 1 - \frac{\tau_{11}\,\tau_{22}}{\tau_{12}\,\tau_{21}}$

j can also be written as

$$j = \sigma_o \underset{\sim}{E} = P\, e\mu \underset{\sim}{E} \tag{13}$$

where μ is the total mobility. By combining together equations (13), (12) and (11) the total mobility is then given by

$$\mu = -\frac{1}{3}\,\frac{\gamma^3 \int K^3 \frac{\partial \phi_{O1}}{\partial K} \frac{e\tau_{11}}{m_1} p^1(K^2)dK + \int K^3 \frac{\partial \phi_{O2}}{\partial K} \frac{e\tau_{22}}{m_2} p^2(K^2)dK}{\gamma^3 \int \phi_{O1} K^2 dK + \int \phi_{O2} K^2 dK} \tag{14}$$

If the distribution function in light hole band can be obtained from that of the heavy hole one by the following relationship $\phi_{O1} = (\frac{m_1}{m_2})^{3/2} \phi_{O2}$, then the equation (14) reduces immediately to equation 2.5.4 which was the expression for the mobility used in the one-band model.

APPENDIX 3

THE RATE OF PHOTOEXCITATION (ω_{ph})

We give in here a brief outline of the model of photoexcitation derived by Barker [14]. The effect of instantaneous optical phonon emission on the rate of photoexcitation is also discussed.

Model of Excitation Spectrum

It is assumed that a single hole is excited into the band for each photon absorbed from the radiation by the neutral impurities. The rate of generation of carriers by a flux of photons of energy $\hbar\omega$ is then proportional to the concentration of neutral impurities, the photoionization cross-section and the intensity of radiation. It is adopted a radiation field approximating to the room temperature blackbody radiation. The number of photons dn in the range of energy ($\hbar\omega$, $\hbar\omega + d\hbar\omega$) is of the Planck form

$$dn \alpha (\hbar\omega)^2 \, d\hbar\omega \, [\exp(\hbar\omega/k_B T_r) - 1]^{-1} \qquad (1)$$

where $T_r \sim 300\ ^{o}K$.

If a photon of energy $\hbar\omega$ excites a carrier into the band with energy ε, then by conservation of energy

$$\varepsilon + Ea \sim \hbar\omega \qquad (2)$$

where Ea is the activation energy. Only photons with energies in the range ($\varepsilon + Ea$, $\varepsilon + Ea + d\varepsilon$) may excite carriers into the band in the range (ε, $\varepsilon + d\varepsilon$). The number of photons in this range is proportional to dn. The excitation rate into the same range of energies is

$$dn \; |M|^2 \; g(\varepsilon) \; \alpha(h\omega)$$

where $g(\varepsilon)$ is the density of states into the band, $\alpha(h\omega)$ is the probability that a correct photon is absorbed and $|M|^2$ is proportional to the transition probability into the band. This rate is just $W\,\omega_{ph}(\varepsilon)$, where W is the total excitation rate and ω_{ph} is the normalized rate of excitation. $W\,\omega_{ph}(\varepsilon)$ is then

$$W\,\omega_{ph}(\varepsilon) \alpha \quad \frac{(\varepsilon+Ea)^2 \; |M|^2 \; \alpha(\varepsilon+Ea)}{\exp\left[\frac{\varepsilon+Ea}{k_B T_r}\right] - 1} \tag{3}$$

For room temperature radiation $k_B T_r \sim 0.025$ eV, $E_a/k_B T_r \sim 2$eV, $(\varepsilon + Ea)^2 \sim E_a^2$ so that a final expression for $W\,\omega_{ph}$ is

$$W\,\omega_{ph} \; \alpha \; \varepsilon^{\ell} \exp\,(-\varepsilon/k_B T_r) \tag{4}$$

where ℓ is a parameter determined by the matrix elements for the electron-photon interaction and the corresponding selection rules for the transition probabilities.

The Reduced Rate of Photoexcitation, one band model

In order to derive this rate, we first determine the distribution of the newly excited carriers into the band. To this end a rate equation is set up

$$W\left[A\varepsilon^{\ell} \exp(-\varepsilon/k_B T_r) - \frac{f(\varepsilon)}{\tau_{rec}(\varepsilon)}\right] + \frac{f(\varepsilon)\; h\omega_{op}}{\tau_{op}(\varepsilon+h\omega_{op})} - \frac{f(\varepsilon)}{\tau_{op}(\varepsilon)} + J_{ac} + \ldots = 0 \tag{5}$$

where the first term is the excitation rate (eq. 4), the third and fourth terms are the net scattering rate out of state ε by emission of optical phonons and J_{ac} is the scattering rate due to acoustic phonons. If the emission of optical phonons occurs in a finite time (τ_{op}) but very much smaller than any other physical time associated with the scattering mechanisms, then equation (5) is reduced to

$$W\ Ac'\ \exp\left(-\varepsilon/k_B T_r\right) + \frac{f(\varepsilon + h\omega_{op})}{\tau_{op}(\varepsilon+h\omega_{op})} - \frac{f(\varepsilon)}{\tau_{op}(\varepsilon)} = 0 \qquad (6)$$

A final assumption is that

$$\tau_{op}^{-1} = \tau_o^{-1} = \text{constant} \qquad \varepsilon \geq h\omega_{op} = .037\ \text{eV}$$

$$= 0 \qquad \varepsilon < 0.037\ \text{eV}$$

In the rate of photoexcitation, photon energies greater than 0.23 eV have been removed by an InSb filter. The excitation rate can be drawn as follows

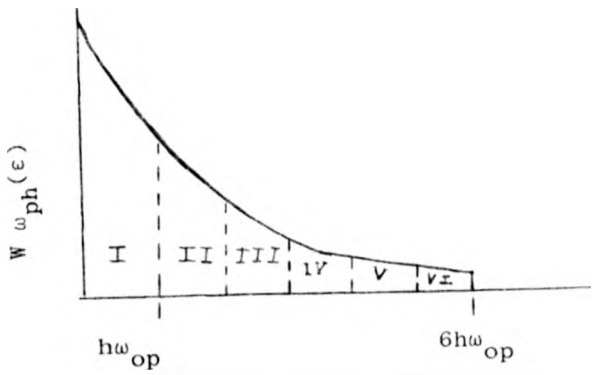

The rate equation for region VI is

$$AW(\varepsilon + 5\hbar\omega_{op})^{\ell} \exp\left(-\frac{\varepsilon+4\hbar\omega_{op}}{k_B T_r}\right) - \frac{f(\varepsilon+5\hbar\omega_{op})}{\tau_o} = 0$$

Therefore the distribution function is

$$f(\varepsilon+5\hbar\omega_{op}) = AW\tau_o \exp\left(-\frac{\varepsilon+5\hbar\omega_{op}}{k_B T_r}\right)(\varepsilon+\hbar\omega_{op})^{\ell}.$$

Similarly the rate equation for region V is

$$AW(\varepsilon+4\hbar\omega_{op})^{\ell} \exp\left(-\frac{\varepsilon+4\hbar\omega_{op}}{k_B T_r}\right) + \frac{f(\varepsilon+5\hbar\omega_{op})}{\tau_o} - \frac{f(\varepsilon+4\hbar\omega_{op})}{\tau_o} = 0$$

and the distribution function is that region when $\tau_o^{-1} \to 0$, is

$$f(\varepsilon+4\hbar\omega_{op}) = AW\,\tau_o\left[\exp\left(-\frac{\varepsilon+4\hbar\omega_{op}}{k_B T_r}\right)(\varepsilon+\hbar\omega_{op})^{\ell} + \exp\left(-\frac{\varepsilon+5\hbar\omega_{op}}{k_B T_r}\right)(\varepsilon+5\hbar\omega_{op})^{\ell}\right] \qquad (7)$$

The distribution functions for the other regions are obtained in a similar way. Finally the rate equation for all carriers in region I is

$$AW(\varepsilon)^{\ell} \exp\left(-\frac{\varepsilon}{k_B T_r}\right) - \frac{f(\varepsilon)}{\tau_{rec}} + \frac{f(\varepsilon+\hbar\omega_{op})}{\tau o} + J_{ac} = 0 \qquad (8)$$

or

$$AW\varepsilon^{\ell} \exp\left(-\frac{\varepsilon}{k_B T_r}\right) - \frac{f(\varepsilon)}{\tau_{rec}} + A \sum_{n=1} (\varepsilon+n\hbar\omega_{op})^{\ell} \exp\left(-\frac{\varepsilon+n\hbar\omega_{op}}{k_B T_r}\right) + J_{ac} = 0 \qquad (9)$$

Therefore the effective rate of photoexcitation is clearly given by the first and third terms of this equation. That is

$$\omega_{ph} = A \exp\left(-\frac{\varepsilon}{k_B T_r}\right) \sum_{n=0}^{5} (\varepsilon+n\hbar\omega_{op})^{\ell} \exp\left(-\frac{\varepsilon+n\hbar\omega_{op}}{k_B T_r}\right) \qquad (10)$$

and the reduced rate of photoexcitation is defined as

$$\bar{\omega}_{ph} \equiv K\,\omega_{ph} = AK \exp\left(-K^2 \frac{T}{T_r}\right) \sum_{n=0}^{5} (\varepsilon+n\hbar\omega_{op})^{\ell} \exp\left(-\frac{\varepsilon+n\hbar\omega_{op}}{k_B T_r}\right) \qquad (11)$$

where $K^2 = \frac{\varepsilon}{k_B T}$, the constant A can be obtained by the use of the normalization condition, equation 2.2.6.

Two-band Model:

The rate of photoexcitation into each one of the bands is derived by identical procedure of that of the one-band model. In the two-band model carriers can migrate into any of the two bands after the emission of an optical phonon, and the probability of these transitions is proportional to the density of states of the final band. Thus, for example, the rate equation for carriers in the region I, band i and $\ell = 0$ becomes

$$AW \exp\left(-\frac{\varepsilon}{k_B T_r}\right) + \frac{P_{ii}}{P_{ii}+P_{ij}} \frac{f_i(\varepsilon+h\omega_{op})}{\tau_o} + \frac{P_{ji}}{P_{jj}+P_{ji}} \frac{f_j(\varepsilon+h\omega_{op})}{\tau_o}$$

$$- \frac{f_i(\varepsilon)}{\tau_{rec_i}} + J_{ac_i} = 0 \qquad (12)$$

where the second and the fourth terms correspond to the total intra- and inter-band scattering rate into the state ε in band i due to the emission of optical phonons, respectively. The multiplicative factors are defined as

$$\frac{P_{ii}}{P_{ii}+P_{ji}} = \frac{m_i^{3/2}}{m_i^{3/2} + m_j^{3/2}} \quad \text{and} \quad \frac{P_{ji}}{P_{jj}+P_{ji}} = \frac{m_j^{3/2}}{m_j^{3/2} + m_i^{3/2}}$$

where i,j = 1,2 and $m_1(m_2)$ is the light (heavy) hole effective mass. The reduced rate of photoexcitation into the light and heavy hole bands are:

$$\bar{\omega}_{ph_1} = \gamma^3 A\, K \exp\left[- K^2 \frac{T}{T_r}\right] \left[1 + \frac{2\gamma^3}{1+\gamma^3} \sum_{n=1}^{5} \exp(- 1.434\, n)\right]$$

$$= .05186B\, K \exp\left(- K^2 \frac{T}{T_r}\right)$$

$$\bar{\omega}_{ph_2} = 1.6BK \exp\left(- K^2 \frac{T}{T_r}\right)$$

the constant B is obtained from the normalization condition (equation 2.2.6)

$$\int (\bar{\omega}_{ph_1} + \bar{\omega}_{ph_2})\, dK^2 = 1$$

Other procedures were also used with no important differences in the final results.

APPENDIX 4

THE ENERGY BALANCE EQUATION

We give here details for each one of the terms of the energy balance equation (equation 3.2.3) when the energy distribution of carriers is given by a Maxwellian function with carrier temperature Te as a parameter. The energy balance equation gives a polynomial equation for the temperature parameter Te.

The total rate of energy loss relative to the bottom of the band due to recombination is

$$W \sum_K \epsilon \frac{\phi(K)\, K}{\tau_{rec}(K)} = W C_o \left(\frac{Te}{T}\right) \int \exp\left(-K^2 \frac{T}{T_e}\right) dK^2$$

$$= W C_o (k_B T_e) \int_0^{\frac{\hbar\omega_{op}}{k_B T_e} = \frac{430}{T_e}} \exp(-Y)\, dY = (k_B T_e) W \bar{C}_o$$

where C_o is a constant that can be evaluated from the normalization equation 2.2.5 and $\bar{C}_o$ is a numerical factor close to 1.

The equation 11, Appendix 3, is the appropriated expression for the reduced rate of photoexcitation. Thus the total rate of energy loss input into the band by the external radiation measured relative to the bottom of the band is then written

$$W \sum_{\substack{K \\ \text{band}}} \epsilon \bar{\omega}_{ph}(K) = (k_B T) A \int_0^{\frac{430}{T_r}} K^2 \sum_{n=0}^{5} \left(K^2 \frac{T}{T_r} + \frac{n\hbar\omega_{op}}{k_B T_r}\right)^{\ell+\frac{1}{2}}$$

$$\times \exp\left[-\left(K^2 \frac{T}{T_r} + \frac{n\hbar\omega_{op}}{k_B T_r}\right)\right] dK^2$$

$$= A_o W (k_B T_r)(\ell + 3/2) \qquad (2)$$

$$\approx 314.22 * W k_B \quad \text{if } \ell = 0$$

Where A is a constant evaluated from the normalization equation 2.2.6 and A_o is a numerical factor close to 1.

The net rate of energy loss into the lattice due to either emission or absorption of acoustic phonons may be obtained from two different methods, [13]. In one of them, the rate of increase of phonons ($\frac{dn_q}{dt}$) with wavevector q is first derived. The net rate of energy loss in the lattice is then obtained by multiplying $\frac{dn_q}{dt}$ by the phonon energy $\hbar\omega_q$ and integrating over all phonon energies. This procedure gives the following expression for the rate of energy loss per carrier into the lattice

$$\sum_{\substack{K \\ \text{band}}} \epsilon\, J(f) = \frac{d\epsilon}{dt} = -\frac{D^2 m_2}{4\pi^3 \rho \hbar} \left[\int_0^{q_{max}} dq\, q^3 (\bar{n}_q + 1) \int_{\frac{\alpha+q}{2}}^{k_{max}} f(k)\, k\, dk - \int_0^{q_{max}} dq\, q^3\, \bar{n}_q \int_{\frac{\alpha-q}{2}}^{k_{max}} f(k) k\, dk \right] \tag{3}$$

Where $k_{max} = (2 m_2 \epsilon_{max})^{\frac{1}{2}}/\hbar$, $q_{max} = \frac{\epsilon_{max}}{\hbar S_L}$, $\epsilon_{max} = 0.037$ eV, $\alpha \left(= \frac{m_2 S_L}{\hbar}\right)$ is the minimum wavevector that a given carrier should have in order to be able to emit acoustic phonons, p is the density of free carriers, and $\bar{n}_q$ is the equilibrium density of phonons.

In the second procedure, the total rate of energy loss ($\frac{d\epsilon}{dt}$) for a carrier with given energy ϵ is first determined. This is carried out by summing over all possible emission and absorption of one-phonon processes, and the total rate of energy loss per carrier to the lattice is then derived by integrating $d\epsilon/dt$ over the distribution of carriers, that is

$$\sum_{K\ \text{band}} \epsilon\, J(f) = \frac{d\epsilon}{dt} = -\frac{D^2\, m_2}{8\Pi^3 \rho h}\left[\int_{\frac{\alpha}{2}}^{k_{max}} f(k)\, kdk \int_0^{2k-\alpha} dq\, q^3(\bar{n}_q+1)\right. \tag{4}$$

$$\left. -\int_0^{k_{max}} f(k)\, kdk \int_0^{2k+\alpha} dq\, q^3\, \bar{n}_q\right]$$

The kind of distribution function we have to our disposal is the main factor which decides the type of procedure to choose. In the case of a Maxwellian function with only one parameter to determine, the equation (3) is the most favourable one. The integration over the q is numerically calculated. However if we assumed that the equipartion of energy is still valid in the range of temperatures ($T < 20^{O}K$) we are dealing with, then the total rate of energy loss per carrier into the lattice has a simple form

$$\frac{d\epsilon}{dt} = -\frac{8\sqrt{2}\, D^2\, m_2^{5/2}\, (k_B T_e)^{3/2}}{\Pi^{3/2}\, \rho h^4}\left[1 - \frac{T}{T_e}\right] C_o + \Lambda \tag{5}$$

where C_o is a numerical factor close to 1 and Λ is small quantity which depends on T. If $C_o = 1$ and $\Lambda = 0$ the expression (5) reduces to the formula obtained by Conwell [13].

Combining together equations (1), (2) and (5) a polynomial equation for Te is obtained

$$A_o\, k_B T_r\, (\ell + 3/2) - C_o\, k_B T_e + \alpha_o\, T_e(T_e - T) = 0$$

where

$$\alpha_o = \frac{8\, D^2\, m_2^{5/2}\, k_B^{3/2} \tau_o}{2^{\frac{1}{2}}\, h^4\, \rho\, \Pi\, T^{\frac{1}{2}}}\ ,\ \tau_o \text{ is the constant lifetime defined}$$

in equation 2.2.8. It is noted that $\langle\tau\rangle = \tau_o \left(\frac{Te}{T}\right)^{\frac{1}{2}}$

$$\sum_{K\ \text{band}} \epsilon\, J(f) = \frac{d\epsilon}{dt} = -\frac{D^2 m_2}{8\Pi^3 \rho h}\left[\int_{\frac{\alpha}{2}}^{k_{max}} f(k)\, kdk \int_0^{2k-\alpha} dq\, q^3(\bar{n}_q+1)\right. \tag{4}$$

$$\left. -\int_0^{k_{max}} f(k)\, kdk \int_0^{2k+\alpha} dq\, q^3\, \bar{n}_q\right]$$

The kind of distribution function we have to our disposal is the main factor which decides the type of procedure to choose. In the case of a Maxwellian function with only one parameter to determine, the equation (3) is the most favourable one. The integration over the q is numerically calculated. However if we assumed that the equipartion of energy is still valid in the range of temperatures ($T < 20^{O}K$) we are dealing with, then the total rate of energy loss per carrier into the lattice has a simple form

$$\frac{d\epsilon}{dt} = -\frac{8\sqrt{2}\, D^2\, m_2^{5/2}\, (k_B T_e)^{3/2}}{\Pi^{3/2}\, \rho h^4}\left[1 - \frac{T}{T_e}\right] C_o + \Lambda \tag{5}$$

where C_o is a numerical factor close to 1 and Λ is small quantity which depends on T. If $C_o = 1$ and $\Lambda = 0$ the expression (5) reduces to the formula obtained by Conwell [13].

Combining together equations (1), (2) and (5) a polynomial equation for Te is obtained

$$A_o\, k_B T_r\, (\ell + 3/2) - C_o\, k_B T_e + \alpha_o\, T_e(T_e - T) = 0$$

where

$$\alpha_o = \frac{8\, D^2\, m_2^{5/2}\, \kappa_B^{3/2} \tau_o}{2^{\frac{1}{2}}\, h^4\, \rho\, \Pi\, T^{\frac{1}{2}}}$$, τ_o is the constant lifetime defined in equation 2.2.8. It is noted that $\langle\tau\rangle = \tau_o \left(\frac{Te}{T}\right)^{\frac{1}{2}}$

$$\sum_{K\ \text{band}} \epsilon\, J(f) = \frac{d\epsilon}{dt} = -\frac{D^2 m_2}{8\Pi^3 \rho h}\left[\int_{\frac{\alpha}{2}}^{k_{max}} f(k)\, kdk \int_0^{2k-\alpha} dq\, q^3(\bar{n}_q+1)\right. \tag{4}$$

$$\left. - \int_0^{k_{max}} f(k)\, kdk \int_0^{2k+\alpha} dq\, q^3\, \bar{n}_q\right]$$

The kind of distribution function we have to our disposal is the main factor which decides the type of procedure to choose. In the case of a Maxwellian function with only one parameter to determine, the equation (3) is the most favourable one. The integration over the q is numerically calculated. However if we assumed that the equipartion of energy is still valid in the range of temperatures ($T < 20^{O}K$) we are dealing with, then the total rate of energy loss per carrier into the lattice has a simple form

$$\frac{d\epsilon}{dt} = -\frac{8\sqrt{2}\, D^2\, m_2^{5/2}\, (k_B T_e)^{3/2}}{\Pi^{3/2}\, \rho h^4}\left[1 - \frac{T}{T_e}\right] C_o + \Lambda \tag{5}$$

where C_o is a numerical factor close to 1 and Λ is small quantity which depends on T. If $C_o = 1$ and $\Lambda = 0$ the expression (5) reduces to the formula obtained by Conwell [13].

Combining together equations (1), (2) and (5) a polynomial equation for Te is obtained

$$A_o\, k_B T_r\, (\ell + 3/2) - C_o\, k_B T_e + \alpha_o\, T_e(T_e - T) = 0$$

where

$$\alpha_o = \frac{8\, D^2\, m_2^{5/2}\, \kappa_B^{3/2} \tau_o}{2^{\frac{1}{2}}\, h^4\, \rho\, \Pi\, T^{\frac{1}{2}}}$$

, τ_o is the constant lifetime defined in equation 2.2.8. It is noted that $\langle\tau\rangle = \tau_o \left(\frac{Te}{T}\right)^{\frac{1}{2}}$